From Choice to Action -

Neural Activity Tracking Decision Making

Thesis

for the degree of

doctor rerum naturalium (Dr. rer. nat.)

approved by the Faculty of Natural Sciences of Otto von Guericke University Magdeburg

by M.Sc. Julia Rogge

born on 18 November 1989 in Berlin

Examiner:

Prof. Dr. med. habil. Markus Ullsperger

Prof. Dr. Marco Steinhauser

submitted on: 24 October 2022

defended on: 25 April 2023

Contents

Abbreviations

BPL	Beta Power Lateralization
DDM	Drift-Diffusion Model
CNV	Contingent Negative Variation
CPP	Centro-Parietal Positivity
EEG	Electroencephalography
ERP	Event-Related Potential
Exp.	Experiment
FDR	False Discovery Rate
FEF	Frontal Eye Field
GPi	Globus Pallidus internus
GLM	General Linear Model
LIP	Lateral Intraparietal Area
LRP	Lateralized Readiness Potential
M1	Primary Motor Cortex
MT	Movement Time
RDM	Random Dot Motion Task
RT	Reaction Time
SAT	Speed-Accuracy Trade-Off
SP	Success Probability
SLLR	Sum Log Likelihood Ratio
TF	Time-Frequency
UGM	Urgency Gating Model

List of Figures

List of Tables

1 Zusammenfassung

Wahrnehmungsbasierte Entscheidungsfindung ist eine komplexe Aufgabe, die sich aus mehreren Teilprozessen zusammensetzt, von der Wahrnehmung von Reizen über die Berechnung von Entscheidungen bis hin zur Ausführung der Handlung. An diesen vielfältigen Prozessen sind verschiedene Gehirnregionen und -netzwerke beteiligt. In dieser Arbeit habe ich mich auf die Beta-Power-Lateralisierung (BPL) konzentriert. Dieses Elektroenzephalogramm(EEG)-Signal resultiert aus einer asymmetrischen Beta-Power Reduktion, die in der kontralateralen Hemisphäre stärker ist als in der ipsilateralen, bezogen auf die kommende Bewegung. Dieses Signal baut sich robust an Elektroden über dem motorischen Kortex vor einer unimanuellen Reaktion auf.

Hier habe ich untersucht, inwieweit diese Lateralisierung mit der Entscheidungsverarbeitung zusammenhängt. Dabei habe ich den zeitlichen Verlauf des Signals in Abhängigkeit von Entscheidungsvariablen wie den Antwortzeitpunkt und die Evidenzstärke untersucht. Insbesondere habe ich dabei erwartet, dass ein neuronales Korrelat der Entscheidungsfindung zeitlich von einem eher handlungsvorbereitenden Signal abgekoppelt werden kann. Des Weiteren habe ich die Hypothese aufgestellt, dass sich die Dringlichkeit einer Entscheidung in den Schwankungen der Signalamplitude widerspiegelt, die notwendig ist, um eine Entscheidung zu treffen. Außerdem habe ich angenommen, dass ein entscheidungsverarbeitendes Signal die Stärke der Evidenz abbildet, die zu einem bestimmten Zeitpunkt während der Verarbeitung gesammelt wurde.

Um diese Annahmen zu testen, habe ich drei Verhaltensexperimente mit gesunden Teilnehmern durchgeführt während ein 64-Kanal-EEG abgeleitet wurde. Dreißig Probanden haben zunächst die "Random-Dot-Motion" (RDM) Aufgabe in zwei Sitzungen (unmittelbare Antworten vs. forcierte Antwortverzögerung) ausgeführt. Die Reize variierten zufällig zwischen sechs Evidenz-Stufen (1,6 % - 51,2 % Bewegung in eine kohärente Richtung). In einem weiteren Experiment führten dreißig Teilnehmer ein einfaches Reaktionszeitparadigma mit variabler Antwortverzögerung (300-1300 ms) durch. Die Probanden mussten auf einen direktiven Pfeilreiz reagieren sobald ein Reaktionshinweis erschien. Weitere 34 Teilnehmer haben zweimal die "Token-Aufgabe" bearbeitet. Diese Aufgabe präsentiert schrittweise Evidenz und erlaubt Antworten zu selbstbestimmten Zeitpunkten, wobei schnellere Antworten in einigen Bedingungen mit

Zeitersparnissen oder monetär belohnt wurden.

Mithilfe von Regressionen auf Einzeldurchgangsebene fand ich heraus, dass sich der Startzeitpunkt der BPL von dem eines motorischen Vorbereitungssignals unterscheidet und auch nicht durch eine erzwungene Handlungsverzögerung beeinflusst wird. Insbesondere bei der Token-Aufgabe, aber teilweise auch bei der RDM, zeigte sich, dass die BPL mit der Menge der gesammelten Evidenz für die zukünftige Entscheidung einige Zeit vor Beginn der motorischen Vorbereitung variierte. Schließlich zeigte sich, dass Entscheidungen unter Zeitdruck durch einen veränderte BPL-Verlauf gekennzeichnet waren.

Insgesamt deuten diese Ergebnisse darauf hin, dass die BPL eine wichtige Rolle bei der Entscheidungsfindung spielt. Sie scheint entscheidungsrelevante Variablen während der gesamten Verarbeitung online zu kodieren und die gewählte Option mit der bevorstehenden Handlung zu verknüpfen. Somit könnte die BPL möglicherweise als Auslesesignal für die Entscheidungsentwicklung dienen.

2 Abstract

Perceptual decision-making is a complex task that consists of several sub-processes from the perception of stimuli to the deliberation process to the implementation of the action. A wide range of brain regions and networks are involved in these diverse processes. In this work, I focused on beta-power lateralization (BPL), an electroencephalogram (EEG) signal that results from asymmetric beta power reduction, which is stronger over the contra- than the ipsilateral hemisphere with respect to the movement. This signal robustly builds up at motor cortical electrodes prior to a unimanual response.

Here, I investigated the extent to which this lateralization is related to decision processing. I examined its variability as a function of decision variables such as timing and evidence. In particular, I expected that a neural correlate of decision making can be temporally disentangled from a more action-related signal. Furthermore, I hypothesized that the urgency of a decision would be reflected in the variation in signal amplitude necessary to commit to a choice. Finally, I expected that a decision-tracking signal encodes the amount of evidence accumulated at a given time during processing.

To test these assumptions, I conducted three decision-making experiments with healthy human participants and 64-channel EEG recordings. First, thirty participants performed the 'random dot motion' task in two sessions (immediate responses vs. fixed response delay). The dot stimuli varied randomly between six levels of evidence (1.6 % – 51.2 % motion into a coherent direction). Second, thirty humans performed a simple delayed response paradigm with variable response delay latencies (300 - 1300 ms). They had to respond to a directive arrow stimulus as soon as the imperative response cue occurred. Third, 34 participants were asked to perform the 'Token Task' twice (without vs. with monetary reward). This task presented evidence in a discrete manner and allowed responses at self-determined times with fast responses being rewarded in certain conditions. I explored the relevance of the manipulations as well as reaction times for the dynamics of the BPL by using a novel single-trial regression approach.

Using single-trial regression analyses, I found that BPL differed from a motor preparation signal in onset times and was not affected by a forced response delay (fixed and variable). In particular, in the Token Task, but also to some

extent in the RDM, BPL was found to vary with the amount of accumulated evidence for the 'choice to-be' some time before motor preparation began. Finally, I found that urgent decision making was reflected by altered BPL dynamics related to response timing.

Overall, these results suggest that BPL plays a crucial role in decision making. It appears to encode decision-related variables throughout processing and to link the choice to the upcoming action. Thus, the BPL could potentially serve as an online read-out of decision development.

3 Theoretical Background

We are exposed to a constant stream of information that we have to process and react upon, sometimes under strong time pressure. In cognitive psychology such tasks have been summarized under the generic term decision making. Everyday, we encounter these cognitive demands, for example in road traffic: visual input from the traffic light or a street sign, auditory input from an emergency siren or a beeping car. All this information must be processed and appropriate actions need to be selected and finally carried out. Our behavior is thus controlled by latent decisions that result from complex computations of our brain. Perceptual decision-making, i.e. decisions based on sensory input, involves a categorical judgment of the information entering the brain (Gold & Shadlen, 2000). Imagine a pedestrian trying to cross a busy road. She has to process a lot of information about approaching cars, their speed, acceleration, distance, the width of the road, maybe she observes other pedestrians for reference or even different types of vehicles. She perceives all this information, categorizes it and decides if and when to cross the street. Such a decision task is usually subject to additional environmental conditions such as urgency or perceptual uncertainty.

In experimental settings, decisions are often less complex and external influences can be carefully controlled or intentionally manipulated. Nevertheless, the tasks require similar cognitive functions: intentionally discriminating between the presence or identity of environmental stimuli (Ding & Gold, 2013) by comparing the evidence for the available options (Gold & Shadlen, 2000). It starts with stimulus perception, where information is collected and evidence for the available options is accumulated. Then, a variable policy is required for ending this process with a commitment to a choice or plan of action (Drugowitsch et al., 2012) which consequently guides behavior (Ding & Gold, 2013). In other words, perception involves the representation, selection and accumulation of sensory input (Newman et al., 2017). Information needs to be encoded and integrated into a decision variable (O'Connell et al., 2012). Finally, an appropriate action has to be selected, prepared, and executed (Newman et al., 2017). Interestingly, these sub-processes do not require strict temporal order or distinct neural areas. Instead, functions partially overlap in space (e.g. Hunt et al., 2013) and feedback loops within and between brain regions (Siegel et al., 2015) oppose the idea of strictly sequential pro-

cessing cascades (Sternberg, 1969). This presents a particular challenge when studying isolated sub-processes and requires careful experimental design and interpretation of results. One of such spatial intersections of cognitive tasks will be considered within this thesis. I will present work on signals over the motor cortex and to what extent they represent information integration, action selection, and motor preparation processes.

In the first chapter, I will provide a theoretical overview of the role of evidence accumulation and urgency in perceptual decision-making. Next, I will introduce and describe the analysis of lateralization signals over motor cortex, the neural system of interest in this project. This motivates the research questions and hypotheses of this thesis, which will be investigated in two empirical chapters. A first set of studies involves two perceptual decision-making experiments where fixed and flexible response delays were enforced to disentangle motor from decision related processing. I recorded electroencephalography (EEG) over the motor cortex to study the relevance of motor cortical signals during decision making. In the second study, I used a paradigm that provided evidence in a slow and discrete manner while response urgency was enhanced to investigate urgency effects on decision making. In the final chapter, I will summarize the findings of both studies and discuss their implications in light of the current literature.

3.1 Evidence accumulation in perceptual decision-making

Decision making literature refers to 'evidence' as the perceptual input that provides us with information about features we try to identify or discriminate. Therefore, we need to have a motivation and goal to which we gather relevant information that helps us to come to a solution - to make a decision. This gathering of information and its termination is indispensable for decision making, the latter I will turn to in the next section. First, I will consider the process of evidence accumulation, which can be illustrated by the following scenario. There is a person approaching and one needs to quickly decide whether one knows this person to act appropriately. Thus, one will gather information about facial features, eyes, nose, mouth, and potentially even listen to their voice, observe their gait, or perceive a particular smell. This input from different modalities is collectively gathered over time to provide evidence for the identity of the person and helps us decide whether or not we know the person. After some time, one option will be favored over the other and finally

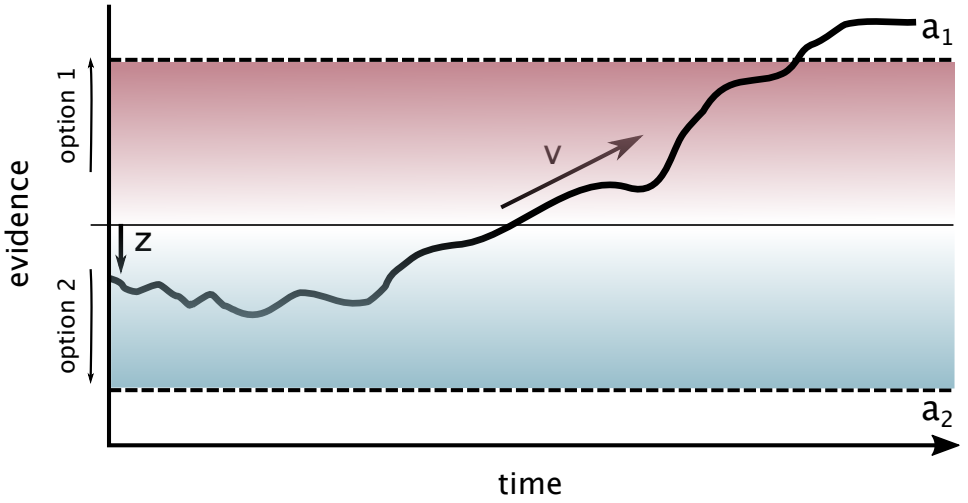

Figure 1. Simple Drift Diffusion Model as an example for the evidence accumulation account in decision making. The accumulator starts with a bias (z) towards option 2 (blue), and then slowly accumulates evidence (v= drift rate) for option 1 (red) until it reaches the decision threshold (a_1) after some time. In behavioral terms this could be the decision process of an agent, who initially tended towards blue. During stimulus presentation, however, the agent receives increasing input in favor of red, and at some point information is sufficient to choose red.

there will be sufficient evidence to commit to a choice. This accumulation of evidence takes place at the order of hundreds of milliseconds but is a highly adaptive and sensitive mechanism.

This idea of evidence accumulation has been formalized by a class of computational models. Currently, the drift-diffusion model (DDM; Ratcliff, 1978; Ratcliff & McKoon, 2008) is most commonly used to describe the process for two-alternative forced choices. It understands evidence accumulation in decision making as a continuous random walk towards either one of the alternatives (see Figure 1). The accumulator unit integrates evidence for both options and gradually builds up as one choice option surpasses the other. The slope of this accumulation process is described by the drift rate (v). Upon reaching one of the thresholds (a) the decision for the corresponding option is made. Sometimes, also starting point biases (z) by prior information or expectation are included.

A number of neural correlates were identified to be involved in evidence accumulation or its integration. This process does not take place within a strict sequence or distinctly specialized areas (see above), but rather within a distributed neural network and through temporally overlapping activation. As

perceptual decision-making is most often studied within the visual modality, I will consider the visual system when describing perceptual areas. However, other perceptual regions may show a similar functional discrimination when stimuli are within the respective modality. Moving stimuli are processed in middle temporal area (Parker & Newsome, 1998) and single unit recordings revealed that single neurons' activity in this region encode evidence strength (Britten et al., 1992). Moreover, high frequency oscillations (high gamma) in human visual area 5 (functional equivalence to middle temporal area in monkeys) are modulated by evidence strength and seem to reflect sensory evidence accumulation (Siegel et al., 2007). Besides, higher-level functions (Tranel et al., 2003) were related in a line of studies to a consistent positive peak of averaged population activity (from EEG recordings) in centro-parietal regions. This centro-parietal positivity (CPP) varied in strength with reaction time (RT) and sensory evidence (Kelly & O'Connell, 2013; Twomey et al., 2016) and was interpreted as a domain general neural marker for the integration of evidence (O'Connell et al., 2012; Twomey et al., 2016). Moreover, sensori-motor regions were found to reflect or integrate evidence strength over time. Initially, studies in monkeys showed that output regions such as frontal eye field (FEF; Gold & Shadlen, 2000, 2003) and the lateral intraparietal area (LIP; Shadlen & Newsome, 2001; Roitman & Shadlen, 2002; Kiani & Shadlen, 2009) varied their activation with stimulus features over time, suggesting that they integrate the accumulated evidence. In humans, similar activity was shown over motor cortical areas. Donner et al. (2009) used MEG to reveal that beta power lateralization (BPL) integrates evidence strength. Others observed such functionality in contralateral (with respect to the choice) beta activity (O'Connell et al., 2012) or described that expectations modulated alpha and beta power motor lateralization (De Lange et al., 2013). Slower fluctuations in motor areas (measured as event-related potentials [ERP]) were also suggested to relate to evidence accumulation. The lateralized readiness potential (LRP, de Jong et al., 1988; Gratton et al., 1988) reflected prior beliefs, decision thresholds and accumulation rates (Van Vugt et al., 2014). Taken together, evidence representations are spread over a variety of cortical regions, from classical perceptual to motor regions. In this thesis, I will particularly shed light on the relevance and distinction of signals recorded over the motor cortex.

An established task to investigate evidence accumulation in perceptual decision-making in the laboratory is the random dot motion task (RDM). The stimuli

were initially used to investigate neural correlates of motion stimulus perception in middle temporal area (Britten et al., 1992; Newsome & Paré, 1988) and proved particularly useful as a perceptual decision task later on. Stimuli in this paradigm are dots moving within a fixed aperture. The subject needs to detect the direction of coherently moving dots. The motion feature of the stimulus is particularly advantageous for manipulating evidence strength. Even though in static displays evidence can by varied, too, the random dot kinematogram appears particularly suitable. It has the opportunity to present fine-grained, almost continuous, modulations in physical stimulus strength by simply adapting the proportion of dots moving into one coherent direction. All other dots move randomly and present noise that can be more or less dominant. Hence, with this task I was able to manipulate physical evidence strength in order to observe similar variations in neural activation, but also effects on behavioral responses. The detailed knowledge of how and where evidence is accumulated in the brain in various contexts is vital for our understanding of decision making as it makes up an indispensable task during decision computation.

3.2 Urgency in perceptual decision-making

Evidence accumulation takes time but it also needs to terminate at some point. The decision maker must complete the accumulation and select an option to adaptively interact with its environment. Some authors (Klaus et al., 2019; Khalighinejad et al., 2020, 2022) argued that choosing when to act is a second decision. While this strong claim may be debated, it seems obvious that some policy on finishing the decision process is inevitable and could be influenced from the task or situational context. The relationship between accuracy and speed is of central importance here. The notion of the speed-accuracy tradeoff (SAT) describes the conflict between accuracy and speed. Behaviorally it manifests itself in reduced accuracy when reactions are fast, and vice versa. This corresponds to assumptions within accumulation models, which state that one cannot acquire as much evidence within this shorter amount of time compared to longer RTs. Thus, we base our choices on less information, which is more error-prone (Schouten & Bekker, 1967; Wickelgren, 1977). It follows that the SAT is directly related to the termination policy of the decision in that speed or accuracy will be favored by terminating the decision process sooner or later (i.e. Reddi & Carpenter, 2000; Drugowitsch et al., 2012). In the example scenario of deciding about the familiarity of a person, speed pressure

would be imposed if this person was already very close once the decision maker notices that an action is required. Possibly, the short amount of time does not allow for noticing every detail of their appearance before a reaction (and a decision) is expected. Thus, it is more likely to make a wrong choice and act inappropriately as compared to a situation where there is a lot of time to observe this person.

Even though, performance decreases with speed, decisions are often made in a haste. One reason is the internal urge to terminate the decision process, which can vary between humans (Yau et al., 2021; Carland et al., 2019). Another reason, as in the given example, are external deadlines that require fast reactions (Wickelgren, 1977). Yet another cause, particularly in laboratory settings, are rewards or instructions for speeded responses (Wickelgren, 1977). Hence, there can be several reasons to finish the decision process before the optimal choice has been prepared. All of the aforementioned reasons are related to urgency which affects cognitive processing and eventually the outcome of the decision (Thura et al., 2012). Such a sense of urgency can be described as time pressure to commit to a decision as soon as possible. When time elapses urgency increases (Drugowitsch et al., 2012). Humans perceive such passage of time and as a result the pressure to respond increases. This is an adaptive mechanism as one cannot endlessly ruminate about a decision. However, in some pathological conditions, e.g. obsessive-compulsive behavior (Banca et al., 2015; Hauser, Moutoussis, Iannaccone, et al., 2017), this ability is in fact suspected to be dysfunctional. Also in normally functioning brains, there is emerging evidence for interindividual variability, as in trait-urgency (for a review see Carland et al., 2019) or a link to the personality trait "need for closure" (Evans et al., 2017), that also affects decision processes. It is crucial to understanding the underlying mechanisms for explaining those behavioral variations. Several decision making models already exist to explain the effect of urgency on decision making.

As I briefly stated above, under the assumptions of accumulation models (see *Evidence accumulation in perceptual decision-making*) it is typically assumed that the decision threshold is reduced in contexts with speed-emphasis (Reddi & Carpenter, 2000; Drugowitsch et al., 2012). This would explain shorter RTs and lower accuracy. In situations with a response deadline or urgency related to elapsing time, one could assume a hazard function of time during

non-performance (Katsimpokis et al., 2020). Such a hazard function has been incorporated into accumulation models by a collapsing bound (Drugowitsch et al., 2012). The threshold is not anymore static but decreases as a function of time spent on the decision. Drugowitsch et al. (2012) found such a mechanism expressed in monkey LIP neurons caused by an external urgency signal. The authors further showed that this urgency signal is in fact independent of the coherence level, i.e. task difficulty. Others suggest an independent urgency signal to play a major modulatory role in decision outcome. This was formalized by the urgency-gating model (UGM; Cisek et al., 2009). The authors postulate that the decision variable and its neural correlates are a product of the current stimulus information (perceptual evidence signal) and an independent urgency signal. This urgency signal increases linearly with elapsing time. Thura and Cisek (2016) suggest that fast decisions are produced through a heightened starting point and steeper build-up of neural activity in the motor system, for both decision and movement related activity. Such an adjustment of the drift rate offers an alternative account to the proposed threshold collapse by Drugowitsch et al. (2012). There is some debate about the necessity of accumulating evidence (Winkel et al., 2014) or whether urgency is sufficient to drive the decision signal (Cisek et al., 2009). Interesting for this discussion may be the dissociation between situational factors. Katsimpokis et al. (2020) found that response deadlines influence the drift rate whereas speed instructions induce threshold regulations.

Urgency does not only impact deliberation time, but also movement time has been linked to speed pressure (Shadmehr et al., 2010). Following this, Thura et al. (2014) suggested to measure movement time (MT, reaching movements) to operationalize response vigor. They observed a relationship between urgency and the vigor of movement in monkeys (Thura et al., 2014) as well as in humans (Thura et al., 2014; Thura & Cisek, 2016).

It was suggested, that an urgency signal originates in the Globus Pallidus internus (GPi; Thura & Cisek, 2017), an output unit of the basal ganglia. Research shows that inactivation of this region in monkeys increases their MT, i.e. vigor (Desmurget & Turner, 2010), indicating a lack of the urgency signal (Thura et al., 2014). In humans with Parkinson's Disease, a pathology characterized by reduced basal ganglia activity, rapid movement is impaired (Mazzoni et al., 2007) which hints at a relevant role of this area in urgency processing.

Furthermore, neural activity patterns in the GPi resemble the hypothetical build-up of urgency (Thura & Cisek, 2016) and can be modulated by speed or accuracy emphasis (provoking more or less urgency) in the task (Thura & Cisek, 2017). Others have shown that the subthalamic nucleus, also a structure of the basal ganglia, modulates decision thresholds and is therefore involved in dynamical adjustments of SAT (Frank, 2006; Cavanagh et al., 2011; Herz et al., 2018). Deep brain electrodes in humans revealed a link between local field potential power in the subthalamic nucleus and behavioral slowing after errors (Siegert et al., 2014). Others (Zaehle et al., 2017) reported a causal relationship between subthalamic nucleus stimulation and impulsivity regulation. Interestingly, beta power in the subthalamic nucleus was phase-coupled to motor cortical beta power and modulated SAT (Herz et al., 2017). Together, these findings suggest that speed or urgency modulations in decision making are based on cortical and subcortical structures as well as their connections. Their exact mechanism, however, remains to be understood. Interestingly, recent findings (Derosiere et al., 2022; Reynaud et al., 2020; Codol et al., 2020) contradict the "shared regulation" hypothesis (Thura et al., 2014) that decision and movement time underlie the same urgency regulation. These studies lack an effect of speed-pressure on vigor. Thus, whether decision and action time are regulated by the same or different mechanism and sources remains unclear.

With the emergence of the urgency account, a new paradigm was introduced to better understand how urgency influences the decision process - the *Token Task* (Cisek et al., 2009). This task requires the participant to decide whether more tokens will end up in a left or right goal. All tokens are visible at all times and move one by one from a central pool to their lateral goal. This sequential presentation of information offers the opportunity to carefully manipulate the amount of evidence given to an observer. The designer of the token sequences can make use of the ground truth of the current evidence (at each moment in time) for each goal. This makes it possible to present different scenarios such as misleading or biased sequences. The original version of the task also allows for manipulating the SAT by offering time savings for fast decisions. Thus, this task offers some advantages over the classical RDM paradigm if one aims to study urgency and evidence accumulation in perceptual decision-making.

3.3 Signals over motor cortex in perceptual decision-making

As stated above, the motor cortex received increasing attention in current cognitive neuroscience literature. Several motor cortical signatures are of interest when studying decision making and action preparation. One of the most famous EEG signals over motor cortex is the readiness potential. The evolving negativation of scalp potentials was first reported and termed "Bereitschaftspotential" (readiness potential) by Kornhuber and Deecke (1965). It emerges around two seconds before voluntary hand movements (Shibasaki & Hallett, 2006) and is most dominant at electrodes above mesial motor cortical areas (Schurger et al., 2021). The readiness potential consists of two components. The first component has a wide symmetrical distribution over the scalp but is strongest at electrode Cz (Shibasaki & Hallett, 2006). This initial deflection comes from activity in supplementary motor area and premotor cortex (Schurger et al., 2021) and is accordingly understood as marking the onset of movement planning and preparation. The late component starts around 400 ms before the movement Kornhuber and Deecke (1964) and is marked by a sudden increase in slope. This negative ramping signal appears maximal contralateral to hand movement (electrodes C1/C2) and originates in primary motor cortex (M1; Shibasaki et al., 1981). Note that the exact timing and distribution varies a lot according to task type, requirements, as well as individuals (Schurger et al., 2021). Importantly, single-hand movements are preceded by this negative potential over motor cortex in both hemispheres, but the strength of the late component (>= 400 ms pre-movement) differs between hemispheres (Deecke et al., 1976).

More than a decade later, this asymmetry in motor cortical negativation before movements was studied more thoroughly (de Jong et al., 1988; Gratton et al., 1988). The lateralized readiness potential (initially termed *corrected motor asymmetry* by de Jong et al., 1988) labels a stronger negativation over the motor cortex contralateral to the effector compared to the ipsilateral hemisphere. It was suggested to be a direct consequence of the late part of the readiness potential and originates also in M1 (for a review see Eimer, 1998). The timepoint at which the readiness potential diverges between hemispheres was understood to reflect the moment of determination for one response side (Kutas & Hillyard, 1980). Today, this slow difference in scalp potentials is often used as a measure of response activation and widely studied in different

contexts mostly using reaction time tasks (Smulders & Miller, 2012). It marks the onset of movement preparation once the selection process, i.e. decision making, is concluded (Kutas & Donchin, 1974; Gratton et al., 1988; Haggard & Eimer, 1999; Kelly & O'Connell, 2013). This, in fact, discriminates the LRP from the readiness potential, which is generally assumed to be specific to voluntary movements and reflects a general preparedness to act (Travers & Haggard, 2021).

Another approach to analyzing scalp potentials is by defining their oscillation frequency and computing the power of each frequency within the signal (see computational details below). Such neural oscillations are linked to specific brain states, functions and regions (first described by Berger, 1929). One widely studied frequency band spans 13-30 Hz, the beta-band. This rhythm has been linked to motor functions for decades. Traditionally, beta-band oscillations were considered to maintain an idling state in the motor cortex (Pfurtscheller et al., 1996), thus preventing any movements during inactivity. The reduction of beta power would according to this view release a 'break' and open up the possibility to act. Today, beta-band oscillations are considered to preserve the current state of the system during inactivity, while attenuation in beta power makes new movements possible (for a review see Engel & Fries, 2010). This hypothesis states that performing any new voluntary movement requires a reduction in beta power (Gilbertson et al., 2005; Androulidakis et al., 2007). Along these lines, beta power was found to decrease after response cue onset (Tzagarakis et al., 2010).

Interestingly and analogous to the low-frequency averaged signals described above (i.e. the readiness potential and the LRP), beta power appears to lateralize prior to one-sided responses (Jasper & Penfield, 1949; Pfurtscheller, 1981). Beta power decreases more strongly in the contralateral than in the ipsilateral hemisphere with respect to the response side (Donner et al., 2009; O'Connell et al., 2012; De Lange et al., 2013). Similarly to LRP, BPL was associated with motor selection in decision making tasks (Kaiser et al., 2001; Doyle et al., 2005). Its robust link to motor output was confirmed when no overt responses to a decision were required and BPL disappeared (Twomey et al., 2016; O'Connell et al., 2012). Thus, it is most likely an effector specific motor preparatory signal. However, it was also shown that BPL amplitude correlated with integrated sensory evidence over a period of time before the

response (Donner et al., 2009). Moreover, BPL was shown to scale with RT and sensory evidence (O'Connell et al., 2012; De Lange et al., 2013). Thus, it was interpreted that this lateralization does not merely represent the final motor selection, but reflects also some decision related variable.

Neural correlates reflecting a decision variable should possess certain features if understood in terms of evidence accumulation theories (see Section 3.1). In the following, I will describe some characteristics that could make beta oscillations a promising candidate for transferring decision information. First, a beta power reduction (inversely) builds up towards a peak just before the response (Kaiser et al., 2001). The authors suggest that such reduced beta power could indicate the time needed for selecting a motor response. Additionally, beta-band power decreased not only after cue, but even further after target presentation (Tzagarakis et al., 2010), indicating that not merely motor preparation is encoded. Second, the rate of this increase in lateralization (slope) varies with stimulus strength if it encodes accumulation of evidence (De Lange et al., 2013). The authors observed for pre-response, but not post-stimulus, that BPL slope varied with stimulus intensity. Others, in contrast, did not find evidence for such an association (Twomey et al., 2016). Third, the latency and amplitude of the peak are relevant parameters as they mark the decision threshold of the accumulator. The time of the peak of contralateral beta (O'Connell et al., 2012) and BPL (Fischer et al., 2018) was shown to be tightly linked to or at RT, respectively. In contrast, beta power peak amplitude was constant regardless of RT (O'Connell et al., 2012) and BPL peak amplitude did not vary with stimulus strength (Twomey et al., 2016). Moreover, a variety of uncertainty levels yielded no peak amplitude differences of beta power (Tzagarakis et al., 2010). Thus, the peak of contralateral beta power or BPL could be indicative of a response threshold. Finally, the onset latency of a decision signal could be predictive of its function. Tzagarakis et al. (2010) reported that beta power changed approximately 120 ms after cue onset even before response target appearance. Its lateralization appeared even several seconds before response onset (Donner et al., 2009) and the starting point was influenced by prior expectations, a relevant variable for decision making (De Lange et al., 2013). To sum up, there is converging evidence that beta power and specifically its lateralization could hold online decision information within the motor cortex. Before turning to the main hypotheses, I will shortly introduce by what means I processed the lateralized EEG signals of interest

for the present studies.

3.4 Processing and analysis of lateralized neural signals

The neural signals that are relevant for this thesis were analyzed by specific methods that I will briefly introduce in this section and describe in more detail in the methods sections of the two main chapters (*Motor cortical signals reflecting decision making and action preparation* & *Beta power lateralization reflects urgency-related response timing during evidence accumulation*).

Electrode Sites. As this thesis focuses on signals related to finger movements, I was interested in electrode locations capturing pre- and primary motor cortical sources. The late readiness potential for hand movements originates primarily from tangential sources in M1 (Nagamine et al., 1996) in the precentral gyrus. The somatotopy of M1 could be advantageously used for locating electrodes directly over hand areas. However, spatial specificity is rather low for EEG recordings (i.e. volume conduction), thus electrode sites are usually selected based on the largest signal strength or previous research. For LRP, C3' and C4' (1 cm anterior to C3/C4) or C3 and C4 have been most commonly used (e.g. de Jong et al., 1988; Eimer, 1998; Haggard & Eimer, 1999; Gratton et al., 1988). Yet, in the vast amount of LRP research there have been a variety of electrode sites used, which also yielded adequate results. The electrode selection for the present experiments was based on previous research, finding strongest BPL in postero-central electrodes (Fischer et al., 2018). The authors used the average of C3 and CP3 for left hemisphere and C4 and CP4 for right hemisphere activity, which I adopted for both motor cortical measures, LRP and BPL.

LRP computation. For the computation of the LRP, different methods have been described (Eimer, 1998). Here I implemented the *averaging method* (Coles, 1989). For right hand responses I subtracted the left hemisphere ERP from the right hemisphere ERP and vice versa for left hand responses. The resulting difference signals were then averaged (taking the sum and dividing by two). This method renders the LRP a negative deflection before the response and its amplitude is half the size of the amplitude obtained by another technique (*double subtraction*, de Jong et al., 1988). This negative polarity of the difference signal (contralateral to response hand stronger negativity than

ipsilateral) corresponds to the polarity of the BPL, and facilitates comparisons between those measurements.

BPL computation. For acquiring oscillatory lateralization there were several steps involved. Firstly, I computed the Time-Frequency (TF) spectra for each electrode of interest and trial. The data was then sorted by contra- and ipsilateral activity, such that C3 and CP3 TF data was re-coded into ipsilateral for left-hand responses and contralateral for right-hand responses. Whereas, C4 and CP4 TF data were considered contralateral for left-hand trials and ipsilateral for right-hand trials. In other words, I re-categorized the electrode data from their specific hemispheric location into their output-related location (ipsi- or contralateral to response side). Then, it was possible to subtract ipsi- from contralateral activity for each location (C and CP) and trial. Eventually, I averaged across positions (i.e. $(C_{ipsi} + CP_{ipsi})/2$ and $(C_{contra} + CP_{contra})/2$) and trials. This rendered a lateralization signal with growing negative deflection before the response and I was able to compare its parameters to the LRP.

Determining onset latencies within a timeseries. Several parameters of ERP and power timeseries can be modulated by experimental manipulations or differ between groups. In the first part of this project, I aimed at differentiating the onset latencies of the ramping signals. Primarily, I was interested in differences in onset latencies between task conditions. Onset latency is often defined as the moment in time at which a signal starts to deviate from zero (Smulders & Miller, 2012). However, this involves the risk of capturing random fluctuations or even more local peaks and troughs of a curve. In order to account for the noisiness and interindividual differences in lateralization trajectories, I applied a jackknife-based method (Miller et al., 1998; Ulrich & Miller, 2001). Separately for each condition, I composed 'new' samples by averaging all but one of the original samples (i.e. participants). This was done for every sample, resulting in a set of averages - the new sample set. This step reduced noise in the timeseries data, but required stricter control during significance testing (Ulrich & Miller, 2001), which I will describe in detail in study 1 (*Motor cortical signals reflecting decision making and action preparation*). Next, I defined the onset of the timeseries peak (negative for the lateralization) by setting a criterion (certain percentage of the maximum peak amplitude) and then identified the timepoint, through interpolation, at which this criterion

was first crossed (Miller et al., 1998). Similarly, this technique can be used to measure peak latencies as well as slopes. Here, however, I focused on the onset time of lateralization and its difference between conditions.

Single-Trial Regression. To disentangle different factors and their specific influence on the temporal evolution of the timeseries data, I applied a single-trial regression approach (Fischer & Ullsperger, 2013; Fischer et al., 2016, 2018). This method is beneficial for a number of reasons. First, it allows to discriminate the influence of a variety of independent predictors, while simultaneously controlling for nuisance variables. Second, it is possible to observe their individual influence over the course of time and preserving the high temporal resolution of the EEG. This permits a fine-grained analysis of predictive strength at specific timepoints with respect to particular events. Third, this method enables us to capture changing variables within a given trial. In traditional trial averaging approaches it is not possible to take such dynamics into account. The present method, however, enabled me to discretely explore the changing influence of evidence strength over the course of a trial (in Exp.3). I epoched data locked to the moment of evidence change. The resulting design matrix did not include a row per trial as would be usually the case for general linear models (GLM) in fMRI or in the GLM for EEG analyses described by Fischer and Ullsperger (2013). Rather it involved several epochs per trial. The model included predictors related to the change in information that was presented along with trial-wise and block-wise regressors. Thus, I was able to detect dynamic changes within each trial while simultaneously taking other static variables into account. More details on these variables follow in the next sections, where I will derive my main research objectives and hypotheses from the literature described above.

4 Research Questions

Decision making is not only a highly complex process and possibly a "window on cognition" (Shadlen & Kiani, 2013), it is also a remarkably distributed task. It involves multiple cortical areas and occurs on different, partially overlapping, time scales. One of the central sub-processes is the accumulation of evidence, which is not yet understood in all its facets, but almost certainly plays a role from perceptual to sensori-motor areas. Another key factor in decision making is the time at which a decision must be completed. Urgency

appears to be an adaptive mechanism for regulating decision timing but its actual mode of action, particularly its effect on evidence accumulation, remains elusive. A possible region where urgency and accumulation of evidence could influence decision making is the motor cortex, maybe reflected in beta oscillations and their lateralization. These signals appear to be promising candidates for determining the current decision state in human motor cortex. By using novel trial-by-trial analysis techniques I am able to not only disentangle the timing and differential influence of multiple predictors, but also to account for dynamic and constant factors within each trial.

The goal of this work is to increase our understanding of evidence accumulation and urgency during perceptual decision-making and mutual interplay between both. For gaining more insight into the decision process I will investigate the role of lateralized beta power recorded over motor cortex. Specifically, the following questions are still open in the literature and will be addressed by the studies within this thesis:

1. What is the role of BPL during the decision process - more than mere action preparation?

2. Does BPL reflect online integration of accumulated evidence as the basis for motor output selection?

3. What role does urgency play in decision making? Specifically, does urgency have an effect on evidence accumulation?

4. Is there an effect of urgency on evidence accumulation in beta power over sensori-motor areas?

5 Hypotheses

With these questions in mind, I will now turn to what I expect to find based on the literature to date. There is already first evidence that BPL is not merely related to action preparation. Initially, this was discussed in a study that described the strength of such hemispheric asymmetry to be related to the integration of evidence over time (Donner et al., 2009). Others reported that BPL was modulated by stimulus properties, i.e. congruency (Fischer et al., 2018). More so, the beta rebound after response was found to bias the upcoming choice (Pape & Siegel, 2016). Thus, BPL parameters have been linked to different decision related variables. Further, it was shown that BPL

peak latency is tightly coupled to RT (Fischer et al., 2018) and peak amplitude does not vary with evidence strength (Twomey et al., 2016) rendering it a candidate for encoding a decision threshold. Contradictory evidence, however, was published regarding the slope parameter, with one study showing a scaling of slope by strength of the stimulus (De Lange et al., 2013), while another could not show this effect (Twomey et al., 2016).

Thus, there are converging, and contradicting, findings as to whether BPL does not merely reflect action preparation but extends to decision related processing. In the present work, I will test this hypothesis by comparing onset latencies of BPL under different delay conditions and make comparisons to another motor cortical signal. I expect that a decision-related signal would not delay its onset in delayed response conditions. Rather, if decision information flows continuously into motor cortex (e.g. Coles et al., 1985; Selen et al., 2012) and BPL could serve for "read-out" (Fischer et al., 2018), one would assume this signal to emerge some time shortly after stimulus onset regardless of an instructed response delay. Even though there are contradicting findings concerning the scaling of evidence strength on the slope of BPL (Twomey et al., 2016; De Lange et al., 2013), activity in monkey motor preparation cells was consistently observed to vary with evidence strength (Gold & Shadlen, 2007; Kiani & Shadlen, 2009; Shadlen & Newsome, 2001). Thus, for a signal encoding decision information, I expect its slope to scale with stimulus strength. This would indicate a faster development of the decision variable (i.e. evidence accumulation) when strong evidence is presented.

In the second part, I will examine the influence of urgency on decision making and its potential reflection in BPL. If urgency reduced the response threshold, corresponding to collapsing bounds (Drugowitsch et al., 2012), the peak amplitude would be expected to be attenuated in high urgency trials and less evidence would suffice to commit to a choice. This, in turn, would support the notion that BPL reflects a decision variable in motor cortex supporting the evidence accumulation account. Moreover, such a finding could increase our understanding about the location of SAT modulations within the cortex. Moreover, if changes in the slope in BPL associated with urgency manipulations were found, this study could support the idea that the pace of evidence accumulation increases with time pressure. This finding would give support to the urgency account of decision making, which predicts an urgency signal to

affect the momentary weighting of evidence (Cisek et al., 2009). This, in turn, would lead to a steeper increase when speed pressure is high.

In sum, I aim to explore the functional role of BPL and expect it to be involved in decision processing by transferring decision evidence as well as encoding urgency. The following studies will shed light onto several open questions related to decision computation and the meaning of BPL within this context.

The following chapter is based on an article published in NeuroImage:

Rogge J, Jocham G & Ullsperger M (2022). Motor Cortical Signals Reflecting Decision Making and Action Preparation. *Neuroimage, 263*, 1-15.
doi: 10.1016/j.neuroimage.2022.119667.

6 Motor cortical signals reflecting decision making and action preparation

To act adaptively within our environment, our decisions need to be translated into motor behavior. Neural oscillations in the beta frequency range (13 - 30 Hz) have been associated with an inhibited state of the motor cortex during rest (Engel & Fries, 2010; Pfurtscheller et al., 1996). In agreement with this, pre-movement reductions in beta power in pre- and primary motor areas have been observed consistently. This presumably facilitates, or enables, motor responding.

For unimanual actions this reduction is greater in the hemisphere contra- versus ipsilateral to the effector side (Jasper & Penfield, 1949; Pfurtscheller, 1981) and, thus, appears to reflect motor selection processes (Doyle et al., 2005; Kaiser et al., 2001). This lateralization of beta power builds up until the action is executed (Kaiser et al., 2001). A similar attenuation of power has been described in the alpha frequency range (Jasper & Penfield, 1949; Pfurtscheller, 1981; Pfurtscheller & Berghold, 1989).

In addition to motor preparation, alpha and beta power in motor cortical areas also appear to reflect the emergence of a categorical choice. During perceptual decision-making, lateralization of alpha and beta power indicates the upcoming decision several seconds before the overt movement, when choices were mapped to left- or right-hand button presses (Donner et al., 2009). Moreover, beta power lateralization (BPL) was associated with decision-related variables such as stimulus strength (O'Connell et al., 2012), choice alternation (Pape & Siegel, 2016), and accuracy (Fischer et al., 2018). Similarly to BPL, alpha power lateralization (APL) has, in addition to action preparation, been related to the formation (Donner et al., 2009) and urgency (Murphy et al., 2016) of a decision.

On top of these changes in oscillatory activity, a slow event-related potential of

very low frequency, the lateralized readiness potential (LRP) has been shown to immediately precede unilateral movements. It is generally conceived as a slow action preparation mechanism (Gratton et al., 1988; Haggard & Eimer, 1999; Kutas & Donchin, 1974), but others also demonstrated an influence of evidence strength on the LRP (Kelly & O'Connell, 2013).

The question arises whether the functional roles of these lateralization signals during decision and response processing can be distinguished. Here, we aim at investigating to what extent these signals are related to decision making and motor preparation, respectively. On the one end of the dimension between decision- and motor-related would be a signal emerging as soon as sensory evidence is presented (with some lag for mere sensory processes), whereas on the other end there would be a signal that emerges just prior to the response. On the basis of previous findings, we hypothesized that APL and BPL incorporate the accumulation of sensory evidence up to a threshold, at which a categorical commitment to one choice alternative is made. These signals are expected to appear earlier in the processing phase. In contrast, we hypothesized that the LRP is less determined by the accumulation of evidence and instead more closely related to preparing the motor command, thus appearing locked to the response.

In two studies, we imposed a delay between presentation of the stimulus and an imperative cue that prompted participants to respond. This allowed us to separate the decision from motor processing temporally. Furthermore, a signal reflecting the accumulation of sensory evidence would be expected to show a ramping that is steeper when the quality of sensory evidence is high (Donner et al., 2009; Gold & Shadlen, 2007; Kiani & Shadlen, 2009; O'Connell et al., 2012; Ratcliff, 1978; Selen et al., 2012; Shadlen & Newsome, 2001; Werkle-Bergner et al., 2014). Thus, we expected APL and BPL, but not the LRP, to display a ramping that scales with evidence strength. We therefore examined at which time during the decision process the two types of signals (APL/BPL vs. LRP) become evident, to what extent they persist during the delay period, and how their onset and slope are modulated by the strength of sensory evidence.

In brief, we find that, when a delay is imposed between stimulus display and an imperative cue, both APL and BPL emerge soon after stimulus onset. In contrast, the LRP only emerges later, after participants are prompted to respond.

6.1 Material and Methods

6.1.1 Ethical approval

The studies conformed to the standards set by the Declaration of Helsinki and was approved by the Ethics Committee of the University of Magdeburg (Registration Number: 40/18). We obtained written informed consent from all participants.

6.1.2 Participants

Experiment 1. We recorded EEG in 34 human volunteers. The data of four were excluded due to technical problems during the EEG recordings. The remaining 30 participants (12 females) were between 20 and 30 (mean ± SEM, 24.4 ± 0.5) years of age. Twenty-seven participants were right-handed (Edinburgh Handedness Score: 81.81 ± 4.6; left-handed participants scored on average -52.62 ± 6.0 on the handedness measurement).

Experiment 2. We recorded EEG in 32 healthy human volunteers, two of them were excluded due to technical problems during the EEG recordings. The remaining 30 participants (14 females) were between 20 and 35 (mean ± SEM: 26.93 ± 0.76) years of age. One volunteer reported a diagnosis of Asperger's Syndrome and depression and another one indicated anxiety and depression disorder, 16 and 3 years before the study was conducted, respectively. All of the participants were right-handed (Edinburgh Handedness Score: 79.68 ± 4.11).

Both Experiments. The following criteria were met in both experiments. All participants had completed high school and attended or finished university education. They were native speakers or fluent in German or English. Instructions were given to them in the dominant language. The majority of participants had no neurological or psychiatric illness and was not taking psychoactive drugs (exceptions above). All of them had normal or corrected-to-normal vision. All of them were naïve to the respective task, reported to feel concentrated/comfortably awake and had slept sufficiently (five to nine hours) the night before. The participants received monetary or credit point compensation for study participation.

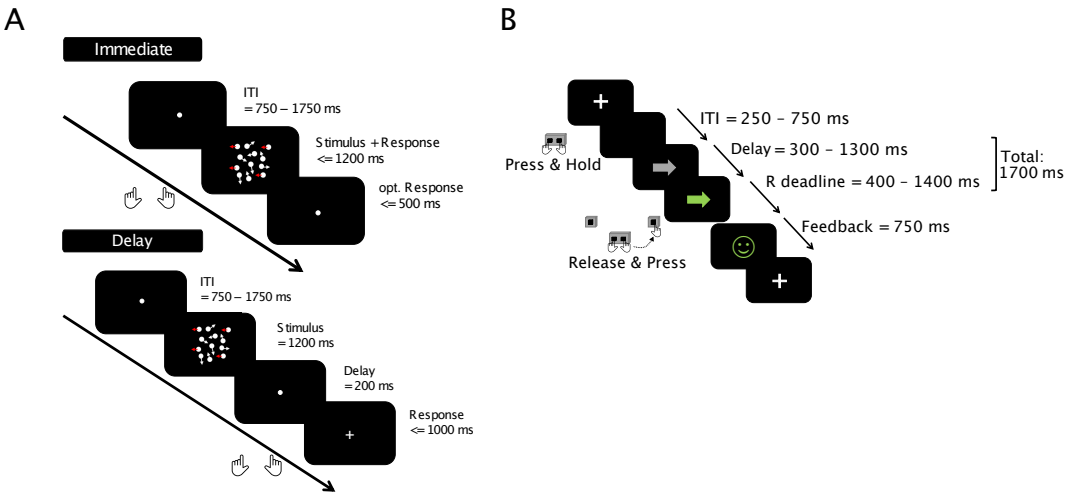

Figure 2-1. Random Dot Motion Task (A) and Delayed Response Task (B). A: Participants performed two versions of the random dot motion task. In 'Immediate', they were free to respond whenever they wanted (within a window of 1700 ms). In 'Delay', participants were only allowed to respond after an imperative cue which appeared 1400 ms after stimulus onset. Motion coherence levels varied randomly between 1.6 and 51.2% of dots moving either left or right. B: In the delayed response task, at trial start, participants were required to depress two keys with their left and right index fingers, respectively. A target (grey arrow) indicated the response (release key and press a button at the indicated side) that had to be excecuted after an imperative cue (arrow turning green). The response window varied randomly from trial to trial, depending on the length of the delay. Feedback was given after the response.

6.1.3 Random Dot Motion Task

The random-dot motion discrimination (RDM) paradigm was adjusted to involve a delay manipulation. Participants were asked to detect the direction of coherent motion within a noisy display of moving dots as fast and as accurately as possible (Figure 2-1A). Responses were given with the left or right thumb on a customized response box.

Stimuli. We presented the task to the participants with the Psychophysics Toolbox 3 (Brainard, 1997; Kleiner et al., 2007; Pelli, 1997) in MATLAB 2012a (MATLAB, 2012). Participants' seating position was fixed at a distance of 100 cm away from a 22-inch LCD monitor with a refresh rate of 60 Hz. The parameters of the stimulus display were adjusted based on (Pilly & Seitz, 2009). The dots were presented in light gray (RGB: 224, 224, 224), in front of a black (RGB: 0,0,0) background. They were bounded within a circular aperture with a diameter of nine degrees of visual angle, which was placed at the center of

the screen. The dot diameter was three pixels and 254 dots were on screen per frame. We used a Brownian Motion dot kinematogram. Signal and noise dots were randomly selected at every frame. All dots moved with the same speed (6.47 visual degrees per second; 4.65 pixels per frame), but motion direction was random for noise dots. Only a proportion of the dots (signal dots) moved coherently in one of the two pre-defined directions: -90 deg (leftward) and +90 deg (rightward). The proportion of signal dots varied pseudo-randomly from trial to trial between six different coherence conditions (0.016, 0.032, 0.064, 0.128, 0.256, or 0.512), subject to the constraint that the coherence level was not allowed to repeat between consecutive trials, if the motion was into the same direction. A fixation dot (diameter = six pixels) was placed at the central point of the screen and aperture. It was present throughout the trial to keep the gaze fixed at the center and avoid eye movements elicited by the moving stimuli.

Task Design and Experimental Procedure. The experiment consisted of two sessions on separate days with a break of one day in between. In one session (Immediate), participants were asked to respond fast and accurately while the stimulus was presented. In the other session (Delay) participants were required to withhold their response until a response cue appeared (fixation cross at the center of the screen) and then had to respond as fast as possible.The order of the sessions was counterbalanced and pseudo-randomized between participants (Immediate first, N = 16). The immediate task took 41.55 ± 0.88 minutes and the delay task took 58.13 ± 0.56 minutes on average. Thirteen volunteers participated before noon, and seventeen after noon.

6.1.4 Delayed Response Task

Task. In the delayed response task (DRT) participants were asked to make responses by the release of a key and a subsequent press of a laterally placed distant key with the index finger (Figure 2-1B). Each trial went off as follows, participants initiated the trial by pressing both central buttons of the response set-up. A target arrow appeared in gray at the center of the screen with some jitter (ITI: 250 - 750 ms) and provided information about which finger to use. The target was either pointing towards left, right, or both sides. In the case of a double-sided arrow, participants were allowed to choose the response side themselves. After a variable delay time (300 - 1300 ms) the

arrow turned green, the imperetaive cue, upon which the response had to be executed (Figure 2-1B). Participants were asked to respond as fast as possible on the side indicated by the target. Responses had to be made within a limited time window, the duration of which was dependent on the delay time. The total duration (target arrow + response time window) always added up to 1700 ms. The actual response deadline was only implicitly given because the arrow stimulus could remain on screen for another 200 ms. After the response or after the deadline they received feedback after a 200 ms interval. Participants learned about their performance by a green smiley, red frowney, or verbal information ('too fast', 'too slow', 'wrong button') for correct, wrong or false alarms, or misses, respectively. A fixation cross appeared at the center of the screen and participants could self-initiate the next trial by pressing and holding both central keys. We presented the task to the participants with the same equipment used for *Experiment 1*.

Task Design and Experimental Procedure. The delay time, and thus also the available response time, were pseudo-randomized with an equal number of trials from 10 delay bins, each spanning 100 ms intervals. Delay times from one bin did not directly repeat one another and an equal number of left, right and double-sided stimuli was presented for each delay bin. In total, 540 trials were presented to each participant, 90 of which were NO-GO trials (no response cue appeared). These trials will not be considered in the following analyses. If participants had more than 10% of unusable trials (misses or false alarms), they had to repeat these at the end of the experiment until we recorded at least 486 trials. The task was divided into two parts, separated by a self-paced break. Additionally, after every block of 22 trials, feedback was provided that informed participants about their previous performance score (percentage correct within the previous block). The experiment started with a training block of 30 trials to familiarize participants with the stimuli and response movement. They were required to respond correctly in at least 80% of the trials to start the actual experiment. The task lasted on average 44.36 $\pm$ 0.61 minutes and was performed in the morning (N = 21) or in the afternoon (N = 9).

6.1.5 EEG Data Acquisition and Preprocessing

We used a customized 61-electrode EEG layout produced by EasyCap (EasyCap GmbH, Herrsching-Breitbrunn, Germany), with sensors (Ag/AgCl) placed in rings equidistantly circling Cz to record electrical brain potentials. Additionally, there were two ocular electrodes placed centrally below each eye and two electrodes measuring electrocardiography. The online reference was at position CPz, the ground was placed between AF4 and Fz. We applied standard electrode gel to reduce impedance rates to below 10 kΩ. We recorded at a sampling rate of 500 Hz using two BrainAmp Amplifiers and the BrainVision Recorder 1.20 (Brain Products GmbH, Gilching, Germany).

EEG data were preprocessed offline using customized MATLAB (MATLAB, 2018) scripts and the EEGLAB toolbox (Delorme & Makeig, 2004). We first applied a high-pass (0.1 Hz) and subsequently a low-pass filter (40 Hz). Afterwards, we epoched data from -2000 ms to 4000 ms (-2000 ms to 5000 ms in Exp. 2) relative to stimulus onset. A customized adaptive artifact removal procedure was used to identify outlier epochs. A maximum of five percent and minimum of ten trials were removed by the algorithm if they exceeded a number of standard deviations (EEGLAB function *pop_jointprop()*).The number of standard deviations (initial SD = 5) was iteratively adjusted (stepsize of 0.1) until the minimum and maximum criteria were met. We used these criteria to ensure that the algorithm (Fischer et al., 2018) finds a reasonable (not too conservative, not too liberal) SD value for the artefact rejection. Through the adaptive artifact rejection algorithm, we identified on average 12.90 ± 0.42 (Exp. 2) artefactual trials before ICA.

Next, we re-referenced the data to common average. For adaptive mixture independent component analysis (AMICA 1.5, Palmer et al., 2012), we prepared the data with a high-pass filter at 1 Hz and performed dimensionality reduction to 40 components by principal component analysis. In Exp. 2, we limited iterations to 500 in order to avoid overfitting. Manual selection yielded between one and four (between one and seven in Exp. 2) artefactual components (eye blinks, horizontal eye movements and heart beat components) for each dataset. The resulting ICA-weights were applied to the original data (0.1 - 40 Hz).

After component rejection, and subtraction of average baseline activity (350 to

100 ms prior stimulus onset) from the time series per epoch, we ran a second adaptive artifact rejection routine to clean the signal from remaining noise epochs separately for left- and right-hand responses. There was no minimum amount of trials to reject, but a maximum of five percent of trials within each category. We started with a cut-off of 4.5 standard deviations. On average we rejected 39.83 ± 0.56 epochs at an SD of 6.02 ± 0.06 (Exp. 2: 21.27 ± 0.63 trials at 5.80 ± 0.12 SD). Finally, the reference channel was added to the data.

6.1.6 Data Analyses

All data were analyzed using customized MATLAB scripts. We considered significance levels of $p < .05$ for all analyses unless stated otherwise.

Psychophysical Analysis. In *Experiment 1*, reaction times (RT) and accuracy were analyzed separately for the two conditions (Immediate and Delay). To account for the general skewness of reaction times we log-transformed the raw RT for all analyses. For both, RT and accuracies, the main interest was in the difference between coherence levels. For an analysis of the psychophysical relationship between coherence level and accuracy, we used signed coherence values: coherence levels for leftward dot motion trials were multiplied by -1. Thereby, we obtained an index of evidence for rightward motion, with negative values indicating counter-evidence. Accuracy was then operationalized by the proportion of right-hand responses *(pR)* per signed coherence level. This means for coherence levels < 0 (leftward motion), lower values of pR correspond to higher accuracies (and vice versa for coherence levels > 0 [rightward motion]).

In order to compare differences in accuracy as a function of sensory evidence strength between Immediate and Delay, we fitted a logistic sigmoid to participants' choice data. For each trial, the probability pR to select the right option is given by:

$$pR = \frac{1}{1 + e^{\frac{COH - b}{\tau}}}, \tag{1}$$

Where COH is the signed coherence (see above), the slope parameter τ defines participants' sensitivity to the sensory evidence (motion strength) and the bias term b accounts for unspecific biases towards the left or right hand, independent of sensory evidence.

In *Experiment 2*, we defined response time (RT) as the time from stimulus onset to release of the central key, and movement time (MT) as the time elapsed from releasing the central key to pressing the lateral target key. Both, RT and MT were log-transformed in order to account for their skewed distributions. Data were split into four evenly spaced bins along the range of delay times. On average the bins contained 66.70 ± 1.00 short, 67.87 ± 0.90 medium-short, 64.57 ± 1.10 medium-long and 37.37 ± 2.49 long trials. Average delay times were 436 ± 1.31 ms, 685 ± 1.23 ms, 931 ± 1.58 ms, and 1150 ± 4.35 ms, respectively. In the following sections, we will refer to the them with *bin 1-4*. We used one-sided t-tests for our directional reaction time hypotheses.

Multiple Regression on RT and Choice. For data of *Experiment 1*, we ran linear regression models (Equation 2) separately for each session to determine the factors influencing RT. We restricted the analyses to correct trials and set up the following linear model:

$$Y = \beta_0 + \beta_1 * COH + \beta_2 * REP + \beta_3 * RT_{prev} + \beta_4 * COR_{prev} + \epsilon \qquad (2)$$

Where the dependent variable Y is the (log-transformed) RT, β_0 is a bias term, COH is the (log-transformed) coherence, REP indicates whether the response on the current trial is a repetition with respect to the previous trial, RT_{prev}= (log-transformed) RT in the previous trial, and COR_{prev} indicates whether the choice on the previous trial was correct.

To determine which factors guided selection of the left vs. right choice option, we used the following logistic regression model:

$$Y = \beta_0 + \beta_1 * COH + \beta_2 * CR_{rep} + \beta_3 * RT + \beta_4 * COR + \epsilon \qquad (3)$$

Where the dependent binary variable Y is the choice of the left or right option, β_0 is a bias term, COH is the signed log-transformed coherence, the binary regressor CR_{rep} indicates whether the participant chose the right option on the previous trial (positive weights for this regressor indicate a response repetition bias), RT is the (log-tranformed) RT on the current trial, and COR indicates whether the choice on the current trial is correct or not. We excluded

the first trial of each block and those with an invalid preceding trial (misses and premature responses). The resulting regression weights were tested for significance using one-sample t-tests against 0. P-values were corrected by family-wise error rate to reduce the risk of type-I error.

LRP Analyses. For LRP analyses, we epoched data locked to onset of stimulus, response and imperative cue (the latter for the delay session only). Epochs ranged from -200 ms prior to until 700 ms after the stimulus (Exp. 2: -200 to 700 ms), from -500 ms prior to 200 ms (Exp. 2: -700 to 150 ms) after the cue and from -200 ms prior to 200 ms (Exp. 2: -150 to 200 ms) after the response, respectively. The LRP was computed from the average of electrodes over right hand motor areas: C3, CP3 (rEL), and left hand motor electrodes: C4, CP4 (lEL). The hemispheric difference was calculated by subtracting the averaged ipsilateral from the contralateral activation:

$$LRP = \frac{lEL(rPress) - rEL(rPress) + rEL(lPress) - lEL(lPress)}{2}, \quad (4)$$

with $rPress$ referring to trial with right hand responses and $lPress$ referring to trials with left hand responses.

LRP timeseries were first computed including averages of all correct trials and then averaged over participants. For the analysis of differences related to coherence (Exp.1), we pooled coherence levels into three conditions, low (0.016 and 0.032), medium (0.064 and 0.128) and high (0.256 and 0.512). For Exp. 2, we computed LRP timeseries also for each delay bin (see *Psychophysical Analysis*). The pooling was done to increase signal-to-noise ratios.

In order to validate the presence of LRP, we performed significance testing in the stimulus-locked time window -100 to +600 ms and the response-locked time window -500 to +100 ms. We averaged the amplitudes of time bins (100 ms) within each subject and tested against zero with one-sample t-tests. The resulting p-values were corrected using the false discovery rate (fdr) procedure with adapted q-values (depending on the number conditions and locks [stimulus-locked and response-locked]):

$$q_{fdr} = \frac{0.05}{N_{cond} * 2}. \quad (5)$$

We additionally performed Bayesian statistics (*bayesFactor Toolbox* for MATLAB) for each of the tests and report the resulting bf10 values to inform about the likelihood of our findings. Values between 0.33 and 3 are considered weak or no evidence. We report moderate (>3), strong (>10), very strong (>30) and extreme (> 100) evidence for the effect. We also report moderate (<1/3) and strong (<1/10) evidence for the null hypothesis.

Time-Frequency Analyses. In *Experiment 1*, we epoched the timeseries from -500 ms prior to 2500 ms after stimulus onset, -2000 ms prior to 500 ms after the response time as well as from -2250 prior to 750 ms after cue onset (for Delay). In *Experiment 2*, epochs were -200 to 700 ms (stimulus-locked), -150 to 200 ms (response-locked), and -700 to 150 ms (cue-locked). The following procedure was applied in both experiments. Only correct trials were included. The time-domain EEG data of all electrodes were transformed by Morlet wavelet convolution to receive time-frequency data. Individual trials were decomposed into a power spectrum with 27 linearly spaced frequencies between 5 and 30 Hz (1 Hz increase per step) with wavelets of six cycles. The resulting time-frequency power was log-transformed but remained baseline-free. The difference timelines (APL/BPL) did not require a baseline correction, as baseline difference was expected (and confirmed by our data) to fluctuate around zero. For specific analyses of APL and BPL over motor cortex, we averaged motor electrode pairs per hemisphere (C3 + CP3 [lEL]; C4 + CP4 [rEL]) and computed the trial-wise lateralization. Frequency-band-specific power lateralization was calculated by averaging over frequencies: $13 - 30$ Hz for BPL and $8 - 12$ Hz for APL, then taking trial averages and finally averaging over participants. For single-trial regression analyses (see below), we preserved APL and BPL per trial and participant.

Onset latencies. We quantified onset latencies of LRP, BPL and APL with a jackknife approach (Miller et al., 1998) in order to find a valid timepoint in signals with low signal-to-noise ratios. We constructed sub-samples by a leave-one-out approach (for more details see Miller et al., 1998). For BPL and APL, we identified the peak amplitude of each sub-sample after stimulus onset and the time-point at which 50% of this amplitude was exceeded. We used an 80% cut-off for coherence condition analyses because signal-to-noise ratios were low and we wanted to avoid noise-related local minima before the actual onset of lateralization. For LRP, we defined the peak amplitude before the response

and identified the timepoint at which 90% of this amplitude was reached, as recommended by Miller et al. (1998). The resulting onset timepoints were then compared between sessions (Immediate vs. Delay) and coherence levels. Importantly, significance testing after jackknifing requires conservative correction of F- and t-statistics. For coherence (*Experiment 1*) and delay bin (*Experiment 2*) comparisons, we followed the guidelines introduced by (Ulrich & Miller, 2001) for factorial designs, dividing the F-statistic by $(n-1)^2$ and correspondingly adjusting the p-values. This procedure, however, does not yield any interpretable variance measures. Thus, we will neither report nor display variance values.

Single-trial regression. To investigate the contribution of other factors, above and beyond motor responses, to APL/BPL, we used robust linear regression (MATLAB function: 'robustfit.m') and set up two general linear models (GLM).

To identify the spatial distribution of lateralization, we ran regressions, separately on the time courses of beta and alpha power of all available electrodes. The GLM for *Experiment 1* included the predictor response side ($HAND$; left = -1, right = +1), while accounting for coherence (COH), log-transformed RT (RT), and repetition of the response side (REP):

$$Y = \beta_0 + \beta_1 * HAND + \beta_2 * COH + \beta_3 * RT + \beta_4 * REP + \epsilon, \qquad (6)$$

where Y is the beta or alpha power, respectively, at each electrode and timepoint.

The GLM for *Experiment 2* included delay duration (DEL), log-transformed RT (RT), log-transformed MT (MT) and response hand ($HAND$ [left = -1; right = +1]):

$$Y = \beta_0 + \beta_1 * DEL + \beta_2 * RT + \beta_3 * MT + \beta_4 * HAND + \epsilon, \qquad (7)$$

where Y is alpha and beta power of all electrodes and timepoints. The models (Equations 6 & 7) allowed us to quantify timepoints of significant lateralization by using the regressor $HAND$ and its effect on the single channels, orthogonal to other task-related variables. Importantly, left hemisphere (contralateral) lateralization was expected to be stronger (more negative) in right-

handed responses (+1) than left-handed responses (-1), thus leading to negative regression-weights, and vice versa for right hemisphere electrodes. Next, we investigated at which timepoints the lateralization of beta and alpha power over motor cortex was predicted by regressors of interest. The GLM for *Experiment 1* included coherence level (COH), log-transformed RT (RT) and response repetition (REP):

$$Y = \beta_0 + \beta_1 * COH + \beta_2 * RT + \beta_3 * REP + \epsilon, \tag{8}$$

where Y is beta or alpha power lateralization at each timepoint. For *Experiment 2*, we used the same model as above (Equation 7), where Y the BPL and APL at each timepoint. All GLMs were prepared as described above (*Time-Frequency Analyses*). The regression time windows in *Experiment 1* were -400 to 1500 ms (Exp. 2: -50 to 1500 ms), -1500 to 900 ms (Exp. 2: -500 to 500 ms) and -1200 to 750 ms (Exp. 2: -1500 to 50 ms), for stimulus-locked, cue-locked and response-locked, respectively. We used a robust regression fit to reduce outlier impact. The models were fit at every time point (step size = 2 ms) smoothed over 4 time points before and after. The resulting time series of regression weights were down-sampled by a factor of 5. This resulted in a 100 Hz time series of regression weights per participant for each electrode, regressor, frequency band and condition (Exp. 1: Immediate and Delay). These timeseries were averaged over participants and tested for significance at each time point with a one-sample t-test against 0. Significance levels were adjusted by false discovery rate to control for multiple comparisons.

Additionally, we performed cluster-based permutation analyses to ensure that we only interpret relevant time windows. Firstly, all single timepoints (without significant neighbor) were disregarded. Secondly, we ran 1000 permutations for each timeseries where we randomly shuffled the signs of the values to create an empirical H0 distribution and critical t-values. Clusters with a t-mass larger than that of the null-distribution were considered significant.

6.2 Results

6.2.1 Coherence and delay affect accuracy and reaction time

In *Experiment 1*, overall, reactions were faster in Delay (mean ± SEM, 254.5 ms ± 10.0 ms) than in Immediate trials (812.5 ms ± 40.7 ms; $t(29) = 13.1363$,

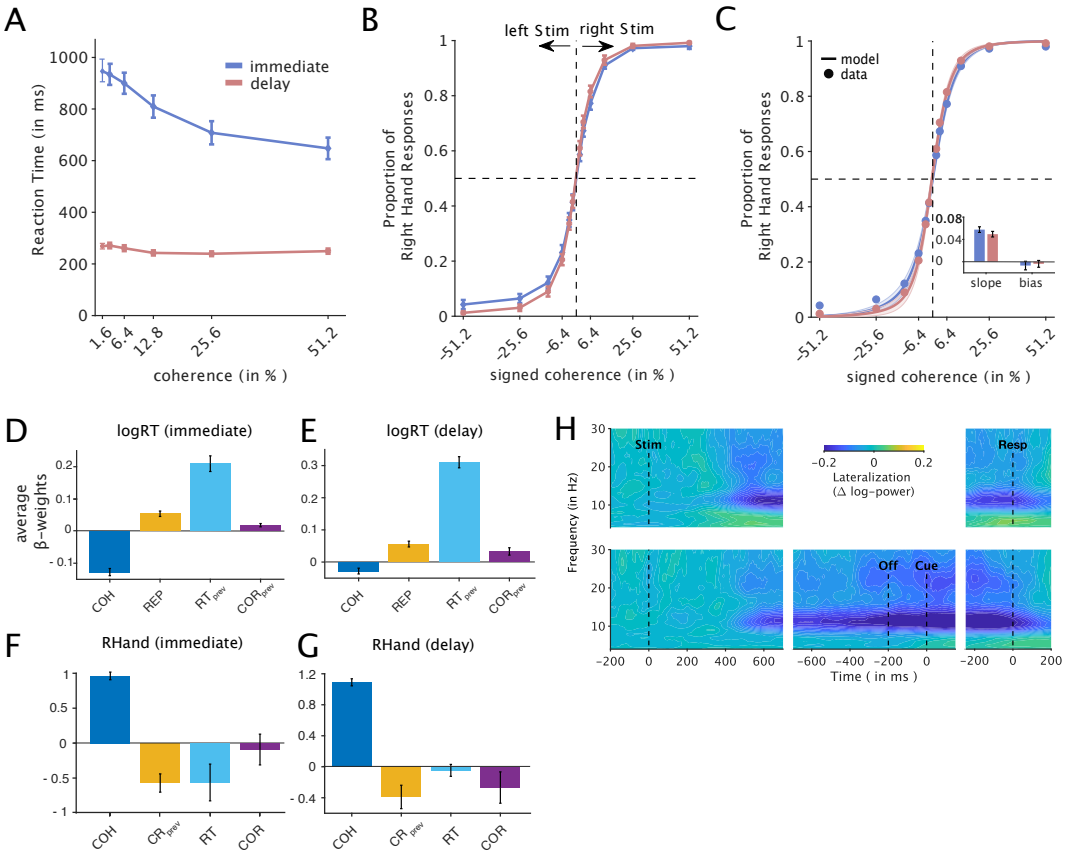

Figure 2-2. Behavior in the random dot motion task. A: Response times decreased with stronger evidence in Immediate (blue) and to a lesser extent in Delay (red). B: Psychometric functions plotting the probability of choosing right as a function of the evidence in favor of the right choice. C: Choice data (from B) and fit of logistic sigmoid. Inset shows the fitted slope and bias term. D, E: Averaged regression weights of the linear multiple regression analysis for log-transformed RT with predictors log-transformed coherence (COH) and bias regressors response repetition (REP), log RT (RT_{prev}) and accuracy (COR_{prev}) in the previous trial in the Immediate (D) and the Delay (E) session. F, G: Averaged regression weights of the logistic regression for response side (L= -1, R= 1) with predictors signed log-transformed coherence (COH), response repetition (CR_{rep}), log RT (RT), and accuracy (COR) in 'Immediate' (F) and 'Delay' (G). H: Time-frequency spectra at electrodes over motor regions (see text for details), difference contra- minus ipsilateral to response side. Upper row = Immediate, lower row = Delay. Left panels show stimulus-locked, right panels show response-locked data, middle panel (delay condition only) shows data locked to response cue. Error bars represent SEM.

$p < .001$, one-sided paired t-test). We expected evidence strength to increase accuracy in both the immediate and delayed task, while reduced RTs were only expected in immediate trials. First, we examined the effect of coherence on RT in correct trials. In both task variants (Figure 2-2A), participants responded faster at high compared to low coherence levels (Immediate: $F(5,145) = 102.85$

$p_{corr} < .001$; Delay: $F(5,145) = 17.712$, $p_{corr} < .001$, rmANOVA). While this was hypothesized for immediate responses, we had not expected such an effect for Delay. Post-hoc tests revealed that, in the delay variant, the significant differences in RT occurred mainly between low and medium to high coherence levels (coherence levels from low [1] to high [6]: 1−4, 1−5, 2−3, 2−4, 2−5, 3−4, 3−5, $p_{corr} < .05$, paired t-test with Scheffé correction). In contrast, in the immediate variant, RT differences were present between all coherence levels ($p_{corr} < .01$), except level 1 and level 2 ($p_{corr} = .04578$). In the immediate variant, RTs were determined by decision time varying with evidence strength and non-decision time, i.e., early stimulus processing, motor preparation and execution. In contrast, in the delay variant decision making was nearly completed before the response cue such that RTs were mainly influenced by stimulus processing of the response cue, movement preparation and execution.

Next, we assessed the effects of coherence on decision accuracy (Figure 2-2B). As expected, the proportion of right responses increased with higher sensory evidence (coherence) in favor of the right option (Differences in accuracy between signed coherence levels: Immediate: $F(11,319) = 459.08$, $p_{corr} < .001$; Delay: $F(11,319) = 606.11$, $p_{corr} < .001$, rmANOVA). Unexpectedly, overall accuracy was slightly higher in Delay compared to Immediate (0.8287 ± 0.0086 vs. 0.8068 ± 0.0094, $t(29) = -2.8420$, $p < .01$, paired t-test). This effect could be driven by the higher likelihood of premature responses in the immediate condition. In the delay version participants were inherently forced to wait with their responses and, thus, were less likely to respond before having finished evidence accumulation. However, this comparison did not take into account the effect of task variant (Immediate vs. Delay) on the psychophysical relationship between coherence level and accuracy. When we fitted a sigmoid function to the choice data, we found that neither the unspecific bias nor the slope parameter tau differed significantly between task variants (b: -0.0069 ± 0.0422 vs. -0.0038 ± 0.0336, $t(29) = -0.6399$, $p = 0.5272$; τ: 0.0576 ± 0.0050 vs. 0.0495 ± 0.005, $t(29) = 1.5882$, $p = 0.1231$, paired t-test, Figure 2-2C, inset) differed significantly between task variants. Thus, the degree to which increasing sensory evidence improved accuracy was not changed by implementing a delay period in this task.

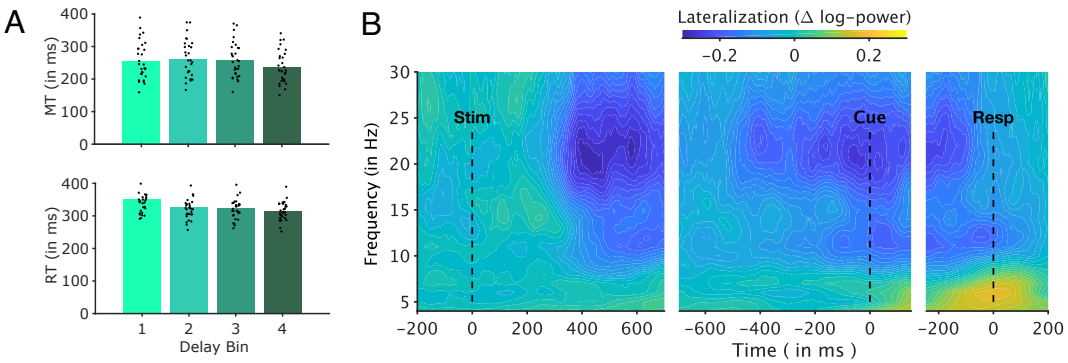

Figure 2-3. Behavior and Lateralization spectra in the delayed response task. A: Movement (top) and Reaction (bottom) times by delay duration: Delay durations were pooled into short [1], medium-short [2], medium-long [3], and long [4] bins. Reaction and movement times decreased with longer delay times (= less time available for response). B: The spectral pattern of lateralized power (contra- minus ipsilateral to response side) at electrodes over motor regions (see text for details), for all trials. The left panel shows stimulus-locked data, the middle panel shows data locked to the imperative cue, and the right panel shows response-locked data.

6.2.2 Response deadline effect on reaction and movement time

In the delayed response task (*Experiment 2*), we expected a decrease in both reaction and movement times with increasing delay. The delay manipulation did not only prolong waiting time, but also reduced the available time to execute the response. As expected, mean RT (± SEM) differed between delay bins (Figure 2-3 A [bottom], bin 1 to 4: 350.22 ± 10.25 ms, 326.52 ± 7.30 ms, 322.97 ± 6.32 ms, 314.29 ± 5.17 ms; $F(3,87) = 17.466$, $p_{corr} < .001$, rmANOVA). Post-hoc t-tests revealed that this effect was mainly driven by a difference between the first bin and all other bins (1−2; 1−3; 1−4: $p_{corr} < .01$, paired t-test with Scheffé correction). Moreover, we observed reduced movement times for the longest delay times (Figure 2-3A [top], bin 1 to 4: 255.74 ± 10.58 ms, 260.08 ± 10.40 ms, 258.75 ± 9.81 ms, 235.92 ± 9.04 ms; $F(3,87) = 38.595$, $p_{corr} < .001$, rmANOVA; paired t-test [Scheffé]: 4−1, 4−2, 4−3: $p_{corr} < .001$). Hence, particularly after a long waiting period, movements appear speeded. This is in line with our hypothesis that the vigor of movements (here the movement time) increases with higher urgency or time pressure. Overall, these findings complement our results of the RDM paradigm (*Experiment 1*). We demonstrate that delaying a response reduces RT and increases urgency, and thus, such delay tasks decouple stimulus processing time from action preparation and execution time.

6.2.3 Other factors guiding performance

To investigate the orthogonal contribution of other factors (in addition to motion coherence) in greater detail, we applied multiple linear/logistic regression to the RT and choice data (*Experiment 1*) of immediate and delay trials (Figure 2-2 D-G). As expected from the analyses above (Figure 2-2 A, B), coherence significantly affected RT and choice in both the Immediate ($p_{corr} <$ .001 for both RT and choice; one-sample t-test, Table 1) and the Delay (RT: $p_{corr} = .0083$; choice: $p_{corr} < .001$) version of the task. These results confirm the above-mentioned effect of sensory evidence strength on decision-making performance even under conditions with a response delay. Further, the analyses revealed an alternation bias, meaning that participants had a tendency to switch response side from trial to trial (e.g. left followed right response), independent of the stimulus direction (Immediate: $p_{corr} < .001$; Delay: $p_{corr} =$ .046) and consecutive choices made with the same hand were significantly slower even in the delay variant (both task variants: $p_{corr} < .001$). Furthermore, the regression revealed that participants' RTs were slowed down on trials following a correct compared to an incorrect response on the previous trial in both task variants (Immediate: $p_{corr} = .0012$; Delay: $p_{corr} = .008$), independent of sensory evidence. This effect can be due to our task environment, involving long response-stimulus intervals, no feedback and frequent errors. These factors were shown to reduce, remove or invert the commonly observed post-error slowing effect (for a review, see Danielmeier & Ullsperger, 2011). Finally, there was an autocorrelation in RTs, as evident from a positive effect of the previous trial's RT (both task variants: $p_{corr} < .001$). This means, that participants had the tendency to stay in one 'speed-mode' for consecutive trials even in trials with a response delay. Importantly, choice direction was not biased by the current accuracy or reaction time (all $p_{corr} > .05$).

6.2.4 Lateralization dynamics throughout fixed and flexible delay periods

To understand where on the spectrum from decision-related to motor activity BPL, APL, and LRP lie, we first explored the dynamics of these signals within the delay period and compared onset times between the immediate and delayed tasks.

In both experiments, the difference (contra- minus ipsilateral) time-frequency

Table 1
Average regression weights for multiple linear regression on RT and Choice

Predictor	Condition	*RT-Model*	*Choice-Model*
COH			
	Immediate	-0.128 ± 0.011***	0.967 ± 0.055***
	Delay	-0.028 ± 0.009**	1.090 ± 0.045***
RT_{prev} / RT			
	Immediate	0.210 ± 0.024***	-0.566 ± 0.264
	Delay	0.310 ± 0.017***	-0.046 ± 0.077
REP / CR_{rep}			
	Immediate	0.054 ± 0.008***	-0.574 ± 0.131***
	Delay	0.056 ± 0.009***	-0.390 ± 0.151*
COR_{prev} /COR			
	Immediate	0.018 ± 0.005**	-0.092 ± 0.221
	Delay	0.033 ± 0.012**	-0.268 ± 0.202

Note. Mean regression weights ± SEM.
* p < .05, ** p < .01, *** p < .001; one-sample t-test

plots (Figure 2-2G & Figure 2-3B) show that lateralization occurred over a broad range of frequencies (alpha and beta band) following stimulus onset. Importantly, this lateralization emerged as early in the delay task as in the immediate task (*Experiment 1*) and was maintained throughout the trial up to the motor response. This finding was supported in *Experiment 2*, where lateralization in alpha and beta range becomes evident before the response cue.

To be able to compare the temporal dynamics of APL and BPL to the LRP (Figures 2-4 and 2-5 A-C), we averaged across frequencies for alpha (8 - 12 Hz) and beta band (13 - 30 Hz). Firstly, we found that BPL in *Experiment 1* emerged already about 400 ms after stimulus onset, before presentation

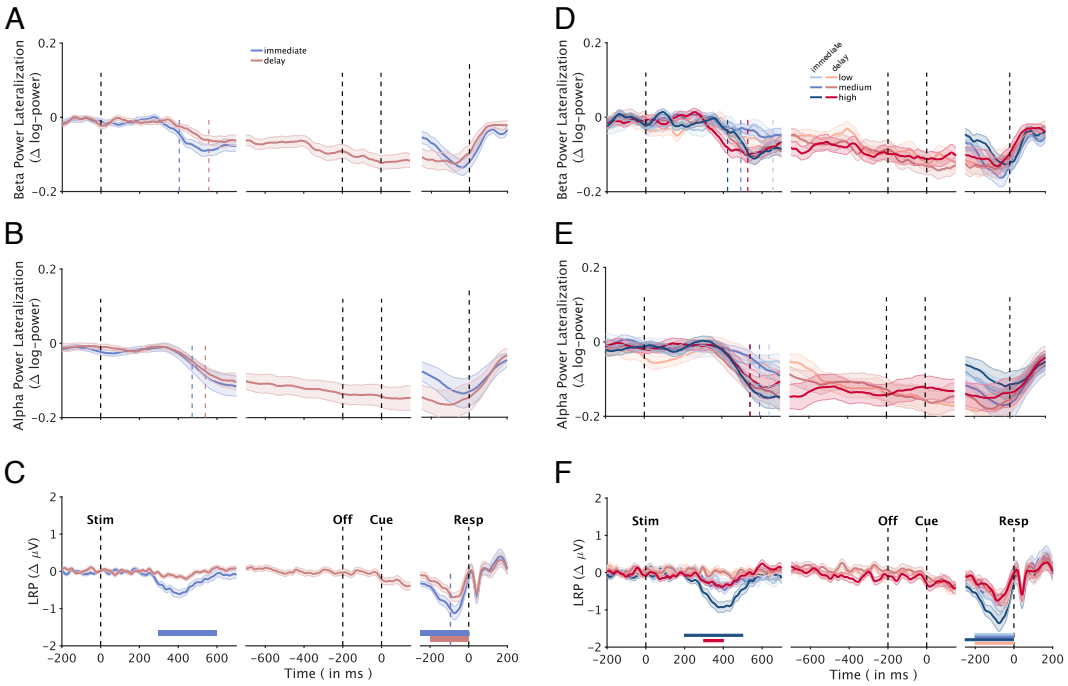

Figure 2-4. A-C: Temporal dynamics of BPL (A), APL (B) and LRP (C) in the Immediate (blue) and Delay (red) condition, averaged over all correct trials. Panels show stimulus-locked (left), cue-locked (center), and response-locked (right) lateralization. Time courses show BPL and APL to emerge after stimulus onset with a peak just before the response in both task variants. In contrast the LRP did not emerge until the imperative cue, evolves steeply and peaks shortly before the response. Horizontal bars at the bottom of each panel (C, F) mark time windows that differ significantly (fdr-correction) from zero and display strong ($bf_{10} > 10$) to extreme ($bf_{10} > 100$) evidence for H1. Onset latencies are displayed without variances (non-interpretable) for Immediate and Delay for all correct trials (vertical colored dashed lines). D-F: Same as in A-C, but separated by coherence level (low, medium and high). Shaded areas represent SEM.

of the response cue and was maintained throughout the delay time until a response was initiated (Figure 2-4A). Stimulus-locked BPL onset latencies did not differ between Immediate and Delay (405.16 ms vs. 558.10 ms; $t(29)$ =

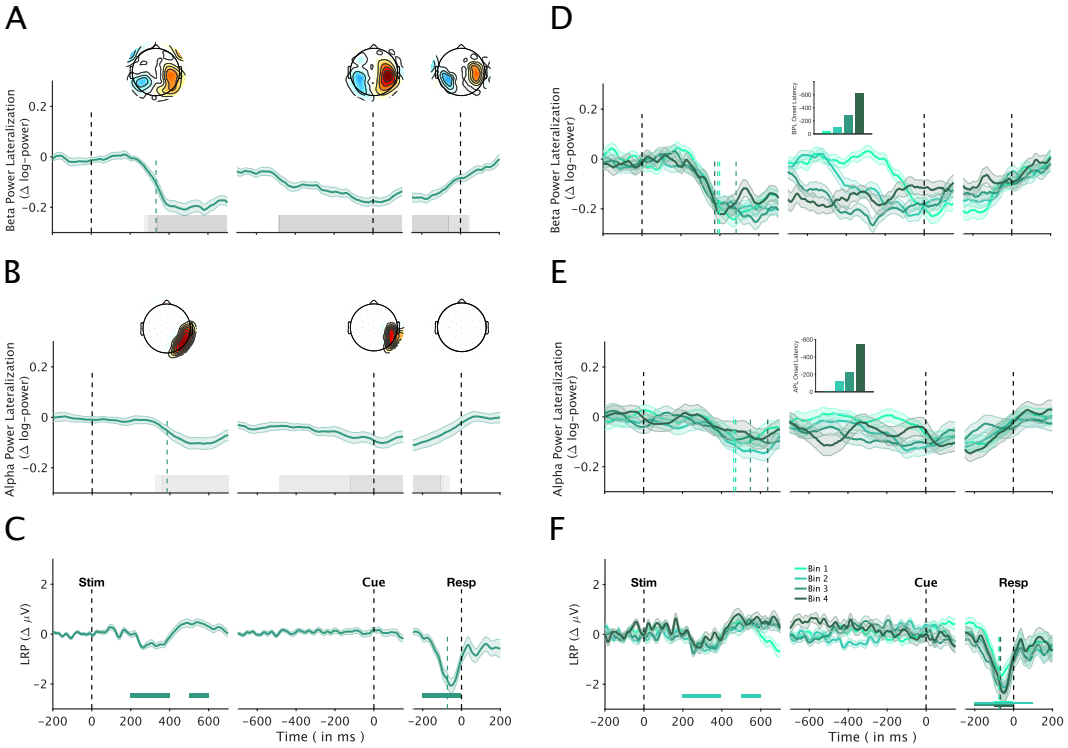

Figure 2-5. Lateralization of beta and alpha power, and LRP during flexible delay times. A, B: The lateralization evolved after stimulus onset across the frequencies of beta and alpha band over all correct trials. Topographies at relevant times (lateralization onset, cue presentation and response) show fdr-corrected regression weights of lateralization (*Hand* regressor in GLM with beta/alpha power as a predictor). The shaded area at the bottom marks significant [cluster-based permutation] time windows of lateralization (darker shading == more electrodes with an effect) given by single-trial regression on C3, C4, CP3, CP4. C: The LRP evolved later after imperative cue presentation peaking shortly before the response. Horizontal bars at the bottom of each panel mark time windows that differ significantly (fdr-correction) from zero and display strong ($bf_{10} > 10$) to very strong evidence ($bf_{10} > 30$) for H1. D, E: BPL and APL dynamics were explored for different delay durations (short [bin 1], medium-short [bin 2], medium-long [bin 3], long [bin 4]). The onset of lateralization is locked to stimulus onset. Vertical dotted lines mark the stimulus-locked onset latency produced by a jackknife averaging procedure, variances are not displayed as they are not interpretable when using this method. Stimulus-locked onset latencies did not differ between delay bins, whereas cue-locked onsets tended to vary with delay duration (inset). F: Different delay durations did not affect the response-locked onset of LRP (vertical dotted green lines). Horizontal bars at the bottom of each panel mark time windows that differ significantly from zero (stim-lock: all $p_{corr} <= .0017$, $bf_{10} > 20.6251$; resp-lock: all $p_{corr} <= .0005$, $bf_{10} > 38.844$). Shaded areas represent SEM..

0.8192, $p_{corr} = 0.2097$, paired t-test; Figure 2-4A).

Single-trial regression analyses (Figure 2-6A, B; upper panels) showed significant lateralization time periods per electrode. The response-side regressor ($HAND$) was expected to correlate negatively with left hemisphere beta power and positively with right hemisphere beta power throughout stimulus processing. Beta power lateralized significantly in electrodes above motor cortex C3 and C4 after stimulus onset regardless of the task variant (horizontal shades

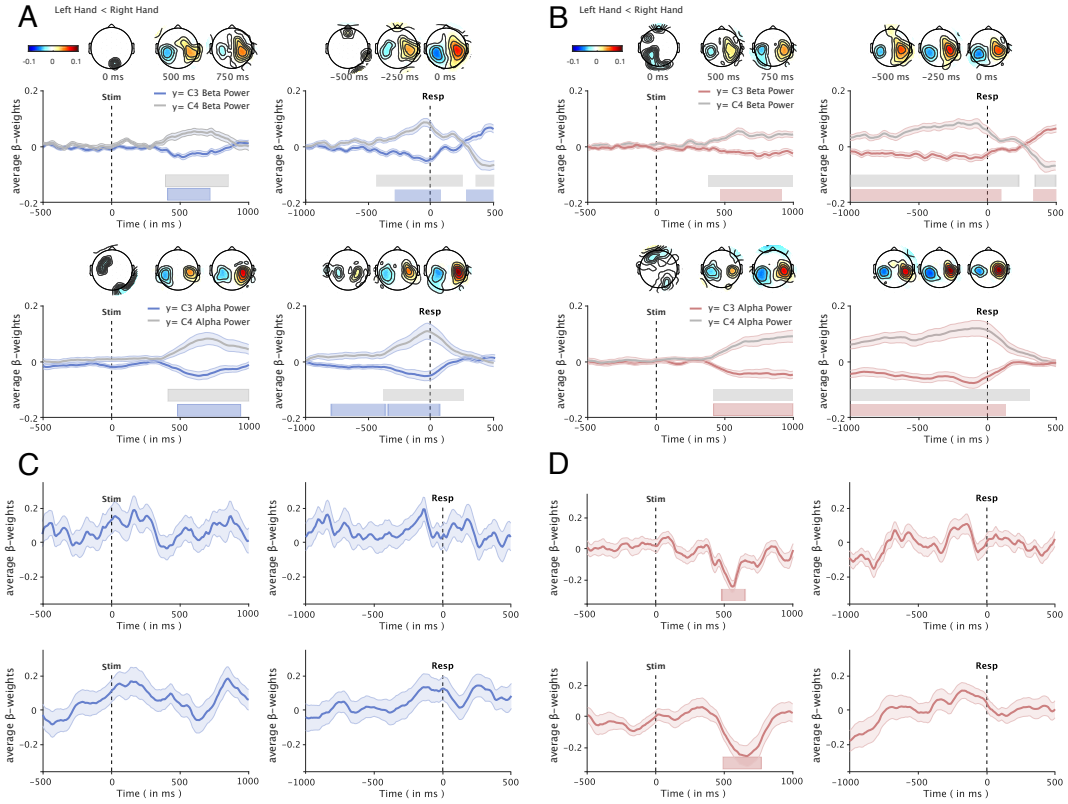

Figure 2-6. Regression weights from response side and coherence regressors. A, B: Regressing response side (left < right) onto beta (top) and alpha power (bottom) time courses revealed continuous significant lateralization over motor cortical electrodes (example results shown for C3 and C4) starting after stimulus onset throughout the delay period until just after response execution (horizontal shades reflect significant timewindows [cluster-based permutation]) for Immediate (A) and Delay (B). Topographies illustrate the fdr-masked regression weights of the lateralization effect over motor cortices at several timepoints. C, D: Regression weights from regressing coherence strength onto BPL (top) and APL (bottom) for stimulus (left) and response-locked (right) time courses, with significant [cluster-based permutation] timewindows marked by the shaded bar in the bottom. Negative regression coefficients for BPL and APL in the delay task variant around 500 - 600 ms after stimulus onset are presumably related to earlier onset times for higher sensory evidence. Shaded areas represent SEM

and topographies in Figure 2-6A, B; stimulus-locked onset of significance for Immediate: +410 ms [C3], +390 ms [C4] and Delay: +470 ms [C3], +380 ms [C4]). Moreover, lateralization remained stable throughout stimulus processing and delay period until shortly after the response (response-locked offset of significance for Immediate: +70 ms [C3], +240 ms [C4], and Delay: +90 ms [C3], +220 ms [C4]). Thus, onset latency and the continuous dynamics appeared comparable between the two task variants. This finding is particularly interesting given that, in Delay, the signal emerged several hundred milliseconds before participants were allowed to respond. This renders the BPL signal dissociable from a motor preparation signal.

The early lateralization effect extended to alpha range frequencies (Figure 2-4B), which showed a temporal pattern comparable to BPL. Here, however, onset latencies differed slightly between Immediate and Delay (471.98 vs. 539.82 ms [post-stimulus]; $t(29) = 1.7874$, $p_{corr} = 0.0422$, paired t-test). Nevertheless, the onset of significant APL is earlier than 550 ms after stimulus onset, long before presentation of the response cue in Delay. Single-trial regression revealed similar effects compared to the findings reported for BPL (Figure 2-4A, B; lower panels). Lateralization occurred after stimulus onset for Immediate (C3: +480 ms, C4: +410 ms) and Delay (C3: +420 ms, C4: +420 ms) and was maintained until just after the response was executed (Immediate: +50 ms [C3], +250 ms [C4]; Delay: +120 ms [C3], +300 ms [C4]).

Comparable to *Experiment 1*, we found in *Experiment 2* that APL/BPL already emerged 400-600 ms after stimulus onset, several hundred ms prior to the imperative cue (Figure 2-5A, B). Single-trial regression analyses revealed that, long before the imperative cue appears, beta and, to a lesser extent, alpha power lateralized in sensori-motor areas (shaded horizontal areas and topographies; beta: 290 ms [post-stimulus] to 30 ms [post-response] and alpha: -120 to 210 ms [peri-cue]). Moreover, the onset latency after stimulus onset (left panels) of the lateralization did not change with changing delay times in beta (Figure 2-5D; bin 1 to 4: 398.49 ms, 388.79 ms, 483.13 ms, 373.23 ms; $F(3,116) = .7637$, $p_{corr} = .5167$, rmANOVA) and alpha frequency range (Figure 2-5E; bin 1 to 4: 462.45 ms, 472.79 ms, 548.44 ms, 637.43 ms; $F(3,116) = .0379$, $p_{corr} = .9901$, rmANOVA). In cue- and response-locked trajectories of BPL, we observed that onset times varied with respect to delay duration (Figure 2-5D, inset): for short delays (bin 1) lateralization started

only briefly before imperative cue onset (bin 1: -43.12 ms) and longer delays were associated with earlier lateralization relative to the cue (bin 2: -98.73 ms; bin 3: -285.78 ms; bin 4: -621.34 ms; $F(3,116) = 2.6922$, $p_{corr} = .0494$, rmANOVA). In sum, these temporal dynamics suggest that APL and BPL are not bound to response execution, but rather to the time when sensory evidence drives a decision, corroborating our results from *Experiment 1.*

In contrast to BPL/APL, the LRP increased shortly and sharply after the onset of the imperative cue and peaked just before response initiation (Immediate: -400 to 2 ms, all $p < .0019$, all $bf_{10} >= 19.2577$; Delay: -200 to 2 ms, all $p < .000817$ all $bf_{10} >= 39.6274$; one-sample t-tests with fdr-correction; Figure 2-4C). It was not present yet during the time of stimulus viewing and decision formation, except for a small and transient lateralization briefly after the stimulus, which reached fdr-corrected significance in the immediate condition only (Immediate: 302 to 500 ms, all $p <.00001$, all $bf_{10} >= 2112.0349$; Delay: -98 to 600 ms, smallest uncorrected p-value = .0062, all $bf_{10} <= 6.8044$; one-sample t-tests; Figure 2-4C, left panel) that seemed to be driven by trials with maximal coherence (Immediate/high: 202 to 500 ms, all $p <.00054$, all $bf_10 <= 57.5512$; Delay/high: 302 to 400 ms, $p < .000007$, $bf_{10} = 3209.2161$; one-sample t-tests with fdr-correction; Figure 2-4F). We found no evidence for a difference in response-locked onset latency between Immediate and Delay (-93.81 ms vs -95.61 ms [pre-response]; t(29) = -0.2966, $p_{corr} = 0.6155$, paired t-test). These trajectories clearly differ from BPL and APL dynamics during stimulus processing, hence pointing at different functional roles of these lateralization signals.

Likewise, the LRP in the simple delayed response task (Figure 2-5C, F) showed a trajectory that is highly similar to the one observed in *Experiment 1.* There was an initial transient deflection after stimulus onset (202 to 400 ms, all $p < .0027$; one sample t-tests with fdr-correction, $bf_{10} >= 14.4519$), driven by the medium-short delays (bin 2: 202 to 400 ms, all $p < .0017$, $bf_{10} >= 38.9540$). Primarily, however, the LRP displayed a short and steep peak just before response execution (-200 to -2 ms, $p < .0032$,$bf_{10} >= 12.004$), which was present in all delay bins within the timewindow from -100 ms to response (all $p < .0021$, one sample t-tests with fdr-correction, all $bf_{10} >= 167.25$, Figure 2-5F [horizontal bars]). Onset times of the peak did not differ between delay bins (bin 1: -75.67 ms, bin 2: -67.74 ms, bin 3: -74.19 ms, bin 4: -67.79 ms;

F(3,116) = 0.0817, p_{corr} = 0.9698, rmANOVA, Figure 2-5F [vertical dotted lines]). Thus, in agreement with our hypothesis, we conclude the LRP is not directly affected by stimulus properties or waiting time, but reflects a general motor preparation process.

6.2.5 Evidence strength modulates Beta and Alpha power lateralization in delay

Next, we asked whether differences in temporal patterns could also be observed between different coherence levels (*Experiment 1*) as would be expected if the strength of lateralization encoded evidence accumulation. APL and BPL differed slightly depending on variations in evidence strength (Figure 2-4D, E). Temporal dynamics of BPL and APL in the decision phase (after stimulus onset) revealed an earlier onset for the highest coherence bin compared to lower coherences (Table 2). The differences in stimulus-locked onset latency in the alpha-band for Delay were significant (F_{corr}(2,87) = 5.7511, p_{corr} = 0.0045, Figure 2-4E, repeated-measures ANOVA). This effect was driven by the significantly shorter onset latency for high compared to medium and low evidence strength (low vs. high: 1205.5 vs. 544.04 ms; medium vs. high: 1195.20 vs. 544.04 ms, post-hoc corrected Scheffé interval). The other comparisons of coherence on onset times were not significant (all $p_{corr} > 0.13$, repeated-measures ANOVA; Figure 2-4D, E). Nonetheless, the observed trend supports our hypothesis about the influence of sensory evidence on lateralization dynamics. In contrast, during the motor preparation phase (pre-response) we could not find such differing APL/BPL dynamics between coherence levels, which further supports the idea that motor preparation is not affected by sensory evidence.

Single-trial regression analyses further support our hypotheses. Most importantly, we found that the *coherence* regressor significantly modulated APL and BPL trajectories in the delayed variant of the task (Figure 2-6D, left panels). The effect occurred several hundred milliseconds after stimulus onset (BPL: +480 to +640 ms, APL: +490 to +760 ms) and can be attributed to later lateralization onset times in lower coherence conditions. This was not found in immediate trials (Figure 2-6C, left panels), in which lateralization strongly varied with reaction times (Figure 2-7D).

In comparison, LRP dynamics were not consistently modulated by sensory

Table 2
Average (± SEM) onset latencies (stimulus-locked) for beta and alpha power lateralizations

	Coherence bin		
	low	*medium*	*high*
BPL			
Immediate	421.75	490.05	655.7
Delay	525.92	1237.40	1246.80
APL			
Immediate	546.17	594.21	643.62
*Delay***	544.04	1195.20	1205.5

Note. Mean onset times for the conditions in milliseconds after stimulus onset without variance (non-interpretable).
** $p_{corr} < .01$, rmANOVA

evidence strength (Figure 2-4F). There was no effect of coherence on onset latency in Immediate (pre-response: -94.80 ms [low], -85.50 ms [medium], -99.67 ms [high]; ANOVA: $F_{corr}(2,87) = 0.6414$, $p = 0.5290$) and Delay (pre-response: -78.03 ms [low], -100.62 ms [medium], -97.24 ms [high]; ANOVA: $F_{corr}(2,87) = 0.6390$, $p = 0.5303$).

However, significance testing of pre-response time windows in Delay revealed a significant LRP deflection only for low evidence strength (-200 to -2 ms, all $p < .00052$, one sample t-tests with fdr-correction, $bf_{10} >= 59.4456$), whereas in Immediate, the LRP was present for all coherence bins (low: -200 to -2 ms, all $p < .00008$, all $bf_{10} >= 320.4341$; medium: -200 to -2 ms, all $p < .00006$, all $bf_{10} >= 52.5054$; high: -300 to -2 ms, all $p < .00014$, all $bf_{10} >= 192.8852$).

6.2.6 Response alternation biased by Beta- and Alpha-power lateralization

As we observed an alternation bias in choice behavior in *Experiment 1* (see *Other factors guiding performance*), we explored the relationship between response alternation and lateralization time courses. First, we qualitatively observed differences in lateralization strength and direction leading up to the

response (Figure 2-7A). Specifically, beta, and, to a lesser extent, alpha power showed lateralization of opposite polarity (against the upcoming choice direction) in *repeat* trials. Eventually, just before the response or shortly after (Immediate BPL), both trial types lateralized towards the correct hemisphere

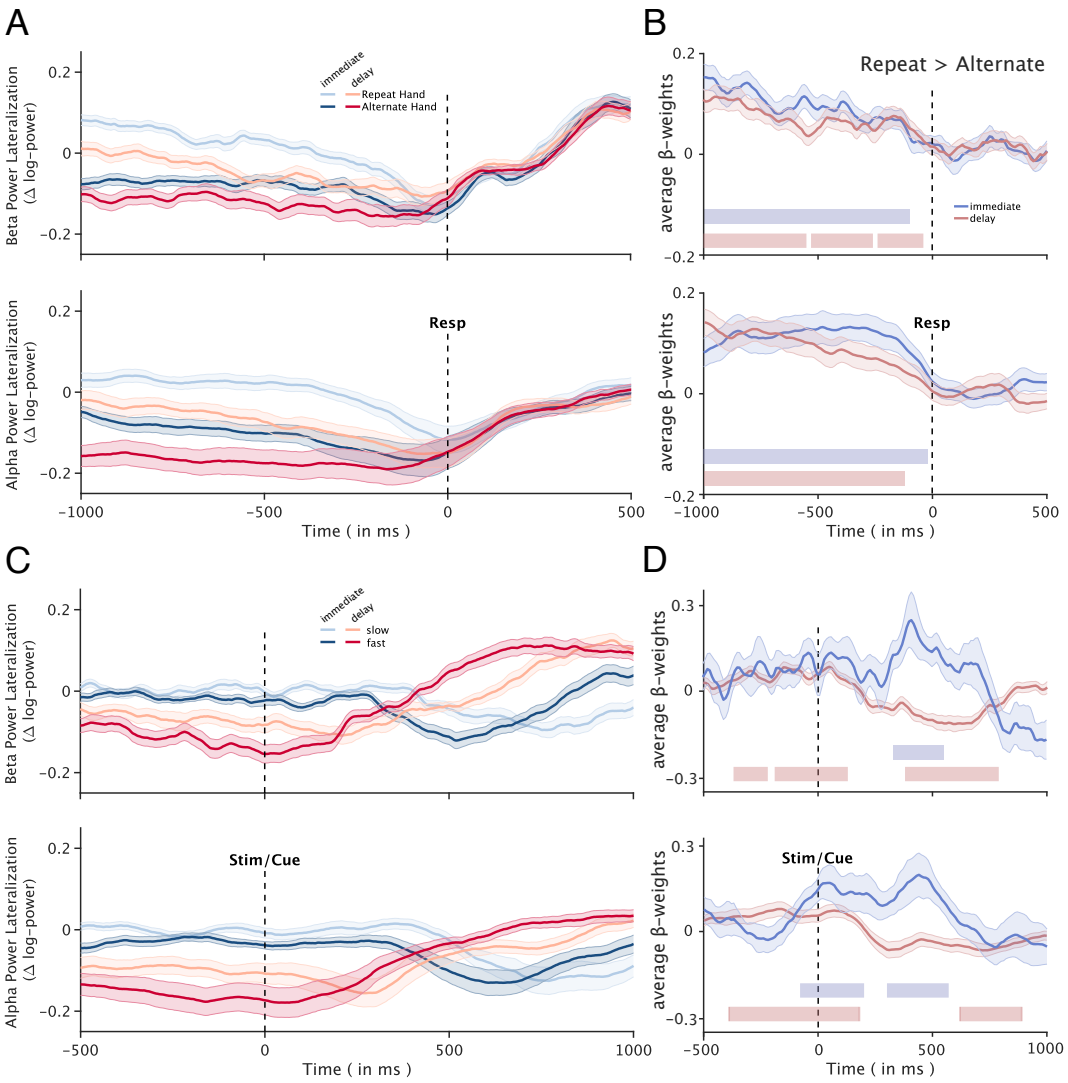

Figure 2-7. BPL and APL are modulated by response alternation and RT. A: In both conditions (blue = Immediate, red = Delay), BPL (top) and APL (bottom) amplitudes and trajectories leading up to the response differ in trials requiring a response alternation (dark), compared to those with same side responses (light). B: Regression weights reveal significantly (shaded horizontal bar, cluster-based permutation) stronger lateralization in alternation trials up until response execution in both conditions and frequency bands. C: A median split of reaction time reveals later onset and later peak latencies for slow responses compared to fast responses in both conditions and frequency bands. D: The regression weights for RT show that differences occur during the time of stimulus viewing (post-stimulus, pre-cue) up until the response. Shaded areas represent SEM.

(contra - ipsi, negative difference in log-power) with similar amplitude. We formally tested these observations using the regression weights of the *Response Repetition* regressor in the multiple single-trial regression (Figure 2-7B). Alpha (lower panels) and beta power lateralization (upper panels) in both Immediate and Delay were significantly biased towards response alternation throughout the trial, until just before response execution (Immediate: -110 ms [BPL], -30 ms[APL]; Delay: -50 [BPL], -130 [APL]), independent of RT and coherence. It appears that the effect of beta rebound (details in the discussion) from the previous trials impinges on the current lateralization in repetition trials long throughout the trial and thus biases toward alternating responses, as we described in the behavioral data.

6.2.7 BPL and APL are modulated by reaction time

Finally, we tested the relationship between BPL/APL dynamics and response speed in *Experiment 1.* Qualitatively, we observed differences in onset and peak latency for both lateralization signals (Figure 2-7 C) when comparing high and low RT trials. We quantified these differences using the regression coefficients of the *RT* regressor (Figure 2-7 D). In the immediate task variant, there was a significant RT effect from +330 to +540 ms (BPL) and from +300 to +560 ms (APL) after stimulus onset. This difference can be explained by later onset times in slow response trials, independent of evidence strength. Similarly, we could show, that, in the delay variant prior to and throughout imperative cue presentation (-370 to +120 ms [BPL] and -500 to +170 ms [APL]) variations related to RT were present. Importantly, these effects were independent of sensory evidence strength. Opposite effects (negative regression coefficients) occurring later in the delayed trials (post-response) could be attributed to a later return to baseline or beta rebound after response execution.

6.3 Discussion

We used two different perceptual decision-making paradigms which varied in the amount of time that was allowed for making a decision and the timepoint at which participants were allowed to express their choice. On the one hand, the RDM task either permitted self-determined duration of evidence accumulation (stimulus viewing) or enforced a fixed time for stimulus viewing, which allowed for relatively long duration of evidence accumulation. On the other hand, the delayed response task inherently required only short evidence accumulation

(low uncertainty of the choice) but forced the volunteer to wait for a variable time with the output of their decision (motor response). These variations in the temporal structure of the task aimed at separating evidence accumulation from activity related to movement preparation and execution in the motor cortex.

We found that, as expected, sensory evidence strength of a stimulus improves perceptual decision-making performance and this effect tends to be reflected in the temporal evolution of BPL and APL. Importantly, effector-specific lateralization develops already several hundred ms before presentation of an imperative cue and persists until the response is executed. In contrast, the LRP occurred markedly later, upon the onset of the imperative cue, regardless of condition and experiment. Moreover, we could show that BPL and APL are related to choice alternation biases across successive trials and thereby influence choice selection.

First of all, we validated that stronger evidence due to higher motion coherence (i.e., lower uncertainty) leads to faster and more accurate decisions, as has been described previously, (De Lange et al., 2013; Gold & Shadlen, 2000, 2003; Kelly & O'Connell, 2013; O'Connell et al., 2012; Twomey et al., 2016). Further, we confirmed that our manipulation allows us to temporally separate decision and motor processes. Enforcing a delay before response execution did not change accuracy, but reduced reaction times, consistently. This suggests that decision processes were completed (in conditions with medium to high evidence) upon the presentation of an imperative cue. Motor preparation and execution, whose implementation time was not affected by coherence, followed afterwards.

Furthermore, we found that after longer delays not only reaction times but also movement times decreased. If we assume that movement time serves as a proxy for vigorous behavior, we here find support for the hypothesis that urgency increases vigor as has been postulated by Thura et al. (2014). Perhaps, a global arousal due to an upcoming spatially unspecific urgency signal increases motor excitability (see below) and thus leads to more vigorous responses. The same authors (Thura & Cisek, 2016) found PMd and M1 cells to up- or downscale activity with elapsing time. This urgency signal originated in subcortical regions, potentially in the GPi (Thura & Cisek, 2016).

In line with our predictions for APL and BPL, we demonstrated that effector-

specific lateralization occurs already before imperative cue presentation and persists until the response is executed. The implementation of a forced delay period before the motor response allowed us to assess to what extent these signals are more closely related to decision- or motor processes. We thus argue that alpha and beta power lateralize already during decision time. Hence, we assume that decision-related information is conveyed to motor cortical areas prior to response preparation and upheld until the response is prompted. Previous results (Kaiser et al., 2001) already suggested that the timing of beta power reduction may be an index for the duration of motor response selection (Alegre et al., 2003) and report such a power reduction even before stimulus presentation when temporal predictability was ensured. Lateralization of beta power in the present study appeared even with unpredictable imperative cues. Similarly, Twomey et al. (2016) reported ongoing BPL throughout a delay. One could argue that a fixed delay duration as in *Experiment 1* could make motor preparation before the imperative cue adaptive to the task. However, we find similar results in the second experiment, where the delay was unexpectable and responses potentially unnecessary (NO-GO trials). In such a setting, it would be adaptive to wait with motor preparation until the imperative cue appears, given that the response window is long enough. However, it was also shown that BPL did not appear if response requirements were unknown (Twomey et al., 2016). Thus, we understand the signal as depending on action selection.

Concerning the onset times of the signal, it is important to note that lateralization of oscillatory power and LRP differ consistently. LRP occurred robustly, regardless of condition and experiment, only near the onset of the imperative cue, indicative of a signal responsible for motor preparation. Only a small temporary deflection towards the correct side, time-locked to stimulus presentation was observable in the immediate task when coherence was maximal, and in the delayed response task. Similar observations in LRP (Scheibe et al., 2009) were interpreted as a primer for the motor system. One could speculate that the strong decision signal resulting from unambiguous evidence carried over and triggered a partial motor activation. However, this early motor preparation would not occur under uncertain conditions, as Scheibe et al. (2009) already demonstrated. With upcoming motor output, we found LRP dynamics robustly bound to the response and thus temporally separable from BPL and APL trajectories. We conclude that additional information is en-

coded to some degree in APL and BPL. We hereby extend existing evidence about a hypothetical decision variable, which tracks the amount of incoming evidence and is computed elsewhere in the brain, reflected, e.g., in the centro-parietal positivity (O'Connell et al., 2012; Twomey et al., 2016). This signal, in turn, feeds into the motor system during stimulus viewing some time before responses need to be executed. We show (Figure S2-1) that CPP and BPL emerge around the same time after stimulus onset, regardless of the response delay. Unfortunately, we could not demonstrate a relationship on a single-trial level as signal-to-noise ratios were insufficient for this kind of analysis. The determination of onset latencies requires averaging over trials. This process questions the traditional view of a strictly sequential cascade of decision making (Sternberg, 1969). It opens the opportunity for temporal and spatial flexibility in neural mechanisms leading to motor output.

Importantly, both, the peak of beta lateralization (Fischer et al., 2018) and the LRP (Van Vugt et al., 2014), have been considered to index a motor threshold. Many decision-making models (e.g. drift diffusion models) assume such a boundary that would typically mark the release of a motor response. Thus, peaks of such "ramping-to-threshold" signals were expected to fall into a window around 20 ms (i.e. the time to for a cortical motor signal to reach the effector) before response execution. Here we found that, on the one hand, BPL can peak already some hundreds of milliseconds before response execution. In the delayed tasks, however, a peak could not be clearly defined as the signal was rather marked by a prolonged plateau phase and even a slow return to baseline (shorty before the response). The LRP, on the other hand, clearly peaked just before the response regardless of condition and task. In contrast, Fischer et al. (2018) reported that peaks of BPL matched exactly the time of response initiation. This could be more likely in speeded forced-choice reaction time tasks with very short reaction and evidence accumulation times, such as the Flanker Task. In these cases, decision and motor processes are overlapping and difficult to separate. Implementation of a delay in our tasks, however, disentangled these two functions and revealed the individual temporal dynamics of APB/BPL and LRP. Thus, we hereby challenge the previous assumptions of a single motor threshold. We speculate that even though a preparation of a motor response is reflected by BPL, we cannot necessarily use its peak as the threshold for initiation of an overt response. It could potentially indicate a heightened excitability of the motor system, which then needs a final

trigger signal to release the action, perhaps reflected by the LRP. However, Van Vugt et al. (2014) and Kelly and O'Connell (2013) found the early LRP to scale with evidence strength, which would argue against it being a merely motor-related signal. It is worth noting, however, that the LRP was measured at non-conventional frontocentral electrodes (CF3 and CF4) in Kelly and O'Connell (2013), which could thus reflect contributions of non-motor dynamics. Nonetheless, Van Vugt et al. (2014) also suggest that the LRP is driven by accumulator units, which we suspect may be reflected by BPL. Possibly, motor actions are already prepared in parallel to evidence accumulation but not measurable at population level. Indeed, it has been shown that preparatory activity in motor cortical areas cancels out at the population level (Kaufman et al., 2014). Only when an action is executed, activity moves from this null space into an output-potent pattern. We speculate that the onset of the LRP marks this transition between patterns. Along these lines, variability in motor excitability has been shown to be task-dependent and indicative of the motor preparation state (Klein-Flügge et al., 2013). More specifically, it was found that cortico-spinal excitability is modulated by the evidence in favor of a particular choice (Klein-Flügge & Bestmann, 2012). Furthermore, a negative relationship between oscillatory brain activity and cortical excitability has been shown previously for alpha band in occipital cortex (Samaha et al., 2017), somatosensory regions (Ploner et al., 2006) and motor cortex (Sauseng et al., 2009) and for beta in posterior parietal cortex (Samaha et al., 2017) and somatosensory areas (Ploner et al., 2006). Thus, it seems conceivable, that beta power likewise inversely modulates excitability of the motor system and thereby makes action initiation more likely.

Common computational models reflect evidence accumulation by an up- or downward ramping (depending on the signal) to a threshold (e.g., drift-diffusion models). In biophysical models of decision making, as in recurrent cortical network models (Wang, 2002), reaching this threshold corresponds to the network reaching a stable attractor state. The network remains in this attractor state until an action is initiated. The dynamics of BPL/APL we observed, namely a ramping to plateau that persisted throughout the delay until a response was carried out, is thus reminiscent of such attractor dynamics. However, there remains some uncertainty about the representation of evidence strength within the motor system. Even though we found sensory evidence strength to modulate BPL and APL ramping in delayed trials, the effect could not be

observed in immediate trials. In contrast, other studies (De Lange et al., 2013; O'Connell et al., 2012) report stronger differences in BPL slopes depending on the decision difficulty (strength of evidence). Even others report that BPL reflects evidence as well as evidence update (Gould et al., 2012) and also the value of the choice (Hunt et al., 2013). Similarly as in our study, Twomey et al. (2016), however, showed no effect of coherence on slope and peak amplitude of BPL. Thus, the question remains why findings related to the functional relevance of BPL are so diverse. One methodological concern is the diversity in lateralization between participants as well as the noisiness of the data within each trial. This in turn, reduced the power of the tests and might hide relevant effects. Therefore, it seems important that future studies further explore interindividual differences in lateralization and behavioral consequences in a larger sample.

Furthermore, we could show a reversed beta-power lateralization after the response (beta rebound), which biases subsequent responses towards alternation. In this study, we could extend the findings of Pape and Siegel (2016) by showing that this bias is only resolved shortly before the upcoming response initiation. If, indeed, alpha and beta activity over motor cortices reflects excitability of the motor system, this would indicate that, following a response, the excitability of the motor cortex contralateral to the effector is reduced. Under certain circumstances, such inhibition of repetition could be adaptive, e.g., to favor exploration over exploitation or to avoid muscle fatigue (Pape & Siegel, 2016).

Moreover, we found that the frequency at which there was motor cortex lateralization extends to the alpha band. Few previous studies show that alpha power decreases (Murphy et al., 2016) and lateralizes (Donner et al., 2009), along with beta power, prior to response execution in decision-making tasks. In the present study, we explored APL and BPL separately. Alpha activity differed only slightly from BPL by being more prominent in the RDM (fixed delay) and less robust in the delayed response task (flexible delay) compared to BPL. We speculate that the predictability of the delay time modulates APL. Alpha power reduction has previously been described as unspecific preactivation, independent of force, speed and muscle group (Pfurtscheller et al., 1998). In the framework of perceptual attention and visual processing, alpha power reductions were associated with covert spatial attention (Barne et al.,

2020). They have been proposed to reflect increased excitability rather than improved accuracy (Lange et al., 2013). In motor cortex, lateralized alpha reductions would, according to this view, release from inattentiveness of the to-be-chosen effector and increase general excitability for the upcoming motor output. Consistent with this idea, Bergmann et al. (2019) related motor cortical alpha power to pulsed facilitation of cortical excitability. Taken together, APL appears as a rather general decision signal, while BPL is potentially more sensitive to external influences such as the decision context; but a strict separation of their functional roles appears difficult.

Overall, our results indicate that current hypotheses regarding the function of BPL may need to be reconsidered. One recent finding (Okazawa et al., 2021) supports the idea that a relationship between evidence and neural signal might be non-linear as representations switch over time, from decision variable to choice. Alternatively, a decision variable might not simply encode evidence strength or certainty (Gold & Shadlen, 2007) of the decision but instead index a readiness to select an option and carry out a subsequent response. This preparedness is probably not only affected by the level of evidence that has been accumulated but also by the time that has passed. Such an "urgency factor" has previously been described to impact reaction times (Reddi & Carpenter, 2000) by reducing the decision threshold, and it may well have modulated the lateralization trajectories in our experiments. Our participants knew, that the time to select a choice and perform a response is more or less limited. They may have been urged to respond prematurely, and potentially our EEG signals were modulated by an additional urgency signal arriving at the motor cortex (Cisek et al., 2009; Thura et al., 2012). Indeed, Kelly et al. (2020) developed a model that used neural data (i.e., alpha and beta amplitudes) to find evidence for the impact of time pressure on the duration of motor preparation as well as changes in drift rates. Thus, future research might address the effect of urgency on lateralization signals in order to understand how it is integrated into the decision variable arriving at the motor cortex.

Taken together, we could separate functions of motor cortical lateralization and suggest that evidence strength modulates cortical excitability. We propose that a better understanding of this process will eventually give researchers an opportunity to use an online index of the current decision stage. Such an index might be valuable in understanding pathological decision making, as well as

healthy behavior under various conditions and in different tasks.

6.4 Supplemental Material 1

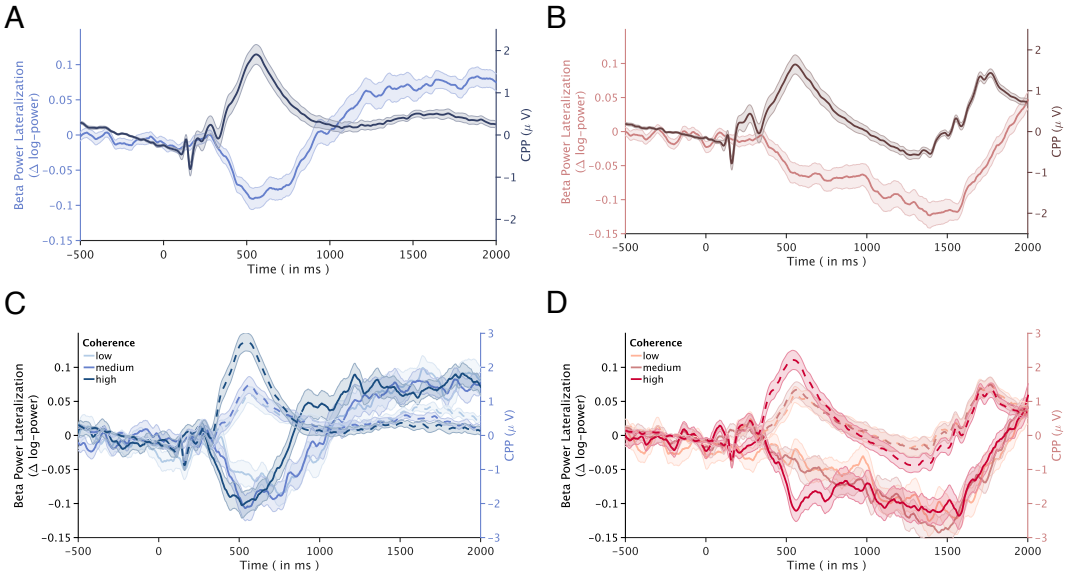

Figure S2-1. CPP and BPL. CPP (dark, average of electrodes Pz, CPz, CP1, CP2) and BPL (light) averaged across all trials and participants for Immediate (A) and Delay (B). Both signals appear after stimulus onset without a dominant lag between them, regardless of the task variant. In Delay, however, BPL is prolonged and returns to baseline much later than in Immediate. C,D: CPP (dashed) and BPL (solid) averaged across coherence bins and participants for Immediate (C) and Delay (D). Shaded areas reflect SEM.

7 Beta power lateralization reflects urgency-related response timing during evidence accumulation

In our dynamic environment we constantly have to make decisions, often in uncertain contexts or under time pressure. For example, if one wants to cross a busy street it is necessary to observe the scene including cars, bikes and traffic signs in order to determine when and where to finally walk across. Such perceptual decisions are choices that are primarily based on sensory input. Gathering such information for perceptual decision-making is called evidence accumulation. In a similar situation, if one is already late for work, decision performance potentially becomes compromised by time pressure. This speed-accuracy trade-off (SAT) results from the fact that decision making takes time, and shortening the decision time compromises the quality of the decision outcome.

In two-alternative forced choice tasks sensory information is integrated over time until it reaches a decision threshold (Bogacz et al., 2006). This assumption is based on evidence-accumulation theories. In accumulation-to-bound models, such as the drift-diffusion model (DDM; Ratcliff, 1978), the process of accumulating evidence throughout deliberation time is formalized. SAT adaptations occur when hasty decision contexts lead to changes in decision policy such that speed is favored over accuracy (e.g. Bogacz et al., 2010; Derosiere et al., 2022; Wickelgren, 1977). It has been shown, that it is possible for humans to adapt their SAT within very short timescales (even within one decision) by adjusting their accuracy criterion (Derosiere et al., 2022; Ditterich, 2006). Theoretically, urgency in decision formation could be realized by a reduction in decision thresholds or increased drift rates reflecting a steeper integration process. Theories involving evidence accumulation typically assume a collapsing threshold over time as prolonged evidence accumulation is costly (Drugowitsch et al., 2012). Empirical observations in humans (Drugowitsch et al., 2015) and monkeys (Gold & Shadlen, 2002) confirmed that reward rate was maximized (sufficient evidence, without being too time consuming) by selecting the decision threshold. Others (Purcell & Kiani, 2016) found even a collapsing bound over the course of several trials as a function of the urgency to switch environments. However, population and single cell activity in pre- and primary motor areas also reflected an increasing slope and baseline over time (Thura et al., 2014). This finding strengthens the assumptions of the urgency gating

model (UGM). The authors assume that in motor cortex the sensory evidence of a decision is encoded on a momentary basis (Cisek et al., 2009; Thura et al., 2014). Instead of building-up or integrating observed evidence over time, the decision signal unfolds based on the strength of current evidence and an independent urgency signal (Cisek et al., 2009; Thura et al., 2014). As a consequence, SAT is realized through adaptations of the urgency signal (Thura et al., 2012) and a decay in the accuracy criterion over time (Cisek et al., 2009). A model that incorporates assumptions of both, the evidence accumulation and the urgency-signal account, is a non-stationary DDM where a time-variant gain mechanism influences drift rate instead of a decision threshold during evidence accumulation (Ditterich, 2006). This model was found to correspond to activity in lateral interparietal neurons of monkeys (Ditterich, 2006). Interestingly, Winkel et al. (2014) empirically compared the predictions of the UGM to assumptions made by the DDM and suggested that evidence accumulation was not replaced by urgency in decision making. Alternatively, it has been proposed that neural circuits involved in temporal integration of evidence and "the cost of time" operate separately (Farashahi et al., 2018). Thus, it remains debated how urgency and evidence accumulation affect decision processing and where these factors are reflected in neural signals.

There is a growing body of evidence suggesting that decision-related variables are represented in parietal regions and then forwarded to and encoded in motor cortex. In support of this idea are EEG signals over parietal (i.e. CPP) and motor areas (beta power over contralateral hemisphere) which corresponded to features of the hypothetical decision variable (O'Connell et al., 2012). In monkeys, lateral interparietal neurons associated with eye movement preparation revealed consistently parameters of a decision variable with firing rates predicting upcoming choice and scaling with the strength of the presented evidence (Bennur & Gold, 2011; Gold & Shadlen, 2001; Roitman & Shadlen, 2002; Shadlen & Newsome, 2001). Also neurons in pre- and primary motor cortex displayed activity that scales with evidence strength and time (Thura et al., 2014). The human motor system, probed via reflexes, was shown to be continuously modulated by time and evidence strength (Selen et al., 2012). This supports the idea that evidence signals are gradually pushed forward towards motor regions, increasing its excitability (Selen et al., 2012). Moreover, hasty decision policies differentially enhanced activity in the outcome relevant hemisphere even for distant effectors (Derosiere et al., 2022). The origin of

temporal adaptation signals has been suggested in basal ganglia structures, specifically in the GPi (Thura & Cisek, 2017, 2016) and the subthalamic nucleus (Frank, 2006). Specifically, beta oscillations in subthalamic nucleus have been associated with muscle activity (Reck et al., 2009). It seems plausible that they project information to motor cortex, where it could potentially be read-out as beta power reduction before movements. Slower cortical signals like the contingent negative variation (CNV) could also play a role as they were shown to relate to beta and alpha power reductions (Funderud et al., 2012). These slow drifts leading up to an event have been associated with movement (Scheibe et al., 2009) and event anticipation (Funderud et al., 2012; van Rijn et al., 2011). Even more relevant in this context appears the beta power lateralization (BPL), which could be a good candidate for reading out current decision processing in the motor cortex. It represents the difference in beta-power reduction between ipsi- and contralateral motor regions, corresponding to the motion side, before unimanual movements. This difference was shown to encode the integral of the evidence represented in visual areas (Donner et al., 2009) and manifested as an early build-up compared to a more motor-related signal (the lateralized readiness potential, Rogge et al., 2022). Moreover, BPL onset was shown to occur locked to stimulus onset, independent of a response delay (Rogge et al., 2022), which indicates an association with decision processing. Important to note, however, is that the emergence of BPL depended on stimulus-effector coupling and remained present after stimulus offset, suggesting more outcome related activity compared to the parietal signal (Twomey et al., 2016). In fast decision making tasks, the peak amplitude of the BPL has been proposed to characterize the decision threshold (Fischer et al., 2018). Alternatively, the slope of the BPL could represent the drift rate of the decision variable in the DDM, which was previously described for CPP and contralateral beta (Kelly et al., 2020; O'Connell et al., 2012).

In the present study, we focus on sequential evidence presentation and urgency manipulations in perceptual decision-making and their effects on BPL dynamics. The understanding of such mechanisms is important for the comprehension of functional decision making. In particular the role of the motor cortex in decision processing remains poorly understood even though it appears to be a central region where latent cognitive processes are transferred into observable motor output activity. We hypothesize that BPL tracks evidence accumulation and encodes an urgency signal. Specifically, we expect

that urgency reduces the peak amplitude of the BPL corresponding to a reduced decision threshold (e.g. Fischer et al., 2018) or evokes speeded evidence accumulation, which would indicate an increase in ramping over time as suggested by Cisek et al. (2009) and Ditterich (2006). Both alternatives would strengthen the perspective that the BPL is a simple non-invasive measure of choice development.

In order to induce urgency, we rewarded fast reactions in two ways: we provided time savings and/or a monetary bonus. It has previously been shown that time on the experiment was rewarding enough to speed up the reactions from participants (Cisek et al., 2009) in a sequential sampling paradigm. This paradigm also allowed us to explore the effect of accumulated as well as momentary evidence on behavior and different neural correlates.

In brief, we found that evidence accumulation and the update of evidence were reflected in BPL dynamics. However, this effect was not directly influenced by speed manipulations. Yet, we found that speed rewards modulated reaction times (RT) via a speed-accuracy trade-off. Additionally, response timing was associated with BPL strength after stimulus presentation. The results of this study will contribute to our understanding of how decision making is tracked in the motor cortex and provide evidence for the relevance of BPL during decision processing.

7.1 Material and Methods

7.1.1 Participants

We recorded EEG in 35 volunteering healthy humans. The data of one participant was excluded because of previous experience with the task. The remaining 34 subjects (21 female) were between 18 and 37 (mean $\pm$ SEM = 25.79 $\pm$ 0.76) years of age. All participants had finished school with Abitur or equivalent (12 to 14 years), of those nine received university degrees, and nine had completed an apprenticeship (practical training). All participants were native speakers or fluent in German or English. Instructions were given to them in the dominant language (English: N = 1). All, but three participants reported no neurological or psychiatric illness and were not taking psychoactive drugs. One person was diagnosed with adjustment disorder two years before study participation, and two were migraine patients under medication without incidence in the week before the experiments. All subjects had normal or corrected-to-normal

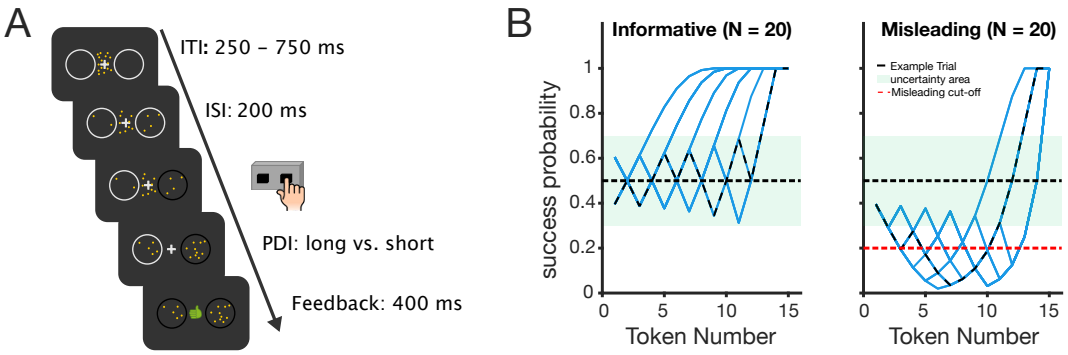

Figure 3-1. Token Task and Trial Sequences. (A) Example trial with correct right-hand press. After a random inter-trial interval (ITI = 250 – 750 ms), one after another, with an inter-stimulus interval (ISI) of 200 ms, each token moves from a central pool to a lateral target (white circles). The participant can respond at any time during the trial and indicate their choice. After the response, all remaining tokens move into their respective goal at slow (170 ms) or fast (20 ms) pace resulting in long vs. short post-decision intervals (PDI). Feedback is presented for 400 ms informing the participant about the correctness of their choice. (B) Specific trial types (informative and misleading) were pre-defined by the development of success probability over the course of the trial. Individual trial sequences are displayed in blue, one specific example is marked with a black dotted line for each type. The uncertainty area (green) covers a range (0.3-0.7) around chance level (0.5). The red dotted line displays a cut-off for misleading trials, where three tokens or more have to be below 0.2 success probability.

vision. Most participants were right-handed (N = 29, Edinburgh Handedness Score: mean ± SEM = 82.04 ± 3.27), left-handed participants scored on average –81.38 (SEM = 10.15), on the handedness measurement. All subjects were naïve to the task. They received monetary or credit point compensation for study participation. The study was approved by the Ethics Committee of the University of Magdeburg.

7.1.2 Task

We implemented a customized version of the Token Task (Cisek et al., 2009; Figure 3-1). Initially, a central pool of fifteen tokens (dots) was presented to the participants. One after another the tokens moved into one of two lateral targets. Participants were asked to decide as fast and as accurately as possible which of two targets most tokens would end up in. Responses were given with the left or right thumb, corresponding to their choice, on a customized response box.

Stimuli. We presented the task to the participants with the Psychophysics Toolbox 3 (Brainard, 1997; Kleiner et al., 2007; Pelli, 1997) in MATLAB 2012a. Their seating position was fixed at a distance of 100 cm away from a 22-inch LCD monitor with a refresh rate of 60 Hz. The participants were presented with a white fixation cross (RGB: 0.9, 0.9, 0.9; diameter: 20 px) at the center of the screen with dark grey background (RGB: 0.2, 0.2, 0.2). This indicated the moment when a participant was allowed to start the trial. Upon pressing the central button of the response box, the trial was self-initiated. After a random intertrial interval (ITI; jitter between 250 and 750 ms) the pool of tokens (diameter: 15 px) were displayed in yellow (RGB: 1.0, 0.8, 0.0) within a fixed circular boundary (200 px diameter) around the center of the screen. Simultaneously, two white circles appeared laterally (diameter of 200 px, at 40 [left] and 60% [right] of maximal screen width, centered along the vertical axis) which marked the targets for the tokens. The fixation cross remained on screen to avoid eye movements throughout the trial. Every 200 ms (interstimulus interval, ISI) one token moved into its designated target, the locations within the target were randomized but tokens were not allowed to cover each other. Once a response was made, the circle of the chosen target side turned black (RGB: 0.9, 0.9, 0.9) and the remaining tokens moved into their target at a pace of either 170 or 20 milliseconds, depending on the current time condition (see below). After a short delay of 300 ms after all remaining tokens had moved to their targets feedback was given for 500 ms. The chosen target circle turned green (RGB: 0.5, 0.8, 0.2) or red (RGB: 1.0, 0.0, 0.0) and a green thumb up/red thumb down (correct/error) or a number indicating the points appeared in green (correct) or red (error), respectively for NO MONEY and MONEY. We designed two specific trial types: misleading trials and informative trials. Their characteristics were based on the development of the success probability (Equation 9 and Figure 3-1) throughout the trial. Success probability measures the objective likelihood for choosing the correct target and dynamically changes with every token movement (Cisek et al., 2009).

$$p(R|N_R, N_L, N_C) = \frac{N_C!}{2N_C} \sum_{k=0}^{min(N_C, 7-N_L)} \frac{1}{k!(N_C - k)!} \tag{9}$$

We restricted directional trials to not decrease their success probability after they crossed the upper limit of an uncertainty window (0.3 – 0.7). In order

to obtain independent trials, the sequence of the first seven tokens had to be unique. For misleading trials, we had the same restriction and additionally required the sequences to stay below 0.2 success probability for at least three token movements. As such, they really mislead the observer to the opposite (incorrect) target in the initial phase of the trial and only later reveal the correct choice. These definitions led to twenty different sequences of left/right token movements for each of the two trial types, directional and misleading trials. Other sequences (random) were selected randomly and only restricted in that they were not allowed to fit the other categories.

Task Design and Experimental Procedure. We invited the subjects twice into the laboratory. On average session 1 lasted 45.98 minutes (SEM = 0.36) and session 2 lasted 42.38 minutes (SEM = 0.66). In the first session they received no financial incentive (NO MONEY), in the second session they could earn bonus money for fast and correct responses (MONEY). An icon reminded the participant of the current reward condition and was visible at all times during the experiment in the top right corner of the screen. The order of the sessions was fixed for all participants. During MONEY, participants earned points depending on their response speed. Starting with 15 points, the number of points decreased by one with every token that moved into its target position. Wrong answers always ended up with 0 points. The reward points accumulated across the session were translated into a bonus payment (14 points == 3 cents). On average participants received a bonus of 4.31 EUR (SEM = 0.17). Participants were instructed before session 1, that they had to achieve an accuracy of 60% in both sessions for receiving their bonus in the end. Thereby, we wanted to restrict guessing strategies and increase motivation to perform well during the first session. Most participants reached the minimum accuracy for both sessions. Eventually, regardless of their performance, they received this bonus money. Within each session, there were eight blocks, which were alternating between fast and slow pace duration, respectively shorter or longer PDI. The starting condition was randomly selected and counterbalanced between participants (N_{FAST} = 17; N_{SLOW} = 17). The type was always instructed before starting the new block and an indicating icon (FAST = rabbit, SLOW = turtle) was visible at all times during the trial in the upper left corner of the screen. During FAST, participants could save time when they responded earlier, as a fixed number of trials needed to be completed throughout the experiment. This option for saving time was instructed before the experiment

and participants could familiarize themselves with the pace during practice trials. After each block participants received feedback about how much time within the experiment had passed via a progress bar, how many points they had collected in the current block and how much bonus money they had earned up until that moment. In sum, we had four different incentive conditions: time savings, monetary reward, both or neither. Each block consisted of eighty trials, forty of which were the predefined sequences (misleading and directional, Figure 3-1). The remaining forty trials were filler trials (random) to avoid learning or recognition. The order of trials was pseudo-randomized as we did not allow more than two repetitions of the same trial type with the same target. Before each session, participants were allowed to familiarize themselves with the task. They practiced eight or 16 (session 2) random FAST (50%) and SLOW trials.

7.1.3 EEG Data Acquisition and Preprocessing

We collected electrical brain potentials with a customized 61-electrode cap (EasyCap GmbH, Herrsching-Breitbrunn, Germany). Passive sensors (Ag/ AgCl) were placed in rings equidistantly around Cz. We added four external electrodes, two ocular electrodes were placed centrally below the eyes and two ECG channels were fixed on the left upper chest. The electrode at position CPz served as the online reference, and a ground electrode was placed between AF4 and Fz. Impedance rates were reduced below 10 kΩ by skin scrubbing and applying standard electrode gel. We recorded with 500 Hz sampling rate using two BrainAmp Amplifiers and the BrainVision Recorder 1.20 (Brain Products GmbH, Gilching, Germany). The raw EEG data for each participant and session were offline pre-processed by using customized scripts in MATLAB 2017a (server) and 2018a as well as the EEGLAB toolbox (Delorme & Makeig, 2004). We first applied a high-pass filter of 0.1 Hz and then a low-pass filter of 42 Hz. Afterwards, we re-referenced all electrodes to common average. The continuous signal was then epoched around 500 ms before and 5000 ms after trial onset (fixation cross). We applied an adaptive detection procedure to detect artefactual epochs using the EEGLAB function *pop_jointprop()*. This algorithm finds a minimum of ten epochs and maximally 5% of trials that are above a certain number of SD away from the mean. It starts with 4.5 standard deviations and iteratively adjusts the size by 0.1 to meet the criteria. On average we rejected 28.09 ± 0.4 trials at 5.56 SD. We identified specific artefacts

from eye movements and muscle contraction with an adaptive mixture independent component analysis (AMICA 1.5, Palmer et al., 2012). For cleaner IC decomposition, we filtered the data more conservatively (high-pass: 1 Hz) and demeaned it prior to ICA. The resulting independent components were manually selected for rejection. The selection procedure was supported by using the ICLabel plugin (Pion-Tonachini et al., 2019). The selected IC components (N = 6.87 ± 0.32) were removed after the reference was added back to the data. Then, we removed the ocular channels and ran another adaptive artefact correction without a minimum rejection criterion. On average we rejected 24.87 ± 0.4 trials at 6.57 SD. Finally, we baseline corrected the epochs from 0 to 200 milliseconds after the fixation cross.

7.1.4 Data Analyses

All analyses were done using MATLAB 2018a or MATLAB 2017a (on server). We considered significance levels of $p < .05$ unless otherwise stated. We excluded misses, premature responses, first and last trials of each block. Reaction times were log-transformed per subject for all analyses. The datasets of each session (NO MONEY, MONEY) were treated independently, and were only compared with each other in second-level analyses.

Behavior. To validate the effect of urgency manipulations (time and monetary incentives) we explored RT and accuracy between the different conditions. We ran a repeated-measures ANOVA on RT and the proportion of correct trials (Pcor with MONEY (monetary incentive, yes or no), TIME (fast or slow block) and TRIAL (informative, misleading, or random) as factors. To validate the speed-accuracy across all participants, we correlated RT with Pcor. We also wanted to know whether the speed-accuracy trade-off was related to speed incentive and occurring within participants. Thus, we computed the difference (Δ) in RT and Accuracy between NO MONEY and MONEY and between FAST and SLOW, for each participant. Then, we correlated Δ RT and Δ Pcor.

Next, we wanted to know whether the normative evidence (success probability, Equation 9) or an approximation of evidence – the sum log likelihood ratio (SLLR, Equation 10, Cisek et al., 2009) explains behavioral observations better. The SLLR is a simple estimation of sensory evidence:

$$E_s(n) = \sum_{j=1}^{n} \frac{log(p(e_j)|S)}{(p(e_j|U))}, \tag{10}$$

where $p(e_j|S)$ is the likelihood of a specific token event ej during correct trials, and $p(e_j|U)$ is its likelihood during trials in which it is not correct. This, simply speaking, results in a momentary ratio of tokens within each target.

For finding the better fitting evidence measure, we ran two simple regression models with the following GLM:

$$Y = \beta_0 + \beta_1 * Evidence + \epsilon, \tag{11}$$

where Y is the RT and the predictor *Evidence* was either SP (Equation 9) or SLLR (Equation 10) at the estimated moment of the choice (two tokens prior to response). This token was selected as an approximation based on average simple reaction times (279 ms, SD = 45 ms) observed by Cisek et al. (2009). The token directly preceding the response (up to -200 ms) was unlikely to be considered for the choice as simple response preparation and execution would take more than 200 ms. We compared the resulting regression weights and R2-values per participant and session between models using paired-samples t-tests to evaluate the fit of the models.

Further, we wanted to explore whether heuristics and other factors had additional effects (above evidence) on choices and decision time. Firstly, we ran this GLM on RT:

$$\begin{aligned} Y = &\beta_0 + \beta_1 * EVIDENCE + \beta_2 * UPDATE + \\ &\beta_3 * TIME + \beta_4 * MONO + \beta_5 * CORRECT + \epsilon \end{aligned} \tag{12}$$

where Y is RT and the predictors were SLLR for the correct side at the moment of choice ($EVIDENCE$), whether the pre-choice update of evidence was towards the choice side $UPDATE$), FAST or SLOW block ($TIME$), how many tokens went into one direction before the choice ($MONO$), and whether the response was correct ($CORRECT$). Secondly, we ran a logistic GLM on the choice:

$$\begin{aligned} Y =& \beta_0 + \beta_1 * EVIDENCE + \beta_2 * UPDATE + \\ & \beta_3 * TIME + \beta_4 * MONO + \beta_5 * CORRECT + \epsilon \end{aligned} \tag{13}$$

where Y is the response side (Right = 1, Left = 0). The predictors were evidence (SLLR) for the right-hand side ($EVIDENCE$), whether the pre-choice token was towards the right-hand side ($UPDATE$), FAST or SLOW block ($TIME$), how many tokens went towards the right target before the choice ($MONO$), and whether the response was correct ($CORRECT$). All regression models included error and correct trials. We only excluded additional trials in which the previous trial had a missed or premature response. Significance of the regression weights was tested against zero per regressor. In second-level analyses, we compared regression weights of each regressor from the model for data of NO MONEY to MONEY with a paired-sample t-test. All p-values were corrected for multiple comparisons using the false discovery rate (FDR) method.

Time-frequency signal. The following transformations were ran on stimulus-, response-, and token-locked data (epoch limits were the same as above). Note, that for token-locked, we extracted several epochs out of the initial trial, thus we will not refer to trial-wise, but epoch-wise analyses in the following. We used Morlet wavelet transformation with six cycles to receive time-frequency data of all electrodes. We defined 27 linearly spaced frequencies from 5 to 30 Hz. The resulting power per frequency and time was log-transformed and baseline free. For further analyses (see Single-Trial Regression) we collapsed over our frequency band of interest: beta power (13-30 Hz). As we were interested in the motor cortical lateralization of beta-power, we computed the epoch-wise difference (contra minus ipsilateral to the effector) in power between two motor electrode pairs (C3 & C4, CP3 & CP4). Then we averaged the Δ-power over electrode pairs. This resulted in one BPL timeline per epoch. We used this outcome to compute single-trial regressions. For exploratory purposes, we also averaged the BPL epoch dynamics over selected conditions (i.e. MONEY, TIME, RT, EVIDENCE, UPDATE) and over participants.

Time-domain signal. We performed two-fold transformations on the time-domain signal. Firstly, we considered epochs locked to the stimulus (-200 to 1000 ms) and to the response (-900 to 300 ms). Regions of interest were central

midline electrodes: Fz, Cz, CPz, Pz. We averaged trials according to different conditions and outcomes: NO MONEY vs. MONEY session, SLOW vs. FAST block, and high (NO MONEY: mean ± SEM = 3014.30 ± 3.49 ms; MONEY: 2645.01 ± 7.99 ms) vs. low (NO MONEY: 2446.99 ± 5.41 ms; MONEY: 1816.77 ± 15.25 ms) RT (based on a median split within participants). Secondly, we divided the trial epochs into new epochs locked to token-onset (0 to 600 ms). This aggregated the number of epochs up to 15 times (number of tokens within one trial), but post-response tokens were excluded. Here, we were able to explore effects directly related to the current state of evidence, both the momentary evidence update (pro vs. contra choice) and the evidence accumulated up to this point. The latter was split into to three evidence bins for averaging purposes: contra (SLLR < 0), low (SLLR > 0 and SLLR < 0.8), high (SLLR > 0.8). The token-locked signals were used for further single-trial analyses.

Single-trial regression. Our main goal in this study was to investigate the individual contribution of urgency and evidence on BPL. Specifically, we used a single-trial regression approach to explore the effect of different factors on these signals over time. Because we wanted to see the effect of the changing evidence within the trial, we used token-locked epochs (locked to the moment when evidence changes). Note, this includes overlaps of different epochs, as the token-to-token interval was 200 ms. The regression was run on the whole epoch from token-onset until 600 ms post-token. Input data (ERP, beta power, BPL) was first smoothed over 8 ms (4 timepoints) and the output was downsampled to 100 Hz. All models involved a robust regression fit to reduce the impact of outliers and were computed separately for each session (NO MONEY and MONEY) for each participant. We excluded token-epochs that appeared after the overt response in all models. First, we ran models for all electrodes including only correct trials:

$$\begin{aligned} Y =& \beta_0 + \beta_1 * EVI_{right} + \beta_2 * UPD_{right} + \\ & \beta_3 * TIME + \beta_4 * RT + \beta_5 * TOKEN + \epsilon, \end{aligned} \tag{14}$$

where Y is the beta power over the course of the epoch. We included the following regressors: evidence for the right side ($EVIright$), evidence update ($UPDright$), Time Condition ($Time$), log-transformed RT (RT), and

we controlled for token number within the trial ($TOKEN$). Secondly, we ran regression models on the BPL signal. Here, we included correct and error trials.

$$\begin{aligned} Y =& \beta_0 + \beta_1 * EVI_{response} + \beta_2 * UPD_{response} + \\ & \beta_3 * TIME + \beta_4 * RT + \beta_5 * TOKEN + \epsilon, \end{aligned} \tag{15}$$

where Y equals BPL and accumulated evidence ($EVI_{response}$) and the momentary evidence update ($UPD_{response}$) are coded relative to the response. All other regressors remained the same as above (Equation 14). Thirdly, we ran the same model on the time-domain EEG data (token-locked) of all electrodes, but excluded error trials. Each model yielded a timeseries of regression weights for each participant and per electrode, and reward condition (NO MONEY and MONEY). At each timepoint, we tested for significant deviation from zero with a simple one-sample t-test. We applied FDR-correction to correct for multiple comparisons. Finally, we applied cluster-based permutation tests to ensure that only robust time windows are interpreted. Therefore, we first excluded all single timepoints (without significant neighbor). Then, we performed 1000 permutations for each timeseries with randomly shuffled signs to produce an empirical H0 distribution and critical t-values. Original clusters which had a t-mass that was larger than that of the null-distribution were considered significant.

BPL Amplitude. For testing whether the BPL peak amplitude varies with response times we used simple linear regression models per subject:

$$Y = \beta_0 + \beta_1 * BPLpeak + \epsilon, \tag{16}$$

where Y equals the (log-transformed) RT per trial. The predictor ($BPLpeak$) was the average BPL amplitude over the time window from -200 ms to -50 ms before the response. The resulting regression weights (per subject) were tested for significance with a simple one-sample t-test.

7.2 Results

The present experiment was designed to investigate the effect of time pressure on decision-making performance and BPL, a neural correlate related to

evidence accumulation and motor output preparation. With our design, we expected to induce a speed-accuracy trade-off by using temporal and monetary rewards for speeded reactions. We also expected to find, that an estimation of evidence better represents behavior than the normative evidence strength. We further hypothesized that other decision-making strategies (heuristics) would influence decision outcome and time and that their utilization differed depending on urgency. Furthermore, we expected that BPL dynamics would be influenced by evidence and heuristics as well as a variation with RT. Moreover, we performed exploratory analyses on global beta power reductions and midline electrode ERPs.

7.2.1 Speed-accuracy trade-off

To validate our urgency manipulations, we first analyzed whether participants show a speed-accuracy trade-off related to the incentives we provided for speeded responses. Reaction time (RT) and the proportion of correct trials (Pcor) decrease with the amount of incentives that were provided for speeded responses (RT: TIME: $F(33,1) = 11.873, p = .0016$, MONEY: $F(33,1) = 72.349, p < .001$, TRIAL: $F(66,2) = 24.073, p < .001$; Accuracy: all $p < .001$; rm-ANOVA; Figure 3-2A, B). The reward types appear to be additive in their effect on RT and accuracy, the more reward we offered, the faster participants responded. Monetary bonus alone seems to motivate stronger response speeding than time savings alone (average difference ± SEM in informative trials: MONEY: 510.1 ± 9.9 ms; TIME: 146.3 ± 7.6 ms; $p < .001$; paired-samples t-test). Furthermore, RT is higher and accuracy is lower in misleading trials, compared to informative trials, which was intended by the design (average difference ± SEM: RT: -34.2 ± 2.2 ms, $p = 0.0133$; Pcor: 0.5188 ± 0.003, $p < .001$; paired-sample t-tests). Those trials initially mislead the evidence towards the wrong target and only later in the sequence provide evidence for the correct side. This leads to more errors in general and particularly in fast response trials. Across all trial types, we find an inter-subject speed-accuracy trade-off (SAT) in all reward conditions (NO MONEY-SLOW: $\rho = 0.7891, p < .001$, NO MONEY-FAST: $\rho = 0.7858, p < .001$, MONEY-SLOW: $\rho = 0.8988, p < .001$, MONEY-FAST: $\rho = 0.9041, p < .001$; Figure 3-2C). Moreover, intra-individual speed-accuracy adjustments are related to the reward we were offering for speeded responses. Within-subjects adaptations in RT (Δ RT) correlate with adaptations in accuracy (Δ Pcor) related to

monetary as well as time incentives (TIME: $\rho = 0.8953; p < .001$; MONEY: $\rho = 0.8765; p < .001$; Figure 3-2D).

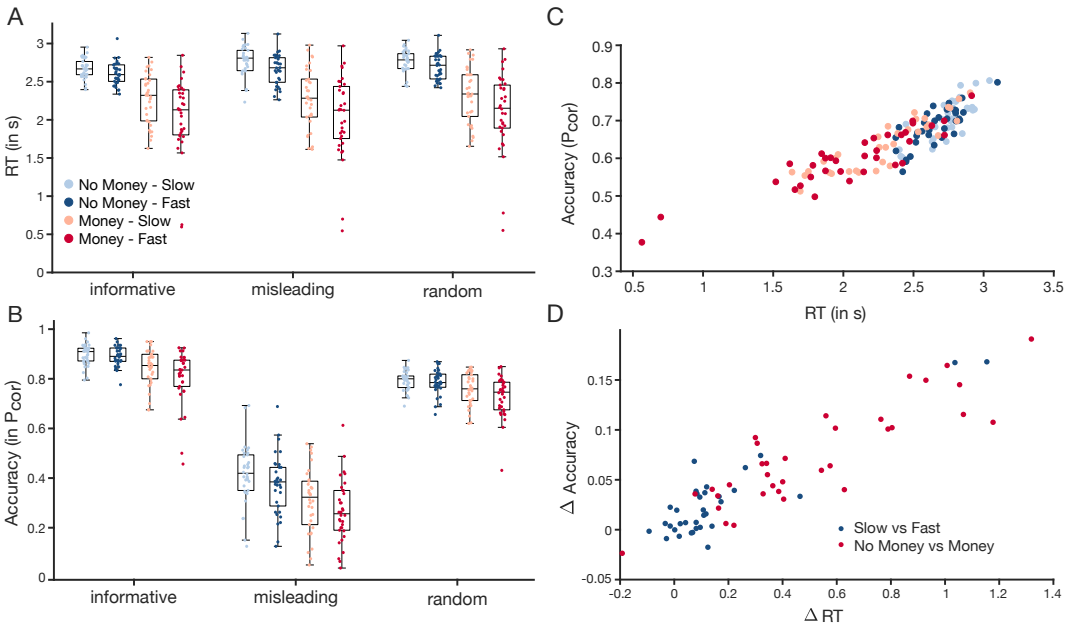

Figure 3-2. Speed-Accuracy Trade-off. Reaction times (A) and accuracy (B) by trial (informative, misleading, random) and incentive type (money and time). Dots represent individual participant average across the respective trials. Per participant accuracy (C) as a function of reaction time displayed separately for each reward condition. Per participant change in accuracy (D) as a function of change in RT for TIME (blue) and MONEY (red). Inter- (C) and intraindividual (D), speed-accuracy trade-off related to reward manipulations. Grouped boxplots were created using MATLAB scripts from Danz (2021).

7.2.2 Errors and Heuristics

Next, we aimed at strengthening our claim that speeded responses were related to our manipulation by inspecting the amount of misses and premature responses (Figure S3-1A, B). In unrewarded trials there were more missed trials as compared to the rewarded condition (TIME: $F(33, 1) = 13.034, p = 0.0010$; MONEY: $F(33, 1) = 39.194, p < .001$; rm-ANOVA). This is to be expected as speed was emphasized in rewarded conditions and thus misses were less likely. The opposite pattern was expected for premature responses, with more early presses in rewarded trials. We, however, could not find a clear difference between the conditions (TIME: $F(33) = 1.9389, p = .1731$; MONEY: $F(33, 1) = 4.028, p = .0530$; rm-ANOVA). Further, we explored potential response side biases (*choices*, Figure S3-1C) and found that in NO MONEY, responses were biased towards the left ($L/R < 0.5$), whereas in MONEY there

was less bias in choices ($F(33,1) = 7.1489, p = .0116$; rm-ANOVA). Temporal reward did not have an effect on choice bias ($F(33,1) = 0.4442, p = .5096$; rm-ANOVA). Together, these results support our expectations that stronger incentives enhance speed pressure and therefore reduce misses and increase premature responses in rewarded conditions. To parse out the influences on decision time and outcome, we wanted to inspect potential strategic variables that could be used to arrive at a decision. Thus, we explored potential heuristics that participants could use to make their choices. We first considered the monotony of the sequence, i.e. the number of tokens moving onto the eventually chosen direction prior to the choice. The results suggest less monotony prior to choices within rewarded conditions (TIME: $F(33,1) = 4.7678, p = .0362$; MONEY: $F(33,1) = 31.909, p < .001$; rm-ANOVA; Figure S3-1D). This could be due to lower RTs in these conditions as trials do not allow as much monotony as in low reward trials. Using multiple regression analyses (see *Heuristics influence RT and Choices*), we examined the independent effects of these predictors. Secondly, we explored whether or not a choice followed the direction of the pre-choice token (time of choice minus two tokens), we will call this evidence *update* from here on. We found, that monetary reward, but not temporal reward, increased the proportion of trials in which the final token side (update) was chosen (TIME: $F(33,1) = 0.1864, p = .6687$; MONEY: $F(33,1) = 38.689, p = .0062$; rm-ANOVA; Figure S3-1E). In sum, we show, that increased use of heuristics due to urgency might play a role in decision formation. We followed up on these findings with multiple regression analyses (see *Heuristics influence RT and Choices*).

7.2.3 Normative or Estimated Evidence?

Next, we looked into the relevance of different evidence variables. We aimed to find out whether the normative evidence or an estimation of evidence explains behavior best. The first measure is the success probability (SP), which is the variable we used to pre-define informative and misleading trial sequences. It takes into account the number of tokens that are still going to move and is thus a precise value of the likelihood for being correct. The second measure is the sum log likelihood ratio (SLLR), which considers only the previously observed token movements (as if we count the number of tokens on each side and take the ratio, while accounting for the likelihood of a left/right win for the movement to the respective side). We found that both types of evidence at the moment

of choice are reduced in urgent trials (SP: TRIAL: $F(66, 2) = 124.02, p < .001$,TIME: $F(33, 1) = 9.9585, p = .0034$, MONEY: $F(33, 1) = 34.731, p < .001$; SLLR: TRIAL: $F(66, 2) = 134.72, p < .001$, TIME: $F(33, 1) = 5.185, p = 0.0293$, MONEY: $F(33, 1) = 30.067, p < .001$, rm-ANOVAs; Figure 3-3A, B). This goes along with a previously observed shift towards faster, less accurate decisions in rewarded trials. An exception are the results in misleading trials. Here, lower evidence at the moment of choice was found in low rewarded trials compared to trials with high rewards. This reflects that evidence only slowly turns towards the wrong side. Thus, in very fast (and urgent) trials, misleading evidence might not have reached its peak yet, whereas in slower (less urgent) trials participants potentially responded later at a moment of strongest misinformation.

In order to find the measurement that better explains our observed decision times, we ran simple regression models and compared the regression weights model fits. We found that on average over participants, beta weights for SLLR were stronger (more negative) than for SP in both sessions (NO MONEY: $p = 2.2467e^{-16}$, MONEY: $p = 2.4061e^{-13}$, paired-samples t-test; Figure 3-3C). Additionally, the model fit (R2) of the models with SLLR as a predictor was significantly higher than of the SP-model in both sessions (NO MONEY: $p = 6.2737e^{-12}$, MONEY: $p = 0.0019$, paired-samples t-tests; Figure 3-3D). These results suggest that higher evidence for the choice predict faster responses when considering trial-wise adaptations. Firstly, these responses can be explained by evidence strength within each urgency condition. However, when comparing between conditions (see above) urgency encourages faster decisions at low evidence strength. Secondly, the stronger beta weights and model fit suggest that SLLR better predicts behavior (RT) in the present task. Thus, we decided to continue using SLLR in the following analyses. Importantly, we need to point out that the variations between conditions and trial types (Figure 3-3A, B) in evidence strength at the choice and the rather low model fit (Figure 3-3C) suggest that neither evidence measure can be the only driving factor for defining the moment of choice. More specifically, evidence strength itself does not represent a threshold that is needed to initiate a response. It is more likely that there are other influential variables and heuristics that influence the moment of response or modulate the response threshold.

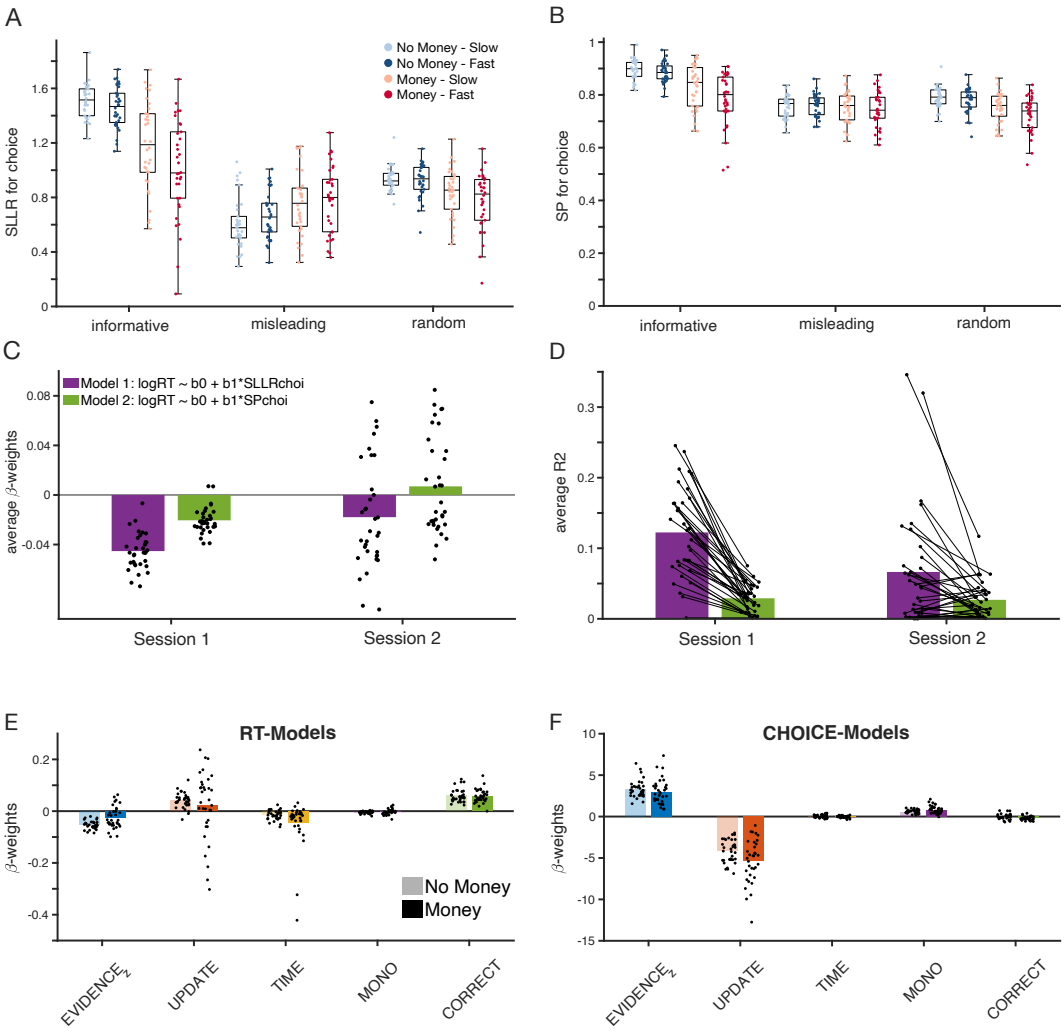

Figure 3-3. Evidence and heuristics. (A) Average sum log likelihood ratio for the choice and (B) success probability for the choice at the time of the response by condition and trial type. (C) Average regression weights per regression model, one per factor (SLLR [purple] and SP [green]) and reward (MONEY vs. NO MONEY) condition. (D) Average model fit (R2) per model organized as in C. Individual participant results are displayed with dots, lines link the values belonging to one participant. Regression weights of multiple regression analyses for RT-models (E) and CHOICE-models (F) with pale colors representing the results from NO MONEY and bright colors are from MONEY. Dots are regression weights from each individual participants. Cross-correlations between predictors can be found in Figure S3-2.

7.2.4 Heuristics influence RT and Choices

In order to understand what variables, besides evidence, influence behavior we performed multiple regression analyses. We will first consider influential factors on reaction time and in separate models the effect on the choice outcome. Here, we will also follow up on the potential relevance of heuristics (see *Errors and*

Heuristics) to understand their independent effect on choice time and outcome. We ran all analyses separately for both sessions (Figure 3-3E, F & Figure S3-2) and tested the regression weights for significance against zero.

RT-Models. This set of models was designed to explore the effects of different factors on response times (Equation 12). We included evidence strength and several heuristics to understand their relative contribution to explain decision time. Note, that negative regression weights mean that lower values of the regressor are associated with slow response trials (higher RT). The amount of evidence (SLLR for the choice) at the choice explains a significant amount of variance in RT in both, NO MONEY and MONEY ($p_{corr} < .01$, one-sample t-test), even if we account for several other factors. In slow response trials, evidence strength at choice was lower, whereas fast responses were performed at higher evidence strength. This could mean, that the response threshold decreases after some time and therefore later reactions tend to be performed at lower evidence. Also evidence update (whether or not, the token preceding the choice moved towards or against the choice direction), explains a significant amount of variance in RT in the first session (NO MONEY: $p_{corr} < .01$), but not in the second (MONEY: $p_{corr} = .3165$). Thus, an update pro-choice was more likely in slower responses, which could be explained by more reliance on this heuristic later in the trial. Participants might show increasing urgency over the course of the trial, and thus utilize simplification strategies in order to make a choice. The lack of this effect in MONEY trials could be related to the high variance in regression weights between participants. This regressor seems to reflect a variable that strongly differentiates decision-making strategies: participants attached more or less weight to the information given by only the pre-choice token. These strategic differences became observable in the much more critical session (MONEY), where individual responses were directly translated into monetary gain. Next, the Time condition was predictive of RT (trend in MONEY), with faster responses in the FAST condition, and slower responses in SLOW (NO MONEY: $p_{corr} < .001$; MONEY: $p_{corr} = .0091, \alpha_{corr} = .006$). This effect confirms our initial finding (see *Speed-accuracy trade-off*) that time savings encourage urgent reactions. Additionally, the models reveal that monotony is a significant predictor in NO MONEY ($p_{corr} < .001$), but not in MONEY ($p_{corr} = .1379$). There were more previous tokens moving monotonously into the choice direction in trials with slower responses. This heuristic, similar to evidence update, could become

only relevant later in the trial when participants need other information than evidence to make their choice under time pressure. Potentially, this strategy was overcome by the generally faster responses in MONEY, such that this heuristic was not necessary to use. The last regressor Correct confirms that speeded trials are less accurate (both: $p_{corr} < .001$). This effect holds on a single-trial level independent of reward condition.

Additionally, we formally wanted to compare the effects between NO MONEY and MONEY. We show that the strength of the regression weights differs only for evidence ($p_{corr} = .0018$; all other: $p_{corr} > .1263$, paired-samples t-test). In line with our hypothesis, decision times depend less on evidence estimations in MONEY, compared to trials without monetary rewards. In sum, we found that, additional to the estimated evidence, other factors and heuristics appear to influence the time for committing to a choice. Importantly, monetary reward (urgency) seems to affect the utilization of evidence for decision timing.

CHOICE-Models. With the following model we aim to explain what factors influence choice direction. We used multiple logistic regression analyses to explore to what extent evidence strength and heuristics affect the decision outcome (left or right hand choice, Equation 13). Note, negative regression weights mean that lower values of the regressor are more likely in right hand responses. First of all, estimated evidence at the moment of choice strongly influences the choice (both sessions: $p_{corr} < .001$, one-sample t-test): the more evidence towards the right the more likely a right hand response and vice versa for left hand responses. Interestingly, the recent update of evidence, i.e. whether or not the pre-choice token moved towards the left or right, inversely influences the choice direction (both sessions: $p_{corr} < .001$). This means, after a pre-choice token towards the right, choices towards the left were more likely. This effect could potentially be explained by our choice of the pre-choice token (two tokens prior to response). Not in every trial or individual, this token necessarily reflects the one bit of information that appeared just before the subject committed to the choice. Thus, we just have an estimation of the pre-choice information and need to be careful with interpretations. As expected, the third factor Time condition does not show any choice bias in both sessions ($p_{corr} > .1692$). The heuristic variable monotony explains a significant amount of variability in choices (both sessions: $p_{corr} < .001$). This means over and above estimated evidence and update, monotony of the sequences

was guiding the choice direction. Finally, we can derive from the model in MONEY that there is some bias towards incorrect in right hand side choices ($p_{corr} < .001$), which is not present in NO MONEY ($p_{corr} = .9990$). Perhaps, uncertain choices, that were more error-prone, tended to be performed with the dominant (right) hand. However, this remains speculation. Finally, we compared the regression weights between the two models in order to discern any urgency effect driven by monetary reward. We found no differences in most of the factors ($p_{corr} > .01$, paired-samples t-test), except for a trend in monotony ($p_{corr} = .0064, alpha_{corr} = .0020$), which suggests that a utilization of this heuristic could be more weighty under urgency. Together, we found that, besides the strength of accumulated evidence, the previous update and monotony of the sequence guide choice outcomes to some extent. The data suggest that under urgency (MONEY) choice outcomes are more strongly affected by a heuristic (*monotony*) than in contexts with low urgency (NO MONEY). However, the speed of responses (see above) under urgency seems to be driven by evidence and reward rather than monotony. In contrast, under low urgency the generally later responses offer more flexibility for response time adaptations and seem to be also affected by the monotony of the sequence.

7.2.5 Influential factors on global beta power

Next, we wanted to explore to what extent task variables are associated with whole-brain beta power. In particular, we used single-trial regression analyses to explain lateralized as well as midline beta-power modulations by accumulated (estimated) *evidence*, evidence *Update*, *Time* condition, *RT* and time on trial (*Token Number*). The outcome of the model was the respective time-series, locked to the each event of token-movement, i.e. when a token moved to its target within a trial. Thus, we do not remain in trial-space of regression analyses, but the epochs consist of several time windows from each trial. Firstly, we show that evidence (for the right response) is predictive of hemispheric lateralization (i.e. left motor cortical electrodes have negative regression weights, thus show stronger beta power reduction in right hand trials compared to left hand trials and vice versa for right hemisphere electrodes, Figure 3-4A). This effect appears significant from around token onset time to 450-600 ms after token onset for relevant motor electrodes C3, C4, CP3, CP4 (specific times can be found in shadings in Figure 3-4). Importantly, this prominent contrast between left and right hemisphere electrodes not only

reflects the lateralization after stimulus presentation but highlights that the strength of lateralization depends on the strength of evidence. This would not be possible to show by merely comparing averaged epochs, but requires to control for other task effects (e.g. *Token Number*), as we have done here with this single-trial regression approach. Secondly, we wondered whether there was an effect of the immediately preceding token (*Update*: pro or contra right hand) on beta-power. This regressor does not take into account the evidence history and thus not the full information presented on screen, but rather presents a heuristic that just considers the isolated novel information of the previous token move. Therefore, it can be understood as the momentary evidence. The regression weights represent again a distinctive motor lateralization. However, in comparison to *Evidence*, the *Update* regression weights are initially opposite to the choice direction (significant only in MONEY) and only sometime later after the token move take effect on the lateralization in the output direction (Figure 3-4B). Thirdly, Time does not have an effect on beta power at any electrode and time point, in both conditions (Figure S3-3A). Fourthly, in contrast, *Reaction Time* is reflected in central to central-posterior regions over the whole course of the epoch in both conditions (Figure 3-4C). Negative regression weights mean stronger beta power in faster trials. This points at a relevance of beta power in urgency as in fast response trials beta power appears to decrease faster and more strongly. Finally, we controlled for the effect of the 'time on trial' (*Token Number*). As expected, there is a strong and global effect (most pronounced over motor electrodes) throughout the full course of the epoch (Figure 3-4D). Beta power decreases with increasing number of token, which inherently means ongoing time in the trial and upcoming response initiation. This effect displays the downward ramping nature of beta power in preparation of a response throughout a trial.

7.2.6 Evidence and Update influence Beta Power Lateralization

Next, we investigated beta power lateralization and influential factors in detail. Therefore, we first considered time courses of the last ~4 token moves before the response obtained by response-locked averaging (Figure 3-5). We found beta-power and its hemispheric lateralization ramping downwards over the course of the trial (Figure 3-5A, B, C). The peak of lateralization was present just before the response and the onset and slope appeared to differ slightly between the sessions (MONEY vs. NO MONEY, Figure 3-5C). When sorting

BPL trajectories by TIME condition (FAST vs. SLOW blocks, Figure 3-5D), we can observe minor differences between the blocks within MONEY, such that BPL onset builds-up steeper and closer to the response in fast trials, which we could not confirm with single-trial regression analyses (see below). The observation of BPL dynamics for slow and fast responses (high vs. low RT, Figure 3-5E) reveals that trajectories in slower trials appear non-lateralized for longer and end up with a lower peak amplitude than fast responses. We confirmed a difference in BPL amplitude before the response related to RT by running a single-trial linear regression model (Equation 16) per participant. The resulting regression weights reveal a significant effect of strength of BPL prior to the response on RTs in both reward conditions (NO MONEY: $t(33) = 2.7244, p = 0.0102$; MONEY: $t(33) = 3.0006, p = 0.0051$; one-sample t-tests).

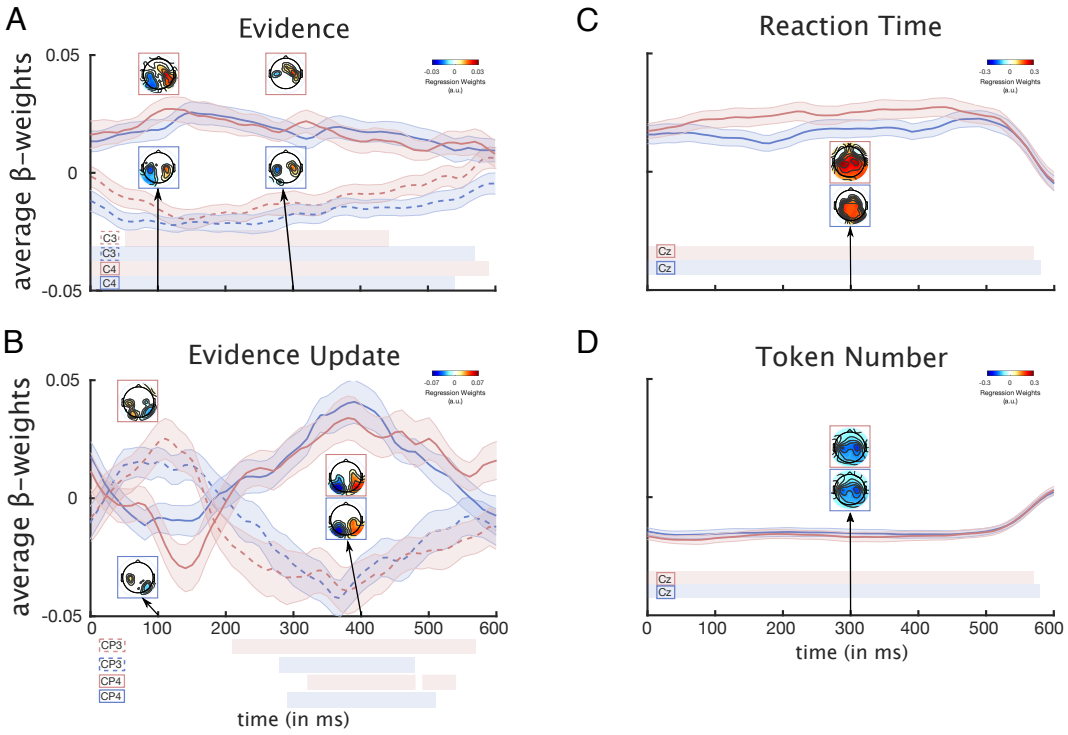

Figure 3-4. Factors influencing Beta Power at whole head and electrodes of interest. Token-locked time courses of the regression weights for Evidence for right hand response (A), Update (B), RT (C), Token Number (D) for relevant electrodes for both sessions, NO MONEY (blue) and MONEY (red). Dashed lines represent time courses for left hemisphere electrodes C3 (A) and CP3 (B), solid lines are from right hemisphere electrodes: C4 (A) and CP4 (B). Significant time windows (cluster-based permutation) are marked with the shading below each panel, separately for each electrode of interest. Time was non-significant at all times and is plotted in Figure S3-3. Topographies display whole head distribution of regression weights at interesting time points. Shade around the line represents SEM.

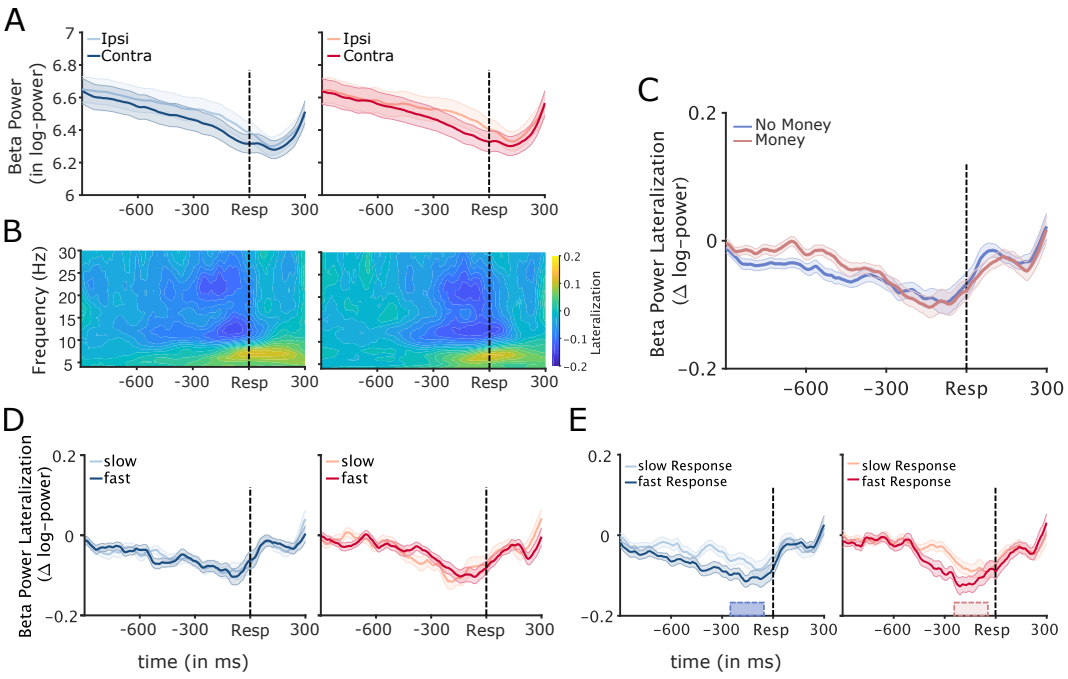

Figure 3-5. Beta Power Lateralization (BPL). (A) Response-locked average over contra- and ipsilateral beta power (13 - 30 Hz) ramps downwards at motor cortical electrodes (C3, C4, CP3, CP4) for both, NO MONEY (blue) and MONEY (red). (B) Lateralization (contra- minus ipsilateral to the effector) time-frequency plots show peak lateralization in beta band just before the response in both sessions (left: NO MONEY, right: MONEY). (C) BPL increases (contra < ipsi) over time towards response with slightly different trajectories in NO MONEY and MONEY. (D) BPL averaged over slow and fast trials (*Time* condition) and (E) averaged over trials with low and high *RT* (fast vs. slow response). A regression model reveals that peak amplitude (-200 to -50 ms before response, shaded bar at the bottom) varies with RT. Shaded areas represent SEM.

Together, these observations indicate that BPL trajectories are modulated by reward manipulations and relate to reaction times. In order to further test these claims and to understand the individual contribution of different factors we applied a single-trial regression approach with multiple predictors.

We developed a GLM with variables that are potentially influential for lateralization strength and latency. We ran this model on token-locked BPL to account for the changing evidence over the course of a trial. We included regressors Evidence, Update, Time Condition, RT and Token Number and computed regression weights for each factor over the course of the epoch (Figure 3-6 & Equation 15). Firstly,the regression weights show that the amount of Evidence (SLLR) has an effect on lateralization after a piece of information was presented (token move; Figure 3-6A). These negative beta-weights display

that stronger lateralization (negative) corresponds to higher evidence values, over and above the effects from token number and RT. Second-level analyses reveal no differences between beta-weights in NO MONEY vs. MONEY (all $p > .05$, paired t-test over timepoints 0 - 300 ms post-token). Secondly, we found that *Update* modulates BPL two-fold (Figure 3-6B): An initial instance occurs early after token movement in the opposite direction (stronger lateralization after contra choice information). A second modulation appeared later on, indicating that lateralization around this time is stronger after pro-choice tokens (negative regression weight). We ran second-level analyses over the whole course of the epoch to compare between the two sessions and found that the regression weights of Update tended to be more influential in MONEY at 110-120 ms and at 280 ms post-token ($p_{uncorr} <= .05$, paired t-tests). By exploring the averaged token-locked BPL signal (Figure 3-6B, right panel), we found that the first period accounts for a stronger effect of Update in MONEY compared to NO MONEY. The second period reflects an earlier onset of the Update effect in MONEY compared to NO MONEY. Taken together these results reflect potential differences in utilizing and reflecting heuristics under time pressure. In contrast to our expectations, Time had no effect on BPL at any timepoint over and above any of the other factors (Figure S3-3B). Perhaps, reaction time explained most variability that was related to this manipulation (TIME: FAST vs. SLOW). We can show, that RT appears as an influential factor consistently throughout the epoch (Figure 3-6C). This means that in fast response trials, BPL is more pronounced compared to slow response trials. In other words, in trials with long RT lateralization towards the chosen response is lower (more positive BPL) arising from later onset and lower peak amplitude in those trials (Figure 3-5E). This points at a potential relevance of urgency in BPL. Reduced RTs are descriptive of rewarded (urgent) conditions (see *Speed-accuracy trade-off*) and following from this, it could be that speed contexts affect BPL ramping which in turn speeds up responses. Finally, we confirm the effect of an ongoing downward ramping lateralization over the course of the trial in both sessions as *Token Number* is inversely related to BPL (Figure 3-6D).

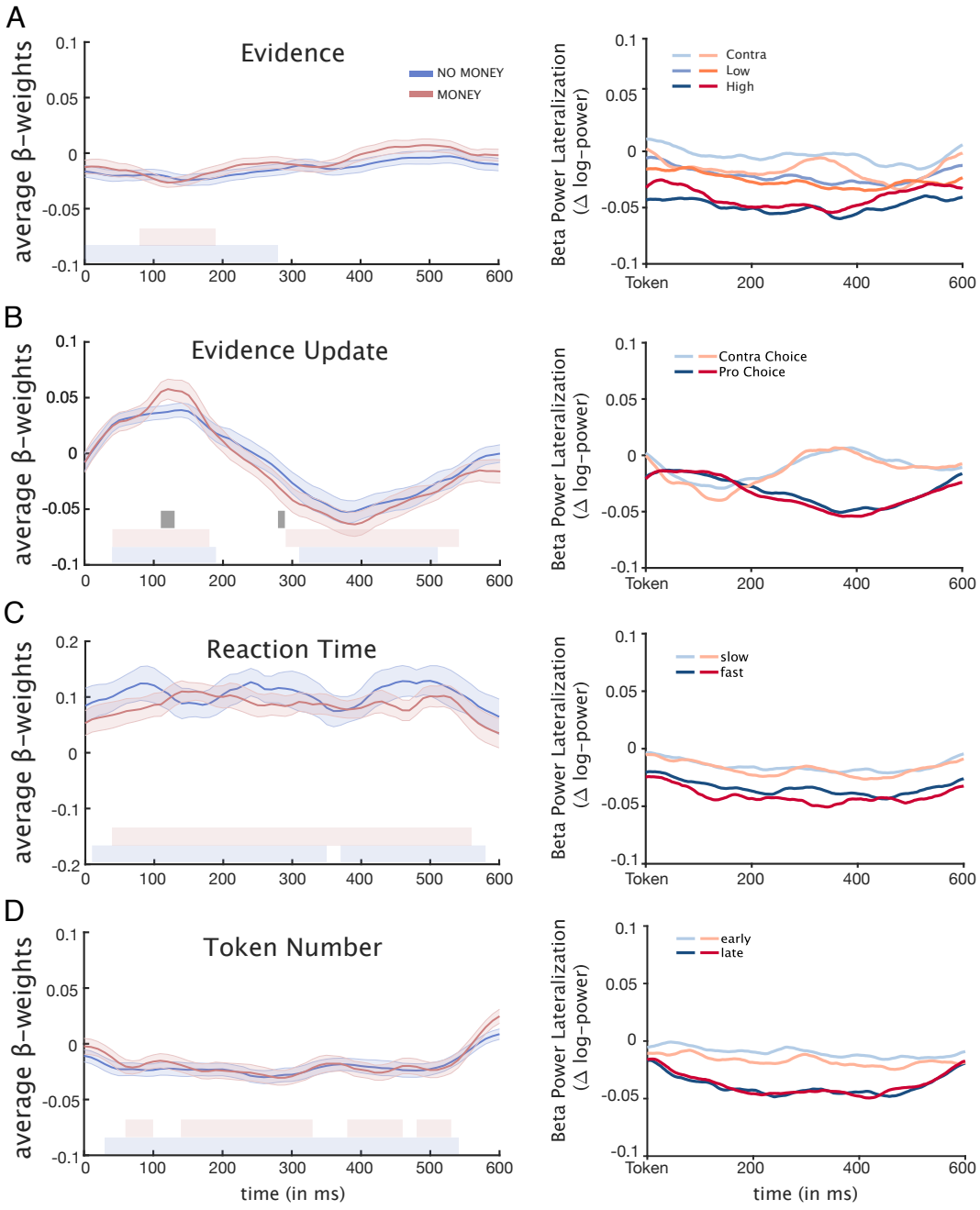

Figure 3-6. Factors influencing BPL. Left panels show token-locked time courses of regression weights for *Evidence* for the choice (A), *Update* (B), *RT* (D), *Token Number* (E) for both sessions (NO MONEY = blue and MONEY = red). Significant time periods (cluster-based permutation) are shaded below each panel. The regressor *Time* did not reveal any effect (Figure S3-3). For predictors *Evidence* and *Update*, we compared regression weights between both sessions at timepoints of interest (grey shaded area marks time periods with significant differences [uncorrected]) between NO MONEY and MONEY. Shaded areas around the lines represent SEM. Right hand panels display averaged token-locked BPL sorted by evidence strength (contra vs. low vs. high evidence for the choice), update direction (contra vs. pro choice direction), RT (low vs. high; median split) and Token Number within the trial (early vs. late; median split).

7.2.7 Influencing factors on central midline time-domain event-related potentials

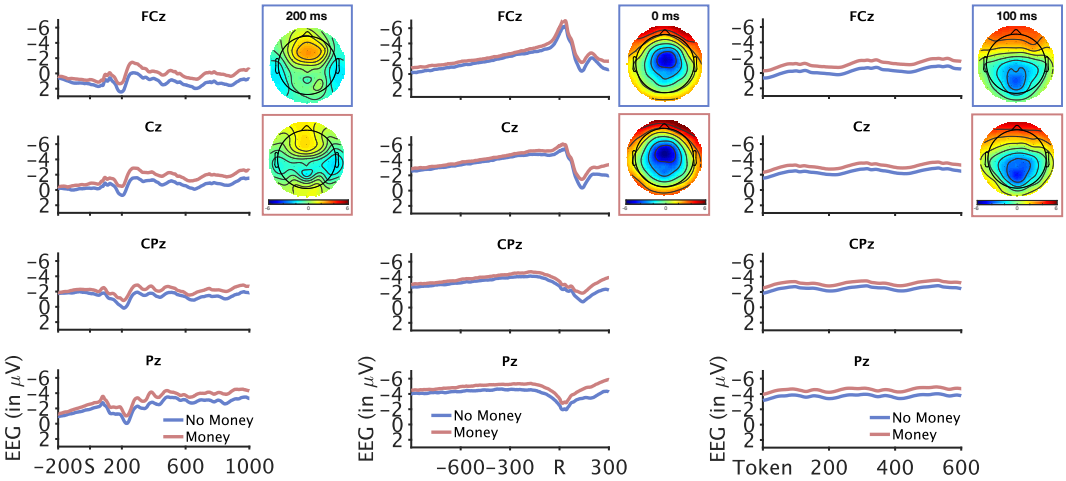

Figure 3-7. Midline electrode potentials by reward condition. The plots show ERPs locked to first token onset (stimulus, left panels), response (middle) and locked to each token onset (right). In midline electrodes and throughout the trial, MONEY (red) shows a consistently stronger negativation than NO MONEY (blue). Topographies show frontocentral to centroparietal negativity at 200 ms post-stimulus onset, at response onset and 100 ms post-token presentation.

Next, we asked whether reward and evidence and response time affected central midline ERPs (e.g. CNV). We observed qualitative differences and quantified the effects with single-trial regression analyses. Firstly, monetary reward reveals a stronger negativity over fronto-central and centro-parietal electrodes (stimulus-, response- and token-onset locked) compared to trials without monetary reward (Figure 3-7). Secondly, we observed a consistent effect of evidence strength on midline electrode negativation throughout the post-token period (Figure 3-7). High accumulated evidence for the response as well as an immediate evidence update for the choice increase negativity after token presentation. Thirdly, we observe slight differences between fast and slow (response time and time incentive, Figure S3-5) trials with a steeper slope of negativation in fast trials mainly over frontocentral and central regions. Upon response this difference disappears. For formal analyses of these observations, we used a single-trial regression approach which reveals independent effects of each regressor on the token-locked time-series of the midline electrodes (Figure 3-8). We found an effect of accumulated evidence on central midline electrodes around 300 – 600 ms post-token, but only under monetary reward. This effect reveals that less negativation occurs with stronger evidence, independent of update, reac-

tion time and reward condition (Figure 3-8A). The immediate evidence update, in contrast, shows intermittent effects on more posterior electrode negativation around 350 – 550 ms post-token in both sessions (Figure 3-8B). Time reward appears relevant in NO MONEY over the course of the token-locked epoch in the frontal central electrode, showing reduced negativation in fast compared to slow trials (Figure 3-8C). Negativation in frontal and frontocentral (only MONEY) electrodes appears to vary with RT over the course of the epoch. Stronger negativation in slower trials regardless of evidence, reward and 'time on trial' (Figure 3-8D). *Token number* (time on trial, Figure 3-8E) affects negativation over midline electrodes in both sessions throughout most of the epoch in that more time on trial leads to more negativation (drift over the trial up to response) which we also show in Figures S3-5 and 3-7.

7.3 Discussion

In this study we aimed at exploring the roles of evidence accumulation and urgency in perceptual decision-making and finding their neural underpinnings. In a slow perceptual decision-making paradigm, we manipulated the evidence given at each time and the amount of time pressure to respond. We found that under urgency evidence strength became less relevant for decision time and responses were faster and less correct independent of trial difficulty. Participants relied more on simplified evidence measures than objective evidence and also utilized heuristics such as the most recent update of evidence for their decisions. The relevance of evidence update became evident in beta power over fronto-lateral electrodes and in the difference between hemispheres (BPL). This effect, however, occurred with a delay after accumulated evidence was reflected. These neural signatures did not appear to be directly affected by urgency – neither temporal nor monetary reward. However, reaction times varied systematically with lateralization dynamics as well as urgency.

Decisions based on simplified evidence accumulation and heuristics. Firstly, instead of normative evidence participants based their decisions on an estimated evidence value (sum log likelihood ratio), which has been introduced by Cisek et al. (2009). A simplified evidence measure appeared to be more feasible to be computed online and good enough for performance in this dynamic task. Moreover, we found that other sources of information were utilized for predicting and timing choices, such as the recent update of evidence. It seems

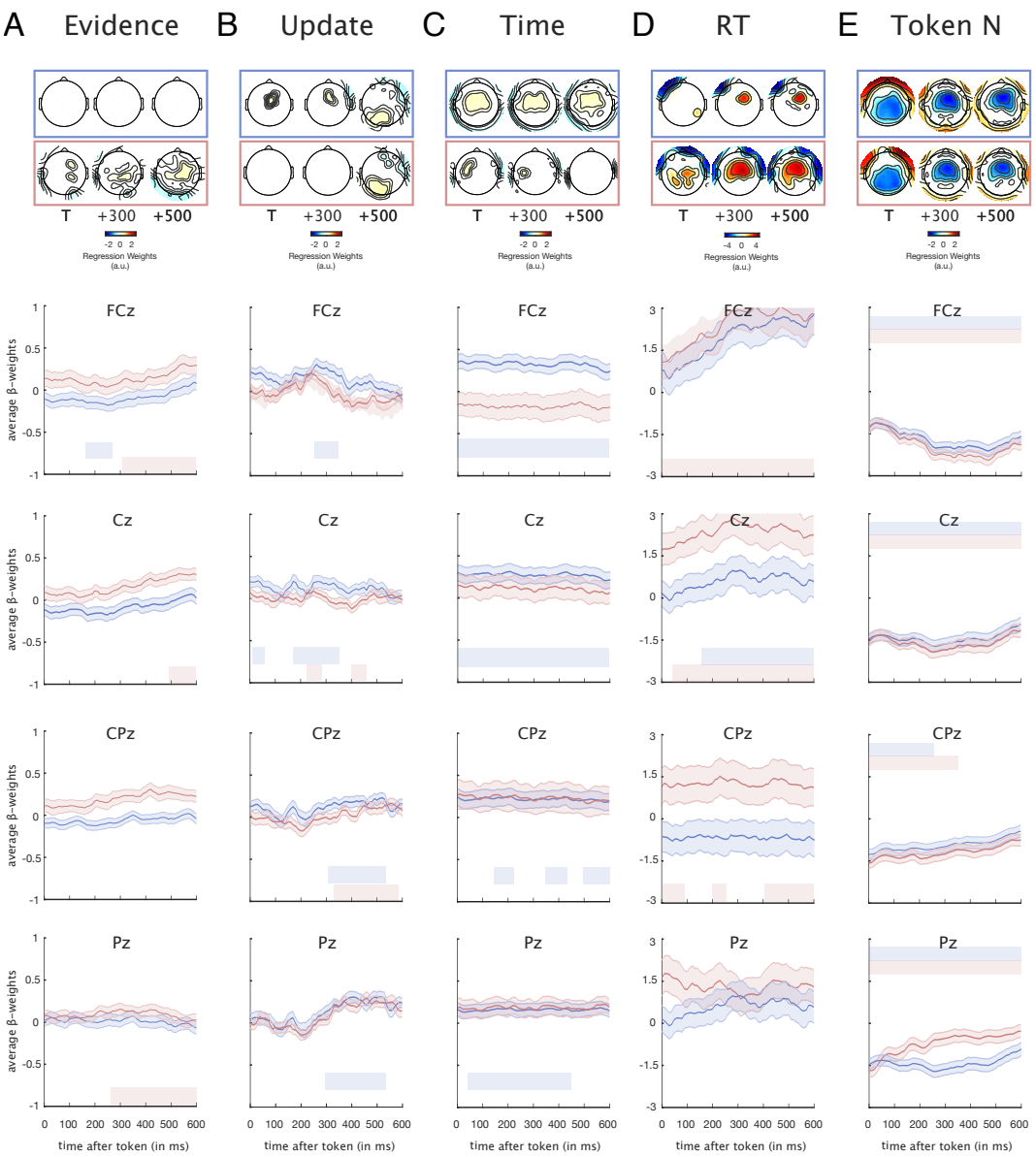

Figure 3-8. Whole-head EEG single-trial analyses. Regression weights over all electrodes (fdr-corrected topographies, referenced at Cz) at specific timepoints (token onset, 300 ms and 500 ms post-token) for the Regressors (A) Evidence, (B) Evidence Update, (C) Time Condition, (D) RT, (F) Token Number. Upper topographies (blue box) for NO MONEY and lower topographies (red box) for MONEY. Panels below display the regression-weight dynamics over the course of the epoch (0 to 600 ms post-token) for central midline electrodes (FCz, Cz, CPz, Pz; from top to bottom). Models were run separately for NO MONEY (blue) and MONEY (red). Shadings around the lines are SEM, shaded bars mark significant (cluster-based permutation) time windows.

that not only the overall evidence plays a role in decision making but also short-term information influences choices. The present findings relate to both, the urgency and the accumulation account of decision processing. We found

support for predictions of the urgency account (Cisek et al., 2009; Thura et al., 2014) which emphasizes the importance of momentary evidence, here evidence update, for decisions. At the same time, our data support the assumptions made by accumulation theories as we present a parametric influence of accumulated evidence on choices. We therefore do not conclusively support one or the other hypothesis, but rather propose, that both account for aspects that drive decisions.

Importantly, we also found that monetary reward for speed tended to make normative, well-informed decisions less likely. Our results indicate, that the speed of responses came at the cost of accuracy by reducing the effort that was put into evidence accumulation and partially relying more on easier available information. Recently it was suggested that urgent decision-making was particularly driven by the actual stimulus, than by a strategy underlying cognitive control (Poth, 2021). This corresponds to our study where resting a decision upon momentary evidence update appeared more likely under speed pressure. In contrast, a strategy underlying cognitive control may involve decisions based on the accumulated evidence and thus making a more informed but potentially time consuming choice. Consistently, we found that both pieces of information were relevant for decision timing and choices, but emphasis on heuristics tended to be stronger in speeded compared to accuracy conditions.

BPL – a neural correlate for integrating evidence. Most importantly, evidence accumulation over time plays a role in all conditions and is also represented in neural activity. Particularly, BPL was of interest in the present study. Even though, in an earlier study we found no evidence for scaled ramping trajectories in fast decision making tasks, e.g. the random dot motion paradigm (Rogge et al., 2022), the present results show that, indeed, BPL varies with evidence strength. The paradigm in this study is different in that it provides sequential evidence and offers a better window into the presented evidence strength at any moment in time. This slow evidence accumulation process appears to be reflected in beta activity over motor cortex and its lateralization strength. Thus, we further strengthen the idea that BPL is not a mere motor preparation signal but tracks decision making online to guide upcoming action selection (Fischer et al., 2018; Hunt et al., 2013).

Different kinds of urgency and boundary collapse. Urgency-related behavioral adaptations can occur due to different modes of speed pressure: instructions, deadlines or even an internal sense of time. Katsimpokis et al. (2020) described that different consequences are expected in tasks involving response deadlines compared to those involving a speed instruction (context). The former type of urgency builds up over time, whereas the latter leads to neural adaptation even before or throughout processing and remains rather constant over time. Deadlines would ultimately lead to long RTs with responses at low evidence, whereas context fosters premature responses. In our task, we applied both, urgency through context and deadlines. The urgent context was given by offering different reward options such as time savings and monetary bonus for faster response (the context was known in advance). Deadlines were implicitly induced by presenting a fixed amount of tokens and requiring the participant to decide and respond within the presentation time. Accordingly, we observed urgency to be evident in speeded responses at low evidence, but also by slow RTs at low evidence strength (i.e. urgency by deadline). Such complex interplay of decision time and evidence at the moment of choice associated with different types of urgency complicates the definition of a decision threshold – behaviorally as well as for a neuronal correlate. We cannot conclusively define whether decision time is based on dynamic bounds or static bounds with evidence gain modulations. Similarly, decision making models do not agree about incorporating speed adjustments into their mechanism. Some models involve dynamic bounds, which comprise of a decision threshold that is not defined by a fixed value of evidence but instead collapses over time at some (variable) rate. This has been considered in DDMs with collapsing bounds (e.g Drugowitsch et al., 2012) and models involving an independent urgency signal (Cisek et al., 2009; Hanks et al., 2014; Thura et al., 2014). Others suggest that starting points of evidence integration are biased depending on decision contexts (speed or accuracy) and that the gain of the decision variable could be increased (Hanks et al., 2014; Heitz & Schall, 2012). The authors propose that this effect results from modulatory recurrent network activity that is up-/down-regulated based on the context (for a review, see Standage et al., 2014).

Interestingly, adaptations in decision bounds have been related to interindividual differences, such as *Need for Closure* (Evans et al., 2017). Moreover, behavioral consequences of urgency (speeded decisions at low accuracy) were

conceptually related to behavioral phenotype of (trait-) impulsive individuals (Carland et al., 2019). Personality traits might, thus, affect our immediate decision making alongside long-term behavioral effects. Given these tendencies, it seems important to control for such effects in future studies.

Urgency Representations and BPL. Next to better understand behavioral consequences of speeded decision making, we considered neural correlates that were potentially affected by urgency. We were particularly interested in the effect of urgency on information integration in motor areas. Importantly, we did not find compelling evidence for the direct effect of urgency manipulations on the neural build-up of beta power reductions and BPL. We could show, however, that signal strength increases over time. This is consistent with other studies showing neural build-up activity as time elapses in cerebellum (Gao et al., 2018; Lin et al., 2020), prefrontal cortex (Jech et al., 2005), lateral intraparietal area (Churchland et al., 2008; Janssen & Shadlen, 2005; Leon & Shadlen, 2003) and motor cortex (Renoult et al., 2006). Interestingly, the noradrenergic system might be relevant too as pupil size increases over time (Joshi & Gold, 2020). As such long-range effects of urgency were found, it is surprising that we cannot observe an effect on BPL in the current study. One reason could be that a lot of variance was explained by RT. This predictor is prominent over time and RT itself is also related to urgency manipulations (i.e. lower RTs in urgent trials compared to no urgency). Therefore, we speculate that the reduction in RT is an expression of urgency, and RT, but not our manipulations directly, varies with beta power reductions and BPL. Similarly, clear variations in neural ramping by RT were previously found in BPL (Fischer et al., 2018) and other signals, such as pre-saccadic lateral intraparietal neuronal firing rates in monkeys (Hanks et al., 2014), CPP (Kelly & O'Connell, 2013; O'Connell et al., 2012), contralateral beta power reductions over motor cortex (O'Connell et al., 2012), alpha power and alpha power lateralization (Murphy et al., 2016). These variations have been interpreted in terms of starting point biases depending on speed (Fischer et al., 2018) and global gain activity under speed pressure (Murphy et al., 2016). Importantly and congruent with our results, RT modulations by motor desynchronization were independent of physical evidence (O'Connell et al., 2012). Thus, we conclude that our results are consistent with previous studies suggesting that urgency relates to RT changes which are reflected in neural activity. The lack of a direct effect of our urgency manipulation (financial and temporal rewards) could be due to too

low efficiency as Murphy et al. (2016) has previously suggested. Particularly, punishments were claimed to be more effective and should be considered for future tasks. The authors added that mild time-dependencies could potentially not be detected in single-trial analyses. In the case of BPL, low signal-to-noise ratio might explain the lack of findings. We noted similar difficulties in previous work (Rogge et al., 2022). This might be less of an issue in time-domain and averaged signals. We therefore included additional analyses for exploring other neural correlates that are potentially related to evidence and urgency integration during decision making.

Effects of urgency on time-domain scalp potentials . Exploratory analyses revealed the influence of task manipulation on time-domain EEG correlates. Of particular interest was the CNV, a signal over central electrodes, which was previously shown to reflect response planning (Scheibe et al., 2009) and event anticipation (Funderud et al., 2012; van Rijn et al., 2011). Importantly, the CNV has been related to alpha and beta power reductions during motor preparation, where particularly high alpha power was suggested to drive the late part of the CNV (Funderud et al., 2012). We also found negativation over central electrodes, which builds up towards the onset of each token (every 200 ms) and additionally presents a slow drift over the course of the trial with highest amplitudes just before the response. Similarly, the CNV ramps up before imperative stimuli. Thus, the present signal is comparable to the CNV, even though our paradigm is not a classic task to evoke a CNV. Most interestingly, however, is that time incentive (in NO MONEY) seems to diminish the strength of this signal over electrode FCz. Thus, more fronto-central regions might be relevant in urgency encoding that is evoked by the current speed context. This holds at least for trials in which urgency is not dominantly driven by financial reward and thus time savings might be motivating enough to adapt cognitive processing. This finding is in line with the idea of global gain modulation by Murphy et al. (2016). A very general increase in brain activity as a result of urgent context could also affect classical ERPs and thus indicate an increase of the general level of expectation and responsiveness as indexed by the CNV. Overall, little is known about the effect of urgency on ERPs in general. However, with single-trial analyses they could potentially serve as a robust non-invasive marker of decision making to gain insight into the effects of urgency.

Conclusion. Taken together, we find that slow evidence accumulation is reflected in beta power attenuation and its hemispheric lateralization after stimulus presentation. Additionally, other decision variables are encoded in BPL and drive behavior. Particularly, the update of evidence (most recent stimulus) appears relevant for choices and choice timing. Even though, we did not find that time pressure affects how evidence is tracked in the motor cortex, we could show that response times themselves are an expression of urgency and those vary strongly and consistently with BPL. Thus, our study adds to existing understanding of the BPL during decision formation, and provides insight into the role of urgency in decision making. Further research is needed to disentangle the relevance of different types of urgency during the decision process and to understand how it is essentially encoded to inform adaptive response times. Finally, this study was crucial for refining a paradigm that could eventually be used while recording subcortical activity, for example from dystonic patients receiving deep brain stimulation in the GPi (Hu & Stead, 2014). This brain structure seems to be of particular interest because urgency-related activity was previously recorded (Thura & Cisek, 2017, 2016). Such a study could shed light on causal effects of subcortical structures on decision and urgency processing.

7.4 Supplemental Material 2

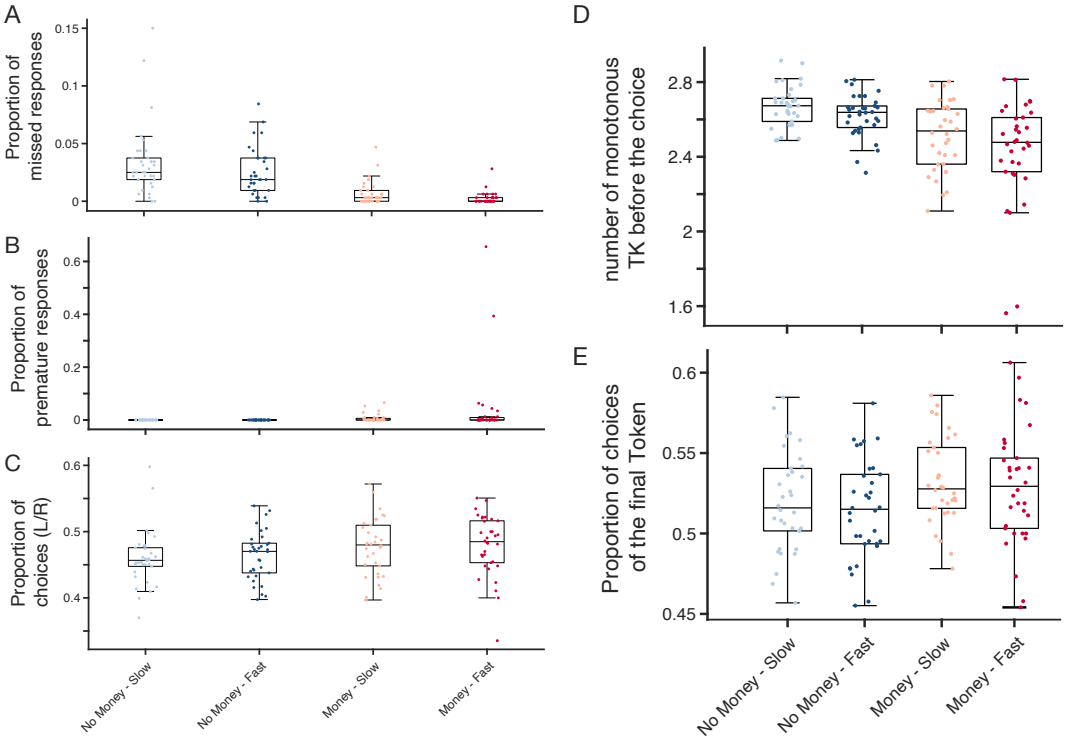

Figure S3-1. Errors and Heuristics. Proportion of missed (A) and premature (B) responses in different conditions. Potential biases and heuristics, that could affect choices and reaction times, were the proportion of choices (C), the monotony of the sequence prior to the response (D) and the proportion of responses that were in the same direction as the previous token (update). We collapsed over all trial types. Individual dots display within-participant average.

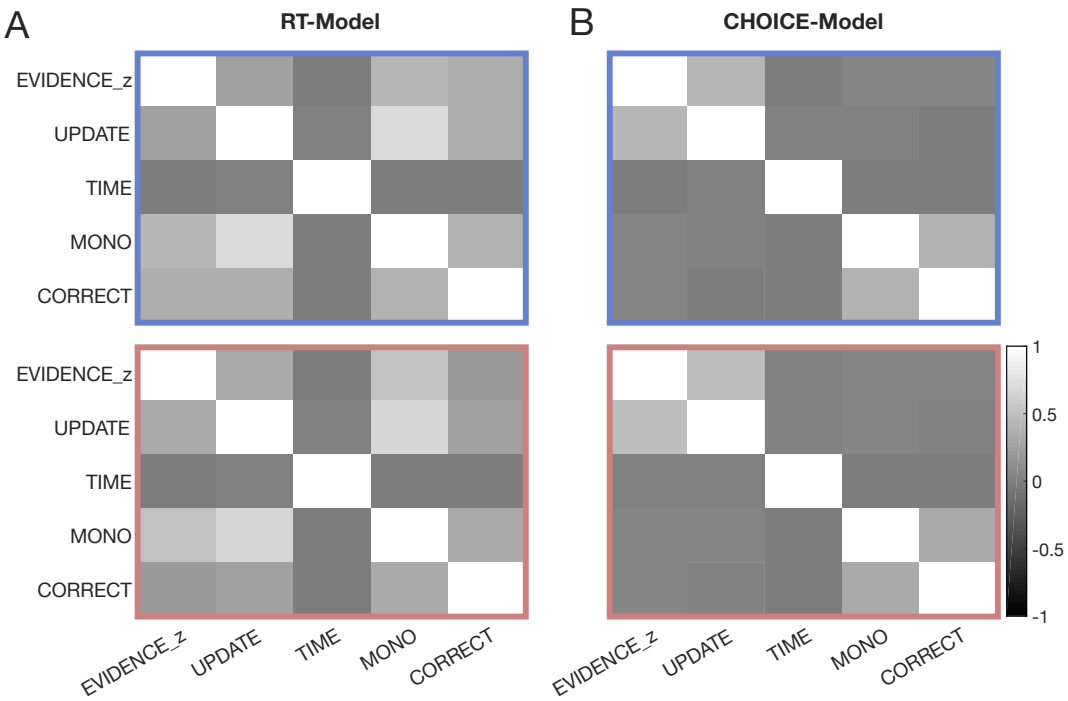

Figure S3-2. Correlation matrices for multiple regression on behavior (Figure 3-3). The averaged correlation strength between all regressors for the RT- (A) and the CHOICE-Models (B), where the top panels are for NO MONEY and bottom panels represent results from MONEY.

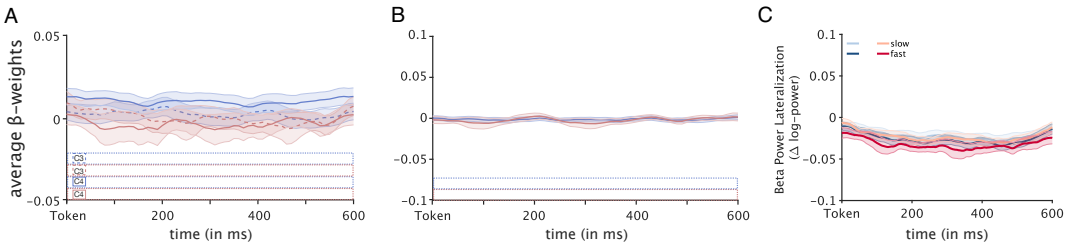

Figure S3-3. Regression weights for Time condition. (A) Time reward does not have an effect for 600 ms after the token presentation on the Beta Power at motor electrodes (C3, C4) in neither condition (NO MONEY = blue, MONEY = red). (B) The same lack of effects for regression on the beta power lateralization. (C) Averaged token-locked BPL sorted by Time condition (SLOW vs. FAST). These results complement Figures 3-4 and 3-6, respectively.

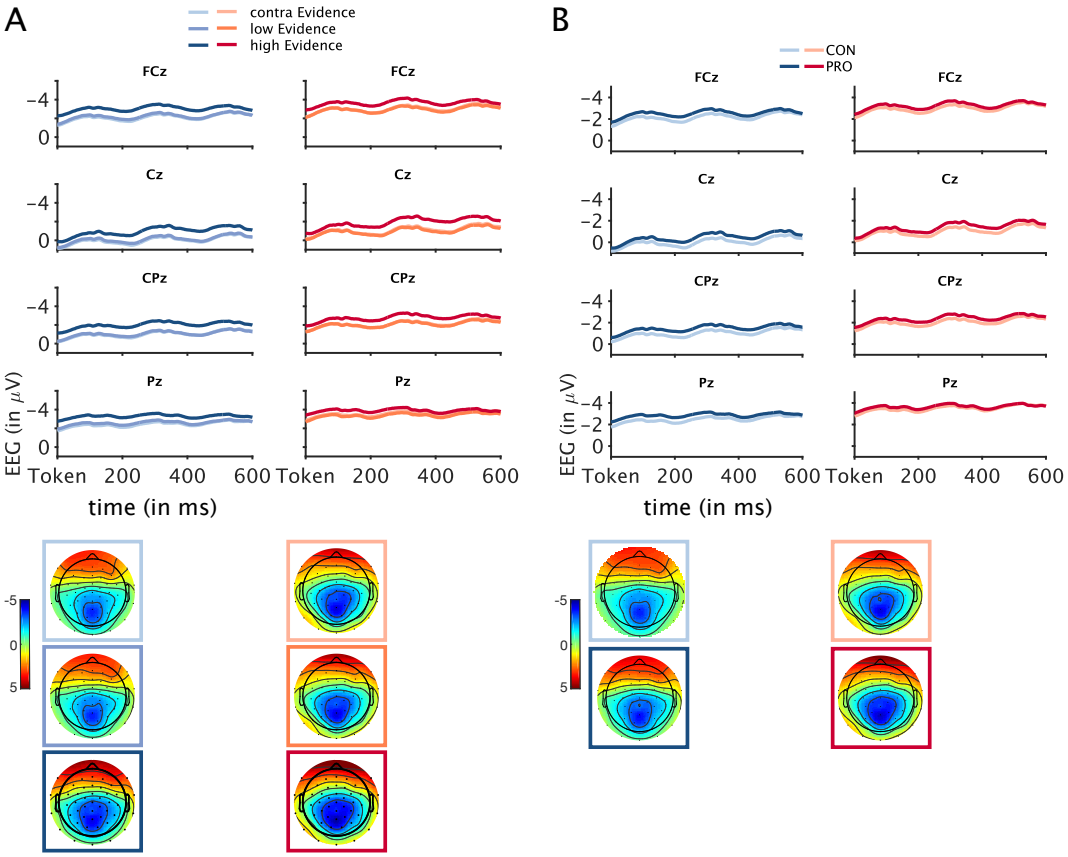

Figure S3-4. Token-locked ERPs by Evidence and Update. Timelines show ERPs of midline electrodes (FCz, Cz, CPz, Pz) up to 600 ms post-token separately for reward condition (NO MONEY = blue vs. MONEY = red). (A) Accumulated evidence (contra vs. low vs. high in choice direction) reveals stronger negativation (up) for high evidence compared to low and contra evidence (the latter two are almost on top of each other). Almost no differences can be observed related to (B) evidence update (contra vs. pro choice). Topographies display whole-head potentials 100 ms after token presentation.

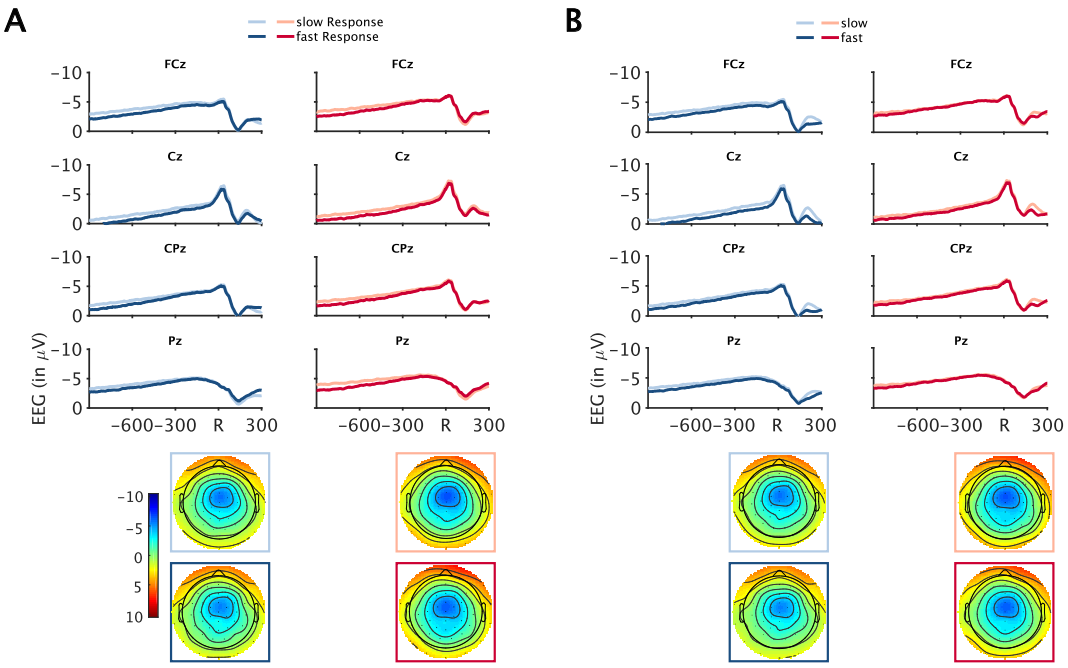

Figure S3-5. Response-locked ERPs by RT and Time. Timelines show ERPs of midline electrodes (FCz, Cz, CPz, Pz) locked to response onset separately for reward condition (NO MONEY = blue vs. MONEY = red), (A) RT (slow = light vs. fast = dark) and (B) Time incentive (SLOW = light vs. FAST = dark). Topographies display scalp potentials at the time of the response.

8 General Discussion

With the work presented here, I aimed at increasing our understanding of the role of lateralized beta power during decision making. I asked which decision-related variables are encoded by the BPL and whether it tracks ongoing processing throughout deliberation time. Moreover, I explored whether urgency influences evidence accumulation and whether this can be read-out from BPL trajectories.

In three studies, I recorded EEG while participants performed different forced-choice perceptual decision tasks. The paradigms varied in the amount of time that was allowed for the response (no vs. fixed vs. flexible delay between stimulus presentation and response cue, Exp. 1 & 3, Exp. 1, Exp. 2, respectively). In addition, the speed of reaction was emphasized to different degrees, with one task including a response deadline (Exp. 2), another (Exp. 3) involving rewards for fast reactions and yet another task (Exp. 1) allowing sufficient time for responding without any speed reward. Furthermore, the paradigms differed in how evidence for the choices was presented to the participants. In one task (Exp 2.) evidence was presented immediately without distractors or noise. In Experiment 1 participants saw immediately all evidence available for the given trial but with more or less noise. In the final task (Exp.3) information was presented sequentially, piece by piece.

I found several influential factors modulating BPL trajectories. Firstly, response delay variations in Experiments 1 & 2 revealed that BPL onset occurred consistently before the response cue regardless of fixed or flexible delay times. Furthermore, BPL trajectories clearly differed from the LRP dynamics. BPL emerged consistently locked to stimulus onset, similarly to no delay trials, whereas LRP onset varied systematically related to response cue times. Secondly, evidence presentation affected BPL dynamics. I found that stimulus strength modulated BPL amplitudes (Exp. 1) and that the momentary BPL strength related to both accumulated evidence and current evidence updating (Exp. 3). Thirdly, I could not find evidence for a direct link between urgency and BPL strength or evidence accumulation (Exp. 3). However, I observed an indirect effect: External speed pressure (rewards) affected behavior in that it decreased reaction times (Exp. 2 & 3); RTs in turn consistently explained variations in the build-up of BPL (Exp. 1 - 3).

In light of these findings, I will discuss the functional role of BPL in the decision process and speculate about perspectives in the following sections.

8.1 Can we use BPL as an online read-out for decision processing?

The presented work emphasizes the relevance of BPL as a window into decision processing. In particular the BPL appears to build a bridge from choice development to corresponding action implementation in specific decision contexts. I assume a predominantly effector-independent decision variable to develop elsewhere in the brain, perhaps reflected by the CPP (O'Connell et al., 2012). The BPL appears to represent this information in the motor output frame by tracking the variable online instead of in an all-or-nothing manner after choices are completed. This dynamic account seems to be adaptive in that it saves time and effort after decision termination as the motor system is already prepared for the intended motor execution.

How and what kind of evidence/decision information is being tracked by the BPL remains elusive. The present studies suggest that slow external evidence presentation can be encoded as an accumulated and momentary value of evidence in BPL. However, it seems less consistently observable when evidence is presented in a quickly rather than discretely. Therefore, I cannot strictly support one or another theory of decision making. While others claim only momentary evidence plays a role (Cisek et al., 2009) or merely accumulated evidence (Winkel et al., 2014), I propose that those frameworks are not mutually exclusive. Instead, they tend to uncover separate aspects of the complex decision-making process. I speculate that different tasks, such as the RDM task at hand and the Token Task, require different modes of processing to some extent. One task presents all evidence at once with different degrees of uncertainty and the decision maker has to infer evidence from a noisy stimulus, whereas in the other task evidence is presented without noise but step-wise. Thus, the accumulation process unfolds based on the external stimulus. Both tasks involve different kinds of uncertainty (perceptual vs. uncertainty related to expectation) which potentially require distinct processing mechanisms. Therefore, different results can be expected in terms of evidence tracking in these tasks. One option to potentially overcome this difference would be to present only the most recent token direction in the last paradigm (Exp. 3). This would require the decision maker to keep an internal representation of the evidence presented without a physical presentation of the current amount

of evidence. However, I did not select such a stimulus as this could be confounded by working memory processes and it does not provide an analogue to the RDM stimulus.

One commonality of all the presented tasks is the response delay. Depending on the task it was enforced or voluntary, fixed or flexible in time. Importantly, BPL occurs across all tasks, regardless of the type of delay, soon after stimulus onset and remains present until a response is initiated. Thus, BPL is not only a robust signal during decision processing but its continued presence throughout delay suggests further functionalities. One could understand the prolonged plateau during the 'wait-to-respond' phases as a kind of motor working memory. Along these lines, other studies (Spitzer et al., 2010; Spitzer & Blankenburg, 2011) found that beta-band power in prefrontal regions is related to somatosensory working memory. Conceptually, this would mean that after a choice has been made and decision making as well as the tracking of the decision variable are complete, the motor cortex remains in its state to enable an action as soon as it is required. Thus, the peak of the BPL does not necessarily indicate the time of response initiation as was suggested by Fischer et al. (2018) but rather marks the moment of terminated decision making (readiness to respond). Another trigger, however, would be needed to initiate the final action execution. From the present results, it becomes likely that the LRP is a potential candidate to mark this moment. It emerges after response cue onset and shows a steep and transient peak which is tightly linked to response onset. One could further speculate, that BPL serves as a gate for this final response trigger. BPL could, metaphorically speaking, act like a brake that is released but requires an additional acceleration force to finally carry out the action.

Such a gating task could also lead to speed-related adaptations: Once responses are allowed to be executed their implementation could be modulated by such a gating mechanism. The actual regulation of the speed of the response is probably encoded in basal ganglia (Frank, 2006; Thura & Cisek, 2017). However, the final implementation of more or less speeded actions could possibly be read out at the cortical level by BPL trajectories. The present results reveal that the strength of BPL differed according to the length of reaction times. Thus, it appears to relate to speed adjustments and might give insight into online processing of speed adjustments. On the other hand, I did not find direct ef-

fects of rewards for fast reactions, although I did find behavioral adjustments. This is not necessarily in opposition of our conclusion. Rather, it shows, that reaction times are directly related to BPL, whereas external speed manipulations may correlate more directly with subcortical structures that regulate speed adjustments. Sudden changes in speed regimes midway through processing, as was previously demonstrated using evidence strength (O'Connell et al., 2012), could deliver more insight into the direct relation between speed instruction and BPL strength. The discrete presentation of evidence, as in the Token Task, could also be beneficial for such purposes, as different levels of evidence could be explored in depth at such moments of interruption.

In conclusion, BPL is a promising candidate for online read-out of the current state of the decision, which is in line with suggestions by Hunt et al. (2013) and Fischer et al. (2018). Presumably, it provides a bridge between decision processing and motor execution by encoding decision- and output-relevant variables.

8.2 Is decision making a sequential process?

From the presented results on BPL over motor cortical regions I infer that decision-related information is tracked in the output frame of reference. This means that at any moment during deliberation time the current state of the decision is encoded by the sign of the lateralization. If the preliminary choice would have to be put into action, one could potentially derive which effector will be used (and thus which choice was dominant at that moment). This, in turn, means that motor cortices not only become involved in the decision process once a choice is finalized. This area appears to play an important role from much earlier on (in Exp. 1 and 2 around 400 ms post-stimulus) by tracking a hypothetical decision variable. In contrast, sequential accounts pose that processing stages occur in succession but might not be completely independent (Sternberg, 1969). Here, however, we found evidence for parallel processing theories because activity over motor cortex was recorded before motor output was required. Similarly, Hunt et al. (2013) concluded that value-guided choices involved parallel processing and Siegel et al. (2015) described the parallel activity in several cortical regions and the relevance of feedback loops for sensori-motor choices. The continuous flow of information theory (Eriksen & Schultz, 1979; Coles, 1989) describes that information processing does not occur sequentially, one sub-function after the another, but that processing stages

overlap. In these studies, visual detection tasks revealed that the motor system was 'primed' for several response options early during visual processing. Over time the alternatives became more and more restricted.

The present results support the idea that information 'leaks' into motor cortical regions throughout processing and therefore aid action preparation or enhance excitability prior to choice commitment. Similarly, Klein-Flügge and Bestmann (2012) previously suggested that corticospinal excitability increased in parallel to decision processing. Consistent with this, I argue that BPL is an inverse correlate of motor cortical excitability that represents the current decision state. Note, that the present results are insofar limited as they do not allow for causal inferences. Here, I present strong links to different decision variables, a robust temporal association with the deliberation time and a dissociation from a signal that tends to merely prepare the action, i.e. the LRP. Together, these findings robustly support a parallel processing account, but whether evidence accumulation/decision processing causes the lateralized activity cannot be answered here. Future research should approach this question by using physical perturbation of motor cortical excitability (TMS) and explore influences on BPL trajectories.

The importance of such a mechanism becomes clear when we look at decisions under time pressure. In those situations, decision making could benefit greatly if excitability is indeed enhanced prior to response preparation. This mechanism appears to promote processing efficiency and could lead to greater rewards or lower losses. In natural environments, for example in foraging tasks, rewards might diminish with elapsing time (competitors) while time itself is costly as the agent looses the opportunity to forage elsewhere. Therefore, a mechanism that shortens the time from choice to action without loss of accuracy appears to be generally adaptive and probably evolutionary preferred.

In sum, the presented studies present evidence against a full sequential processing mode. Rather, decision variables are reflected simultaneously in a variety of brain regions, and processing appears to be parallel, at least to some degree.

8.3 How to find a representation of urgency in the cortex?

In light of the present results, one particular question remains to be answered: Can I find a direct cortical representation of the speed-accuracy trade-off, and

if so where and how is it encoded? In contrast to the hypotheses, I found no direct link between urgency manipulations or the resulting SAT on the strength of BPL in the present studies. One potential reason for the missing effect is the strong relationship between response times and BPL (see detailed discussion in *Urgency Representations and BPL*). In the following, I would like to give suggestions on how this problem could be addressed. Future studies should aim at disentangling the response speed from the influence of urgency. For that it would be useful to explore similar reaction times at different levels of urgency. An experiment could be designed such that urgency is manipulated by different deadlines at similar difficulty. In speed trials, where time is running out fast (i.e. early deadline), a response at 200 ms is rather urgent whereas in trials with late deadlines a response at the same time would be less urgent.

Additionally, the effects of response vigor on cortical signals open many opportunities to be explored in more depth. It was previously suggested that vigor is a behavioral implementation of urgency (Thura et al., 2014). Thus, if neural signal strength correlated with the magnitude of vigor conclusions about an alternative or additional mechanism through which urgency is encoded in the cortex could be drawn. So far the link was described between experimental manipulation (urgency by context) as well as time-on-trial (urgency by deadline) and behavioral invigoration (saccade timing). The origin of urgency and thus the invigoration of movements was suggested in basal ganglia output activity via the GPi (Carland et al., 2019). To my knowledge, this signals' cortical implementation into the decision signal has not yet been described. Therefore, it would be interesting to correlate subcortical SAT-adaptation signals, i.e. record GPi activation with deep brain stimulation electrodes, with the cortical signal related to decision implementation into the action (i.e. the BPL). At the same, time variations in vigor should be correlated with both signals' amplitudes to directly link the behavioral output to the neural correlates. It would be possible to measure the amount of vigor in humans by the velocity of the response action (as was done in the present Exp 2.), but probably also by the compression force exerted on a response device.

Together, the present findings cannot conclusively answer where and how urgency is implemented in the cortical representation of decision making. However, future studies can use previous findings as well the present results to develop new experimental designs to better understand the role of urgency in

decision processing.

8.4 Relevance of BPL for clinical settings

I presented a neural correlate that can potentially serve a an online read-out of current decision processing. It seems likely that future research could examine such markers to gain insight into dysfunctional decision-making processes. Executive functions are compromised in many psychiatric and neurological disorders but often individually affected sub-functions are not specifically determined. However, specialized treatments could serve the patients' recovery well. Thus, more fine-grained diagnostics are needed (Müller & Klein, 2019). If we understand the sub-skills, their neural underpinnings and behavioral signature, we could develop better diagnostic tools. In the current context, it was already shown that compulsive behavior or pathology (Banca et al., 2015; Rotge et al., 2008; Hauser, Moutoussis, Iannaccone, et al., 2017; Hauser, Moutoussis, Dayan, & Dolan, 2017) and substance abuse (Redish et al., 2008) potentially relate to dysfunctional evidence accumulation resulting in delayed or impulsive decision termination, respectively. I suggest that a neural marker of evidence processing, such as the BPL, could improve individualized diagnostics of executive functions. The non-invasive recording of online task processing could provide an insight into dysfunctional patterns of evidence accumulation. Furthermore, tasks that target very particular sub-functions are necessary to aid diagnostics. For example, specific paradigms requiring decision making and evidence accumulation, like the ones presented here, could be adapted for clinical test batteries. Accuracy and reaction times would give first insights into performance deficits at one particular function. EEG measurements of neural correlates could further complement initial behavioral test results.

8.5 Conclusion

Commitment is only meaningful insofar as an action is initiated.
(Thura et al., 2014)

This quote concisely illustrates the tight link between decision and action. The work I presented here tries to uncover a neural correlate of this link.

I found that BPL uniquely represents decision information within the action frame of reference. It seems that decision information is forwarded to motor cortex continuously throughout the deliberation process. Therefore, we can

gain insight into the current state of the decision.

To date there is plenty of evidence related to decision variables elsewhere in the brain and many findings are based on animal models. However, human decision making processing remains partially elusive. Most importantly, we do not know exactly how choices turn into actions.

Here, I presented a neural correlate that could serve as a link between decision processing and action by incorporating several relevant pieces of information from different brain areas. Thereby, it reflects the readiness of the motor cortex to prepare for a particular action. It builds the bridge from top-level decision processing to downstream motor preparation and execution units.

References

Alegre, M., Gurtubay, I. G., Labarga, A., Iriarte, J., Malanda, A., & Artieda, J. (2003). Alpha and beta oscillatory changes during stimulus-induced movement paradigms: Effect of stimulus predictability. *Neuroreport*, *14*(3), 381–385.

Androulidakis, A. G., Doyle, L. M., Yarrow, K., Litvak, V., Gilbertson, T. P., & Brown, P. (2007). Anticipatory changes in beta synchrony in the human corticospinal system and associated improvements in task performance. *Eur. J. Neurosci.*, *25*(12), 3758–3765.

Banca, P., Vestergaard, M. D., Rankov, V., Baek, K., Mitchell, S., Lapa, T., ... Voon, V. (2015). Evidence Accumulation in Obsessive-Compulsive Disorder: the Role of Uncertainty and Monetary Reward on Perceptual Decision-Making Thresholds. *Neuropsychopharmacology*, *40303*(10), 1192–1202.

Barne, L. C., de Lange, F. P., & Cravo, A. M. (2020). Prestimulus alpha power is related to the strength of stimulus representation. *Cortex*, *132*, 250–257.

Bennur, S., & Gold, J. I. (2011). Distinct Representations of a Perceptual Decision and the Associated Oculomotor Plan in the Monkey Lateral Intraparietal Area. *J. Neurosci.*, *31*(3), 913–921.

Berger, H. (1929). Über das Elektrenkephalogramm des Menschen. *Arch. Psychiatr. Nervenkr.*, *87*(1), 527–570.

Bergmann, T. O., Lieb, A., Zrenner, C., & Ziemann, U. (2019). Pulsed Facilitation of Corticospinal Excitability by the Sensorimotor μ-Alpha Rhythm. *J. Neurosci.*, *39*(50), 10034–10043.

Bogacz, R., Brown, E., Moehlis, J., Holmes, P., & Cohen, J. D. (2006). The Physics of Optimal Decision Making: A Formal Analysis of Models of Performance in Two-Alternative Forced-Choice Tasks. *Psychol. Rev.*, *113*(4), 700–765.

Bogacz, R., Hu, P. T., Holmes, P. J., & Cohen, J. D. (2010). Do humans produce the speed-accuracy tradeoff that maximizes reward rate? *Q. J. Exp. Psychol.*, *63*(5), 863.

Brainard, D. H. (1997). The Psychophysics Toolbox. *Spat. Vis.*, *10*(4), 433–436.

Britten, K. H., Shadlen, M. N., Newsome, W. T., & Movshon, J. a. (1992). The analysis of visual motion: a comparison of neuronal and psychophysical performance. *J. Neurosci.*, *12*(12), 4745–4765.

Carland, M. A., Thura, D., & Cisek, P. (2019). The Urge to Decide and Act: Implications for Brain Function and Dysfunction. *Neuroscientist*, *25*(5), 491–511.

Cavanagh, J. F., Wiecki, T. V., Cohen, M. X., Figueroa, C. M., Samanta, J., Sherman, S. J., & Frank, M. J. (2011). Subthalamic nucleus stimulation reverses

mediofrontal influence over decision threshold. *Nat. Neurosci.*, *14*(11), 1462–1467.

Churchland, A. K., Kiani, R., & Shadlen, M. N. (2008). Decision-making with multiple alternatives. *Nat. Neurosci.*, *11*(6), 693–702.

Cisek, P., Puskas, G. A., & El-Murr, S. (2009). Decisions in Changing Conditions: The Urgency-Gating Model. *J. Neurosci.*, *29*(37), 11560–11571.

Codol, O., Holland, P. J., Manohar, S. G., & Galea, J. M. (2020). Reward-Based Improvements in Motor Control Are Driven by Multiple Error-Reducing Mechanisms. *J. Neurosci.*, *40*(18), 3604–3620.

Coles, M. G. (1989). Modern Mind-Brain Reading: Psychophysiology, Physiology, and Cognition. *Psychophysiology*, *26*(3), 251–269.

Coles, M. G., Gratton, G., Bashore, T. R., Eriksen, C. W., & Donchin, E. (1985). A psychophysiological investigation of the continuous flow model of human information processing. *J. Exp. Psychol. Hum. Percept. Perform.*, *11*(5), 529–553.

Danielmeier, C., & Ullsperger, M. (2011). Post-Error Adjustments. *Front. Psychol.*, *2*, 233.

Danz, A. (2021). *boxplotGroup.* MATLAB Central File Exchange.

De Lange, F. P., Rahnev, D. A., Donner, T. H., & Lau, H. (2013). Prestimulus Oscillatory Activity over Motor Cortex Reflects Perceptual Expectations. *J. Neurosci.*, *33*(4), 1400–1410.

Deecke, L., Grözinger, B., & Kornhuber, H. H. (1976). Voluntary finger movement in man: Cerebral potentials and theory. *Biol. Cybern.*, *23*(2), 99–119.

de Jong, R., Wierda, M., Mulder, G., & Mulder, L. J. (1988). Use of Partial Stimulus Information in Response Processing. *J. Exp. Psychol. Hum. Percept. Perform.*, *14*(4), 682–692.

Delorme, A., & Makeig, S. (2004). EEGLAB: an open source toolbox for analysis of single-trial EEG dynamics including independent component analysis. *J. Neurosci. Methods*, *134*(1), 9–21.

Derosiere, G., Thura, D., Cisek, P., & Duque, J. (2022). Hasty sensorimotor decisions rely on an overlap of broad and selective changes in motor activity. *PLOS Biol.*, *20*(4), e3001598.

Desmurget, M., & Turner, R. S. (2010). Motor sequences and the basal ganglia: kinematics, not habits. *J. Neurosci.*, *30*(22), 7685–90.

Ding, L., & Gold, J. I. (2013). The basal ganglia's contributions to perceptual decision making. *Neuron*, *79*(4), 640–9.

Ditterich, J. (2006). Evidence for time-variant decision making. *Eur. J. Neurosci.*, *24*(12), 3628–3641.

Donner, T. H., Siegel, M., Fries, P., & Engel, A. K. (2009). Buildup of Choice-

Predictive Activity in Human Motor Cortex during Perceptual Decision Making. *Curr. Biol.*, *19*(18), 1581–1585.

Doyle, L. M., Yarrow, K., & Brown, P. (2005). Lateralization of event-related beta desynchronization in the EEG during pre-cued reaction time tasks. *Clin. Neurophysiol.*, *116*(8), 1879–1888.

Drugowitsch, J., Deangelis, G. C., Angelaki, D. E., & Pouget, A. (2015). Tuning the speed-accuracy trade-off to maximize reward rate in multisensory decision-making. *Elife*, *4*(e06678), 1–11.

Drugowitsch, J., Moreno-Bote, R., Churchland, A. K., Shadlen, M. N., & Pouget, A. (2012). The Cost of Accumulating Evidence in Perceptual Decision Making. *J. Neurosci.*, *32*(11), 3612–3628.

Eimer, M. (1998). The lateralized readiness potential as an on-line measure of central response activation processes. *Behav. Res. Methods, Instruments, Comput.*, *30*(1), 146–156.

Engel, A. K., & Fries, P. (2010). Beta-band oscillations - signalling the status quo? *Curr. Opin. Neurobiol.*, *20*(2), 156–165.

Eriksen, C. W., & Schultz, D. W. (1979). Information processing in visual search: A continuous flow conception and experimental results. *Percept. Psychophys.*, *25*(4), 249–263.

Evans, N. J., Rae, B., Bushmakin, M., Rubin, M., & Brown, S. D. (2017). Need for closure is associated with urgency in perceptual decision-making. *Mem. Cogn.*, *45*(7), 1193–1205.

Farashahi, S., Ting, C. C., Kao, C. H., Wu, S. W., & Soltani, A. (2018). Dynamic combination of sensory and reward information under time pressure. *PLOS Comput. Biol.*, *14*(3), e1006070.

Fischer, A. G., Danielmeier, C., Villringer, A., Klein, T. A., & Ullsperger, M. (2016). Gender Influences on Brain Responses to Errors and Post-Error Adjustments. *Sci. Rep.*, *6*(1), 1–11.

Fischer, A. G., Nigbur, R., Klein, T. A., Danielmeier, C., & Ullsperger, M. (2018). Cortical beta power reflects decision dynamics and uncovers multiple facets of post-error adaptation. *Nat. Commun.*, *9*(1), 5038.

Fischer, A. G., & Ullsperger, M. (2013). Real and Fictive Outcomes Are Processed Differently but Converge on a Common Adaptive Mechanism. *Neuron*, *79*(6), 1243–1255.

Frank, M. J. (2006). Hold your horses: A dynamic computational role for the subthalamic nucleus in decision making. *Neural Networks*, *19*(8), 1120–1136.

Funderud, I., Lindgren, M., Løvstad, M., Endestad, T., Voytek, B., Knight, R. T., & Solbakk, A. K. (2012). Differential Go/NoGo Activity in Both Contingent Negative Variation and Spectral Power. *PLoS One*, *7*(10), e48504.

Gao, Z., Davis, C., Thomas, A. M., Economo, M. N., Abrego, A. M., Svoboda, K., ... Li, N. (2018). A cortico-cerebellar loop for motor planning. *Nature*, *563*(7729), 113.

Gilbertson, T., Lalo, E., Doyle, L., Di Lazzaro, V., Cioni, B., & Brown, P. (2005). Existing Motor State Is Favored at the Expense of New Movement during 13-35 Hz Oscillatory Synchrony in the Human Corticospinal System. *J. Neurosci.*, *25*(34), 7771.

Gold, J. I., & Shadlen, M. N. (2000). Representation of a perceptual decision in developing oculomotor commands. *Nature*, *404*(6776), 390–394.

Gold, J. I., & Shadlen, M. N. (2001). Neural computations that underlie decisions about sensory stimuli. *TRENDS Cogn. Sci.*, *5*(1), 10–16.

Gold, J. I., & Shadlen, M. N. (2002). Banburismus and the brain: Decoding the relationship between sensory stimuli, decisions, and reward. *Neuron*, *36*(2), 299–308.

Gold, J. I., & Shadlen, M. N. (2003). The influence of behavioral context on the representation of a perceptual decision in developing oculomotor commands. *J. Neurosci.*, *23*(2), 632–651.

Gold, J. I., & Shadlen, M. N. (2007). The Neural Basis of Decision Making. *Annu. Rev. Neurosci.*, *30*(1), 535–574.

Gratton, G., Coles, M. G., Sirevaag, E. J., Eriksen, C. W., & Donchin, E. (1988). Pre- and Poststimulus Activation of Response Channels: A Psychophysiological Analysis. *J. Exp. Psychol. Hum. Percept. Perform.*, *14*(3), 331–344.

Haggard, P., & Eimer, M. (1999). On the relation between brain potentials and the awareness of voluntary movements. *Exp. Brain Res.*, *126*(1), 128–133.

Hanks, T. D., Kiani, R., & Shadlen, M. N. (2014). A neural mechanism of speed-accuracy tradeoff in macaque area LIP. *Elife*, *2014*(3).

Hauser, T. U., Moutoussis, M., Dayan, P., & Dolan, R. J. (2017). Increased decision thresholds trigger extended information gathering across the compulsivity spectrum. *Transl. Psychiatry*, *7*(12), 1296.

Hauser, T. U., Moutoussis, M., Iannaccone, R., Brem, S., Walitza, S., Drechsler, R., ... Dolan, R. J. (2017). Increased decision thresholds enhance information gathering performance in juvenile Obsessive-Compulsive Disorder (OCD). *PLoS Comput. Biol.*, *13*(4), 1–19.

Heitz, R. P., & Schall, J. D. (2012). Neural Mechanisms of Speed-Accuracy Tradeoff. *Neuron*, *76*(3), 616.

Herz, D. M., Little, S., Pedrosa, D. J., Tinkhauser, G., Cheeran, B., Foltynie, T., ... Brown, P. (2018). Mechanisms Underlying Decision-Making as Revealed by Deep-Brain Stimulation in Patients with Parkinson's Disease. *Curr. Biol.*, *28*(8), 1169–1178.

Herz, D. M., Tan, H., Brittain, J.-S., Fischer, P., Cheeran, B., Green, A. L., ... Brown, P. (2017). Distinct mechanisms mediate speed-accuracy adjustments in cortico-subthalamic networks. *Elife*, *6*, e21481.

Hu, W., & Stead, M. (2014). Deep brain stimulation for dystonia. *Transl. Neurodegener.*, *3*(1), 2.

Hunt, L. T., Woolrich, M. W., Rushworth, M. F. S., & Behrens, T. E. J. (2013). Trial-Type Dependent Frames of Reference for Value Comparison. *PLoS Comput. Biol.*, *9*(9), e1003225.

Janssen, P., & Shadlen, M. N. (2005). A representation of the hazard rate of elapsed time in macaque area LIP. *Nat. Neurosci.*, *8*(2), 234–241.

Jasper, H., & Penfield, W. (1949). Electroeorticograms in man: Effect of voluntary movement upon the electrical activity of the preeentral gyrus. *Arch. Psychiatr. Nervenkr.*, *183*(1-2), 163–174.

Jech, R., Dušek, P., Wackermann, J., & Vymazal, J. (2005). Cumulative blood oxygenation-level-dependent signal changes support the 'time accumulator' hypothesis. *Neuroreport*, *16*(13), 1467–1471.

Joshi, S., & Gold, J. I. (2020). Pupil Size as a Window on Neural Substrates of Cognition. *Trends Cogn. Sci.*, *24*(6), 466–480.

Kaiser, J., Birbaumer, N., & Lutzenberger, W. (2001). Event-related beta desynchronization indicates timing of response selection in a delayed-response paradigm in humans. *Neurosci. Lett.*, *312*(3), 149–152.

Katsimpokis, D., Hawkins, G. E., & van Maanen, L. (2020). Not all Speed-Accuracy Trade-Off Manipulations Have the Same Psychological Effect. *Comput. Brain Behav.*, *3*(3), 252–268.

Kaufman, M. T., Churchland, M. M., Ryu, S. I., & Shenoy, K. V. (2014). Cortical activity in the null space: Permitting preparation without movement. *Nat. Neurosci.*, *17*(3), 440–448.

Kelly, S. P., Corbett, E. A., & O'Connell, R. G. (2020). Neurocomputational mechanisms of prior-informed perceptual decision-making in humans. *Nat. Hum. Behav.*, *5*, 467–481.

Kelly, S. P., & O'Connell, R. G. (2013). Internal and External Influences on the Rate of Sensory Evidence Accumulation in the Human Brain. *J. Neurosci.*, *33*(50), 19434–19441.

Khalighinejad, N., Bongioanni, A., Verhagen, L., Folloni, D., Attali, D., Aubry, J. F., ... Rushworth, M. F. (2020). A Basal Forebrain-Cingulate Circuit in Macaques Decides It Is Time to Act. *Neuron*, *105*(2), 370–384.e8.

Khalighinejad, N., Manohar, S., Husain, M., & Rushworth, M. F. (2022). Complementary roles of serotonergic and cholinergic systems in decisions about when to act. *Curr. Biol.*, *32*(5), 1150–1162.

Kiani, R., & Shadlen, M. N. (2009). Representation of confidence associated with a decision by neurons in the parietal cortex. *Science*, *324*(5928), 759–764.

Klaus, A., Alves Da Silva, J., & Costa, R. M. (2019). What, If, and When to Move: Basal Ganglia Circuits and Self-Paced Action Initiation. *Annu. Rev. Neurosci.*, *42*, 459–483.

Kleiner, M., Brainard, D., Pelli, D., Ingling, A., Murray, R., & Broussard, C. (2007). What's new in psychtoolbox-3. *Perception*, *36*(14), 1–16.

Klein-Flügge, M. C., & Bestmann, S. (2012). Time-Dependent Changes in Human Corticospinal Excitability Reveal Value-Based Competition for Action during Decision Processing. *J. Neurosci.*, *32*(24), 8373–8382.

Klein-Flügge, M. C., Nobbs, D., Pitcher, J. B., & Bestmann, S. (2013). Variability of Human Corticospinal Excitability Tracks the State of Action Preparation. *J. Neurosci.*, *33*(13), 5564–5572.

Kornhuber, H. H., & Deecke, L. (1964). Hirnpotentialanderungen beim Menschen vor und nach Willkurbewegungen dargestellt mit Magnetbandspeicherung und Ruckwartsanalyse. *Pflugers Arch. J. Physiol.*, *281*(1), 52.

Kornhuber, H. H., & Deecke, L. (1965). Hirnpotentialänderungen bei Willkürbewegungen und passiven Bewegungen des Menschen: Bereitschaftspotential und reafferente Potentiale. *Pflüger's Arch. für die gesamte Physiol. des Menschen und der Tiere*, *284*(1), 1–17.

Kutas, M., & Donchin, E. (1974). Studies of Squeezing: Handedness, Responding Hand, Response Force, and Asymmetry of Readiness Potential. *Science*, *186*(4163), 545–548.

Kutas, M., & Hillyard, S. A. (1980). Reading senseless sentences: Brain potentials reflect semantic incongruity. *Science*, *207*(4427), 203–205.

Lange, J., Oostenveld, R., & Fries, P. (2013). Reduced occipital alpha power indexes enhanced excitability rather than improved visual perception. *J. Neurosci.*, *33*(7), 3212–3220.

Leon, M. I., & Shadlen, M. N. (2003). Representation of time by neurons in the posterior parietal cortex of the macaque. *Neuron*, *38*(2), 317–327.

Lin, Q., Manley, J., Helmreich, M., Schlumm, F., Li, J. M., Robson, D. N., ... Vaziri, A. (2020). Cerebellar Neurodynamics Predict Decision Timing and Outcome on the Single-Trial Level. *Cell*, *180*(3), 536–551.e17.

MATLAB. (2012). *version 7.14 (R2012a).* Natick, Massachusetts: The MathWorks Inc.

MATLAB. (2018). *version 9.4 (R2018a).* Natick, Massachusetts: The MathWorks Inc.

Mazzoni, P., Hristova, A., & Krakauer, J. W. (2007). Why Don't We Move Faster? Parkinson's Disease, Movement Vigor, and Implicit Motivation. *J. Neurosci.*,

27(27), 7105–7116.

Miller, R. J., Patterson, N. T., & Ulrich, H. R. (1998). Jackknife-based method for measuring LRP onset latency differences. *Psychophysiology*, *35*(01), 99–115.

Müller, S. V., & Klein, T. (2019). *Diagnostik und Therapie von exekutiven Dysfunktionen bei neurologischen Erkrankungen.* Deutsche Gesellschaft fuer Neurologie.

Murphy, P. R., Boonstra, E., & Nieuwenhuis, S. (2016). Global gain modulation generates time-dependent urgency during perceptual choice in humans. *Nat. Commun.*, *7*(1), 13526.

Nagamine, T., Kajola, M., Salmelin, R., Shibasaki, H., & Hari, R. (1996). Movement-related slow cortical magnetic fields and changes of spontaneous MEG- and EEG-brain rhythms. *Electroencephalogr. Clin. Neurophysiol.*, *99*(3), 274–286.

Newman, D. P., Loughnane, G. M., Kelly, S. P., O'Connell, R. G., & Bellgrove, M. A. (2017). Visuospatial Asymmetries Arise from Differences in the Onset Time of Perceptual Evidence Accumulation. *J. Neurosci.*, *37*(12), 3378–3385.

Newsome, W. T., & Paré, E. B. (1988). A selective impairment of motion perception following lesions of the middle temporal visual area (MT). *J. Neurosci.*, *8*(6), 2201–2211.

O'Connell, R. G., Dockree, P. M., & Kelly, S. P. (2012). A supramodal accumulation-to-bound signal that determines perceptual decisions in humans. *Nat. Neurosci.*, *15*(12), 1729–1735.

Okazawa, G., Hatch, C. E., Mancoo, A., Machens, C. K., & Kiani, R. (2021). Representational geometry of perceptual decisions in the monkey parietal cortex. *Cell*, *184*(14), 3748–3761.e18.

Palmer, J. A., Kreutz-Delgado, K., & Makeig, S. (2012). AMICA: An Adaptive Mixture of Independent Component Analyzers with Shared Components. *Tech Rep.*, 1–15.

Pape, A. A., & Siegel, M. (2016). Motor cortex activity predicts response alternation during sensorimotor decisions. *Nat. Commun.*, *7*(1), 1–10.

Parker, A. J., & Newsome, W. T. (1998). Sense and the single neuron: probing the physiology of perception. *Annu. Rev. Neurosci.*, *21*, 227–277.

Pelli, D. G. (1997). The VideoToolbox software for visual psychophysics: Transforming numbers into movies. *Spat. Vis.*, *10*(4), 437–442.

Pfurtscheller, G. (1981). Central beta rhythm during sensorimotor activities in man. *Electroencephalogr. Clin. Neurophysiol.*, *51*(3), 253–264.

Pfurtscheller, G., & Berghold, A. (1989). Patterns of cortical activation during planning of voluntary movement. *Electroencephalogr. Clin. Neurophysiol.*, *72*(3), 250–258.

Pfurtscheller, G., Stancák, A., & Neuper, C. (1996). Post-movement beta synchronization. A correlate of an idling motor area? *Electroencephalogr. Clin. Neurophysiol.*, *98*(4), 281–293.

Pfurtscheller, G., Zalaudek, K., & Neuper, C. (1998). Event-related beta synchronization after wrist, finger and thumb movement. *Electroencephalogr. Clin. Neurophysiol.*, *109*(2), 154–160.

Pilly, P. K., & Seitz, A. R. (2009). What a Difference a Parameter Makes: a Psychophysical Comparison of Random Dot Motion Algorithms. *Vision Res.*, *49*(13), 1599–1612.

Pion-Tonachini, L., Kreutz-Delgado, K., & Makeig, S. (2019). ICLabel: An automated electroencephalographic independent component classifier, dataset, and website. *Neuroimage*, *198*, 181–197.

Ploner, M., Gross, J., Timmermann, L., Pollok, B., & Schnitzler, A. (2006). Oscillatory activity reflects the excitability of the human somatosensory system. *Neuroimage*, *32*(3), 1231–1236.

Poth, C. H. (2021). Urgency forces stimulus-driven action by overcoming cognitive control. *Elife*, *10*(e73682), 1–14.

Purcell, B. A., & Kiani, R. (2016). Hierarchical decision processes that operate over distinct timescales underlie choice and changes in strategy. *Proc. Natl. Acad. Sci. U. S. A.*, *113*(31), E4531–E4540.

Ratcliff, R. (1978). A theory of memory retrieval. *Psychol. Rev.*, *85*(2), 59–108.

Ratcliff, R., & McKoon, G. (2008). The diffusion decision model: theory and data for two-choice decision tasks. *Neural Comput.*, *20*(4), 873–922.

Reck, C., Florin, E., Wojtecki, L., Groiss, S., Voges, J., Sturm, V., ... Timmermann, L. (2009). Differential distribution of coherence between beta-band subthalamic oscillations and forearm muscles in Parkinson's disease during isometric contraction. *Clin. Neurophysiol.*, *120*(8), 1601–1609.

Reddi, B. A., & Carpenter, R. H. (2000). The influence of urgency on decision time. *Nat. Neurosci.*, *3*(8), 827–830.

Redish, A. D., Jensen, S., & Johnson, A. (2008). A unified framework for addiction-Vunerabilities in the decision process. *Behav. Brain Sci.*, *31*, 415–487.

Renoult, L., Roux, S., & Riehle, A. (2006). Time is a rubberband: Neuronal activity in monkey motor cortex in relation to time estimation. *Eur. J. Neurosci.*, *23*(11), 3098–3108.

Reynaud, A. J., Saleri Lunazzi, C., & Thura, D. (2020). Humans sacrifice decision-making for action execution when a demanding control of movement is required. *J. Neurophysiol.*, *124*(2), 497–509.

Rogge, J., Jocham, G., & Ullsperger, M. (2022). Motor cortical signals reflecting decision making and action preparation. *Neuroimage*, *263*, 1–15.

Roitman, J. D., & Shadlen, M. N. (2002). Response of Neurons in the Lateral Intraparietal Area during a Combined Visual Discrimination Reaction Time Task. *J. Neurosci.*, *22*(21), 9475–9489.

Rotge, J. Y., Clair, A. H., Jaafari, N., Hantouche, E. G., Pelissolo, A., Goillandeau, M., ... Aouizerate, B. (2008). A challenging task for assessment of checking behaviors in obsessive-compulsive disorder. *Acta Psychiatr. Scand.*, *117*(6), 465–473.

Samaha, J., Gosseries, O., & Postle, B. R. (2017). Distinct oscillatory frequencies underlie excitability of human occipital and parietal cortex. *J. Neurosci.*, *37*(11), 2824–2833.

Sauseng, P., Klimesch, W., Gerloff, C., & Hummel, F. C. (2009). Spontaneous locally restricted EEG alpha activity determines cortical excitability in the motor cortex. *Neuropsychologia*, *47*(1), 284–288.

Scheibe, C., Schubert, R., Sommer, W., & Heekeren, H. R. (2009). Electrophysiological evidence for the effect of prior probability on response preparation. *Psychophysiology*, *46*(4), 758–770.

Schouten, J. F., & Bekker, J. A. (1967). Reaction time and accuracy. *Acta Psychol. (Amst).*, *27*, 143–153.

Schurger, A., Hu, P. B., Pak, J., & Roskies, A. L. (2021). What Is the Readiness Potential? *Trends Cogn. Sci.*, *25*(7), 558–570.

Selen, L. P., Shadlen, M. N., & Wolpert, D. M. (2012). Deliberation in the motor system: Reflex gains track evolving evidence leading to a decision. *J. Neurosci.*, *32*(7), 2276–2286.

Shadlen, M. N., & Kiani, R. (2013). Decision Making as a Window on Cognition. *Neuron*, *80*(3), 791–806.

Shadlen, M. N., & Newsome, W. T. (2001). Neural basis of a perceptual decision in the parietal cortex (area LIP) of the rhesus monkey. *J. Neurophysiol.*, *86*(4), 1916–36.

Shadmehr, R., De Xivry, J. J. O., Xu-Wilson, M., & Shih, T. Y. (2010). Temporal Discounting of Reward and the Cost of Time in Motor Control. *J. Neurosci.*, *30*(31), 10507–10516.

Shibasaki, H., Barrett, G., Halliday, E., & Halliday, A. M. (1981). Cortical potentials associated with voluntary foot movement in man. *Electroencephalogr. Clin. Neurophysiol.*, *52*(6), 507–516.

Shibasaki, H., & Hallett, M. (2006). What is the Bereitschaftspotential? *Clin. Neurophysiol.*, *117*(11), 2341–2356.

Siegel, M., Buschman, T. J., & Miller, E. K. (2015). Cortical information flow during flexible sensorimotor decisions. *Science*, *348*(6241), 1352–1355.

Siegel, M., Donner, T. H., Oostenveld, R., Fries, P., & Engel, A. K. (2007). High-

Frequency Activity in Human Visual Cortex Is Modulated by Visual Motion Strength. *Cereb. Cortex*, *17*(3), 732–741.

Siegert, S., Herrojo Ruiz, M., Brücke, C., Huebl, J., Schneider, G. H., Ullsperger, M., & Kühn, A. A. (2014). Error signals in the subthalamic nucleus are related to post-error slowing in patients with Parkinson's disease. *Cortex*, *60*, 103–120.

Smulders, F. T., & Miller, J. O. (2012). The Lateralized Readiness Potential. In E. Kappenman & S. Luck (Eds.), *Oxford handb. event-related potential components* (pp. 229–251). Oxford University Press.

Spitzer, B., & Blankenburg, F. (2011). Stimulus-dependent EEG activity reflects internal updating of tactile working memory in humans. *Proc. Natl. Acad. Sci. U. S. A.*, *108*(20), 8444–8449.

Spitzer, B., Wacker, E., & Blankenburg, F. (2010). Oscillatory correlates of vibrotactile frequency processing in human working memory. *J. Neurosci.*, *30*(12), 4496–4502.

Standage, D., Blohm, G., & Dorris, M. C. (2014). On the neural implementation of the speed-accuracy trade-off. *Front. Neurosci.*, *0*(8 JUL), 236.

Sternberg, S. (1969). The discovery of processing stages: Extensions of Donders' method. *Acta Psychol. (Amst).*, *30*(C), 276–315.

Thura, D., Beauregard-Racine, J., Fradet, C.-W., & Cisek, P. (2012). Decision making by urgency gating: theory and experimental support. *J. Neurophysiol.*, *108*(11), 2912–2930.

Thura, D., & Cisek, P. (2016). Modulation of Premotor and Primary Motor Cortical Activity during Volitional Adjustments of Speed-Accuracy Trade-Offs. *J. Neurosci.*, *36*(3), 938–956.

Thura, D., & Cisek, P. (2017). The Basal Ganglia Do Not Select Reach Targets but Control the Urgency of Commitment. *Neuron*, *95*(5), 1160–1170.

Thura, D., Cos, I., Trung, J., & Cisek, P. (2014). Context-Dependent Urgency Influences Speed–Accuracy Trade-Offs in Decision-Making and Movement Execution. *J. Neurosci.*, *34*(49), 16442–16454.

Tranel, D., Cooper, G., & Rodnitzky, R. L. (2003). Higher Brain Functions. In P. M. Conn (Ed.), *Neurosci. med.* (pp. 621–639). Totowa, NJ: Humana Press.

Travers, E., & Haggard, P. (2021). The Readiness Potential reflects the internal source of action, rather than decision uncertainty. *Eur. J. Neurosci.*, *53*(5), 1533–1544.

Twomey, D. M., Kelly, S. P., & O'Connell, R. G. (2016). Abstract and Effector-Selective Decision Signals Exhibit Qualitatively Distinct Dynamics before Delayed Perceptual Reports. *J. Neurosci.*, *36*(28), 7346–7352.

Tzagarakis, C., Ince, N. F., Leuthold, A. C., & Pellizzer, G. (2010). Beta-band activity during motor planning reflects response uncertainty. *J. Neurosci.*, *30*(34), 11270–7.

Ulrich, R., & Miller, J. (2001). Using the jackknife-based scoring method for measuring LRP onset effects in factorial designs. *Psychophysiology*, *38*(5), 816–827.

Van Vugt, M. K., Simen, P., Nystrom, L., Holmes, P., & Cohen, J. D. (2014). Lateralized readiness potentials reveal properties of a neural mechanism for implementing a decision threshold. *PLoS One*, *9*(3), e90943.

van Rijn, H., Kononowicz, T. W., Meck, W. H., Ng, K. K., & Penney, T. B. (2011). Contingent negative variation and its relation to time estimation: A theoretical evaluation. *Front. Integr. Neurosci.*, *5*, 1–5.

Wang, X.-J. (2002). Probabilistic Decision Making by Slow Reverberation in Cortical Circuits. *Neuron*, *36*(5), 955–968.

Werkle-Bergner, M., Grandy, T. H., Chicherio, C., Schmiedek, F., Lövdén, M., & Lindenberger, U. (2014). Coordinated within-trial dynamics of low-frequency neural rhythms controls evidence accumulation. *J. Neurosci.*, *34*(25), 8519–8528.

Wickelgren, W. A. (1977). Speed-accuracy tradeoff and information processing dynamics. *Acta Psychol. (Amst).*, *41*(1), 67–85.

Winkel, J., Keuken, M. C., van Maanen, L., Wagenmakers, E. J., & Forstmann, B. U. (2014). Early evidence affects later decisions: Why evidence accumulation is required to explain response time data. *Psychon. Bull. Rev.*, *21*(3), 777–784.

Yau, Y., Hinault, T., Taylor, M., Cisek, P., Fellows, L. K., & Dagher, A. (2021). Evidence and urgency related EEG signals during dynamic decision-making in humans. *J. Neurosci.*, *41*(26), 5711–5722.

Zaehle, T., Wagenbreth, C., Voges, J., Heinze, H. J., & Galazky, I. (2017). Effects of deep brain stimulation of the subthalamic nucleus on perceptual decision making. *Neuroscience*, *343*, 140–146.

Attachments

Declaration of Honor

I hereby declare that I prepared this thesis without the impermissible help of third parties and that none other than the aids indicated have been used; all sources of information are clearly marked, including my own publications. In particular I have not consciously:

- fabricated data or rejected undesirable results,
- misused statistical methods with the aim of drawing other conclusions than those warranted by the available data,
- plagiarized external data or publications,
- presented the results of other researchers in a distorted way.

I am aware that violations of copyright may lead to injunction and damage claims by the author and also to prosecution by the law enforcement authorities. I hereby agree that the thesis may be electronically reviewed with the aim of identifying plagiarism. This work has not yet been submitted as a doctoral thesis in the same or a similar form in Germany, nor in any other country. It has not yet been published as a whole.

Magdeburg, 24 October 2022

Julia Rogge